Master of Science Thesis

Water Quality Impact of Floating Houses

A study of the effect on Dissolved Oxygen levels

E. Foka

November 2014

Faculty of Civil Engineering · Department of Water Management

Water Quality Impact of Floating Houses
A study of the effect on Dissolved Oxygen levels

by

E. Foka

in partial fulfillment of the requirements for the degree of

Master of Science

in Civil Engineering

at the Delft University of Technology,

to be defended publicly on Wednesday November 19, 2014 at 11:00 AM.

Supervisor:	Prof. dr. ir. N. van de Giesen	
Thesis committee:	Ir. M. Rutten,	TU Delft
	Dr. ir. R. de Graaf,	Deltasync
	Ir. F. Boogaard,	TU Delft/Tauw
	Dr. ir. A. Grefte	TU Delft

An electronic version of this thesis is available at http://repository.tudelft.nl/.

Summary

The growing agglomeration and climate change are two challenges for the urban areas, which result in the reduction of permeable surface, the increase of surface runoff and a change in the temperature and precipitation patterns. These, in addition to the uncertainty of the climate change, point towards the need for adaptive sustainable solutions.

Floating urbanization is an old concept, which recently is gaining attention since it combines solutions for the above-mentioned problems. A number of aspects need to be investigated in order to move forward with the implementation of floating urbanization. One of them is the effect on the water quality and ecology. Since water quality is a complex problem this thesis will focus on the effect of floating houses on Dissolved Oxygen levels.

A small floating residence in the area of Delft will serve as a case study. In this area a measurement campaign in the months of July to September 2013 was conducted in order to collect data, which later served to assess the impact of the floating houses. The results from the field measurements were further evaluated by analyzing which physical property or weather condition is responsible for the observed Dissolved Oxygen differences. Later on, a numerical model was developed in order to analyze in more detail the sources of these effects on Dissolved Oxygen. In particular the consequences of shadow and wind tunnel effect, induced by the floating houses, were studied.

The results of the measurements and numerical simulations showed that there are differences on the Dissolved Oxygen levels in the upper part of the water column. The average measured differences are close to 10% (1mg/L), similar to the results obtained by the numerical models. Nevertheless, both of the floating houses effects (shadow and wind tunnel) are active on the same region of the water column, which makes it difficult to isolate their contributions. Finally, the small amount of data collected and the uncertainty that is inherent in water quality modeling hinder us from drawing a definite conclusion regarding the effects of floating houses on Dissolved Oxygen levels. Further research and improvements on data collection and model development is recommended.

Acknowledgements

This thesis is the final requirement for completing the program of Master of Science at the Department of Water Management of the Delft University of Technology. The current report could not be started nor finished without the valuable help of my graduation Committee.

First I would like to thank Prof. Nick van de Giessen for trusting me and giving me the opportunity to get involved in a new research topic. My daily supervisor Martine Rutten who, despite her heavy work schedule, gave me helpful support and guidance. Dr. Rutger de Graaf and Floris Boogaard for promoting the concept of floating urbanization and water quality research, giving me important information and a good motivation. Finally, I would like to thank dr. Anke Grefte, who was willing to be part of my graduation committee even with a short notice.

An important part of a thesis was the data collection. Therefore I would like to thank the employees from the Hoogheemraadschap Delfland for the substantial help for my measurements and in specific Mr. Rolf Hoefnagel.

Another important ingredient for finishing my thesis was the wholehearted support of my friends. I would like to thank Sam, Sonia, Marietta, Daniele, Anastasia, Maria, Giorgos and Giannis for being there to support me in some difficult moments and give me wise advice.

The last ingredient and equally important is family. I will start with my family in Delft: My gratitude to Artur is infinite like the universe and human stupidity. To my family in Greece: I want to thank my mother and my sister for their patience, unconditional love and care.

Finally I want to dedicate this thesis to my Dad, who would be very fascinated by the concept of Floating Houses.

Delft, The Netherlands — E. Foka
November 2014

Contents

List of Figures

List of Tables

Nomenclature

Latin Symbols

A	Surface area	$[m^2]$
BOD	Biological Oxygen demand	[mg/L]
C	Dissolved Oxygen concentration	[mg/L]
c_p	Specific heat of water	[cal/(°C kg)]
C_{sat}	Saturated Dissolved Oxygen concentration	[mg/L]
$Chla$	Concentration of plant biomass	[mg/L]
D	Decomposition	[mg/(L s)]
F_s	Reaeration	[mg/(L d)]
g	Standard acceleration due to gravity	$[m/s^2]$
G_{max}	Maximum plant growth rate for optimal light conditions	$[d^{-1}]$
G_0	Global radiation	$[W/m^2]$
H	Water depth	[m]
I_0	Solar radiation at subsurface depth	$[W/m^2]$
k	Constant heat exchange coefficient	$[d^{-1}]$
k_a	Reaeration rate	$[d^{-1}]$
k_b	First order decay coefficient	$[d^{-1}]$
k_l	Oxygen transfer coefficient	[m/d]
k_{rs}	Respiration rate coefficient	$[d^{-1}]$
k_x	Turbulent diffusivity in x direction	$[m^2/d]$
k_y	Turbulent diffusivity in y direction	$[m^2/d]$
k_z	Turbulent diffusivity in z direction	$[m^2/d]$

N^2	Stability frequency of stratification	$[s^2/d]$
P	Photosynthesis	$[mg/(L\,d)]$
q	Internal distribution of solar radiation	$[cal/(m^2\,d)]$
Q_r	Total rainfall	[mm]
r_{oa}	Oxygen production per unit mass of plant biomass	$[mgO_2/mgChla]$
r_p	Pearson correlation coefficient	[−]
r_s	Spearman correlation coefficient	[−]
S	Sediment Oxygen demand	$[mg/(L\,d)]$
S_b	Sediment Oxygen demand at 20°C	$[mgO_2/(m^2\,d)]$
S_c	Schmidt number	[−]
SD	Secchi disk depth	[m]
S_t	Internal and external sources and sinks per unit volume	$[mgO_2/(L\,d)]$
T_a	Air temperature	[°C]
T_w	Water temperature	[°C]
u	Velocity component in the x direction	[m/s]
U_D	Wind direction	[°]
U_w	Wind speed	[m/s]
v	velocity component in the y direction	[m/s]
w	Velocity component in the z direction	[m/s]
$YCHO2$	Ratio of mg of plant biomass to mg of oxygen used in respiration	[−]
z	Depth	[m]

Greek Symbols

η	Extinction coefficient	$[m^{-1}]$
θ_b	Temperature adjustment coefficient in decomposition	[−]
θ_{rs}	Temperature adjustment coefficient in respiration	[−]
θ_s	Temperature adjustment coefficient in sediment oxygen demand	[−]
ρ	Water density	$[kg/m^3]$
τ	Optical depth	[m]
φ_ℓ	Attenuation of growth due to light	[−]
ω	Constant associated to the extinction coefficient	[−]

Abbreviations

0D	Zero dimensional
1D	One dimensional

2D	Two dimensional
3D	Three dimensional
BOD	Biological Oxygen demand
COD	Chemical Oxygen demand
CTD	Conductivity temperature depth
DO	Dissolved Oxygen
NAP	Normaal Amsterdam Peil (Amsterdam Ordnance Datum)
RMSE	Root Mean Square Error
SOD	Sediment Oxygen demand
WFD	Water Framework Directive

Chapter 1

Introduction

1.1 Problem definition

Big delta cities such as Rotterdam, New Orleans etc. will face two challenges in the near future: the growing agglomeration of population and climate change. The growing agglomeration of population in urban areas leads to a continuous process of conversion of rural land into urban land. The reduction of rural land for example, contributes to the decrease of the available land for food production. On the other hand, since urban areas are mainly impervious, they suppress water infiltration, generating an imbalance in the urban water cycle. It is expected that there will be an increase of storm-water flow combined with sewer overflows in urban areas [Howe et al., 2011]. Regarding the climate change, it is expected to produce an increase or decrease of temperatures and more heavy rainfall events. We need to keep in mind that climate change is characterized by uncertainty. Therefore, a more sustainable adaptive plan is of high importance.

Coastal cities in the Netherlands are facing (i) the possibility of flooding from river and sea level rise, as well as (ii) an increase in pluvial floods. On top of this, land scarcity is another of the problems that urban planners have to face along with the transformation of permeable land surface into impermeable. Legal requirements demand 10% of the development to be kept for water storage [Nilessen and Jeroen, 2011]. This requirement opens a way for a new adaptive urban development model: Floating houses. Figure 1.1 shows a schematic representation of the problem definition.

The development of the urban environment over the water has the potential of [De Graaf, 2012]:

- Decreasing land scarcity
- Improving the adaptability to flood events/decreasing flood damages
- Producing resources

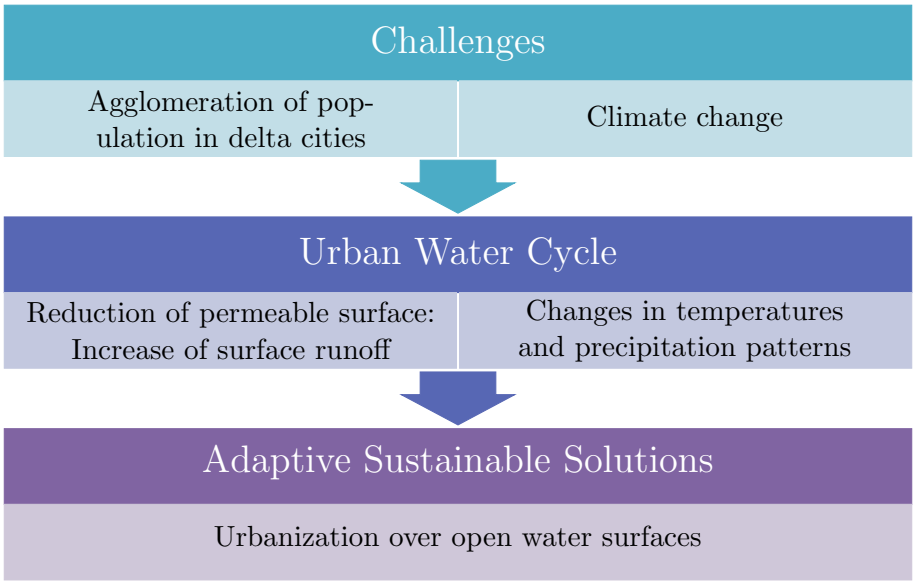

Figure 1.1: Problem definition flow path.

1.2 Current situation

Floating houses and amphibious constructions are part of a broader spectrum of measures against urban flood risk in floodplains. These measures consist of methods that allow temporary flooding of the lower parts of the building, use of waterproof building materials and construction of permanent or temporary barriers [De Graaf, 2012]. Both floating houses and amphibious constructions can adjust to water level variations. The difference between the two is the fact that floating houses are constantly surrounded by water while amphibious houses float in the event of a flood [De Graaf, 2012].

The concept of living on water is not new. At this moment numerous houseboats are established in the Netherlands and all around the world. However, it is a new approach with a future implementation perspective. The current design of the floating houses allows the expansion of a city over the water surface such as ponds, lakes and eventually the ocean.

Furthermore, the concept of urbanization over water includes sustainability practices such as the production of energy by the effluents of the main land city, change of eating habits of the residents (e.g. fish cultivation will reduce the consumption of meat and subsequently the energy used for its production). Therefore, the floating cities will help closing the linear resources metabolism that characterize the current cities [De Graaf, 2012], see Figure 1.2.

Although the aspects regarding the design, construction and selection of materials for floating houses have been investigated, there are a number of other aspects that are still not resolved nor investigated. Some of these are listed below [De Graaf, 2012]:

Technical: How to integrate current floating housing technologies and the application of floating houses in a larger scale.

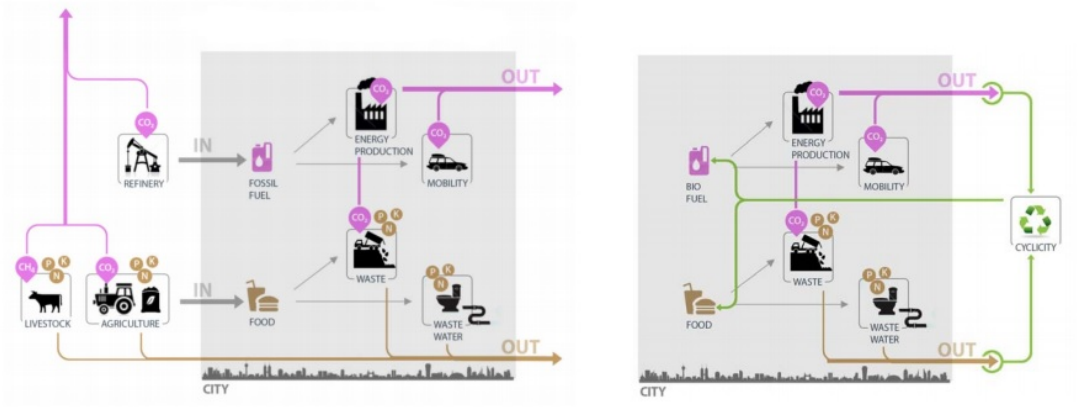

Figure 1.2: Linear metabolism of conventional cities (left) and cyclicity concept of conventional city connected to a floating city (right) (Deltasync).

Design: The development of an urban planning specifically for floating urbanization.

Environmental: What is the impact of floating houses on water quality and ecology?

Economic: The development of a real estate economic model suitable for the floating urbanization.

Governance: The behaviour of the residents of the floating cities needs to be further studied, especially because the floating cities will give the opportunity for a more decentralized policy making. Also, it is still unknown if the floating cities will be regarded as a state of their own or will be part of another nation state.

1.3 Importance of this report

The focus of this work is on the impact of floating houses on the water quality, particularly on Dissolved Oxygen and water temperature. Small floating objects, such as boats, can create hiding places for fishes. However, bigger floating objects like the floating houses can have a negative impact on fish and plants by depriving water from sunlight, which in turn hinders the production of oxygen through photosynthesis, [Graaf, 2009, De Graaf, 2012]. Also, floating objects minimize the air-water interface thus the oxygen exchange rate. More research needs to be done towards the understanding and quantification of the effect of floating houses on water quality.

Furthermore, this environmental knowledge gap is an obstacle for further development and application since local government authorities appear to be reluctant to issue building permits for floating houses, without this topic being studied. However, water boards recognize the innovation that floating houses provide and are willing to contribute to this research.

Therefore, the objective of this research is to investigate if the floating houses influence the Dissolved Oxygen and water temperature of the applied water body. If so the driving causes will be investigated.

1.4 Research questions and Hypotheses

Taking into consideration what was mentioned above, the research question can be stated as follows:

> *What are the effects of floating houses on the Dissolved Oxygen levels of the applied water body?*

The research question will be answered by investigating the following hypotheses:

- *The shadow of the floating houses reduces available sunlight. This lowers the Dissolved Oxygen levels in their vicinity due to reduced photosynthesis.*
- *Depending on their orientation, wind tunnel effect can be produced by the floating houses increasing the turbulence of the water. This increases the mixing in the water column, which reduces the Dissolved Oxygen vertical gradient.*
- *Close to the floating houses the water temperature gradient in the vertical direction will decrease due to shading.*
- *Below the floating houses a hypoxic area is created and oxygen is transferred laterally by the adjacent water column. This lowers the Dissolved Oxygen levels in their vicinity.*

1.5 Outline of the report

This research consists of seven chapters. Chapter 2 elaborates on the water quality aspects and how they can be influenced by the presence of floating houses. After establishing the reasons why Dissolved Oxygen was chosen to be evaluated, the numerical modeling of water quality is introduced. In Chapter 3 a description of the area that served as the case study of the current thesis is introduced to the reader. Chapter 4 describes the methodology followed in the current research. There, the reader is introduced to the instruments used for the measurements and the physical expressions employed in the numerical modeling. In Chapter 5 and Chapter 6 the results from the field measurements and the numerical modeling are presented and discussed, respectively. Finally, Chapter 7 includes the conclusions and recommendations for future research.

Chapter 2

Literature Review

In this chapter water quality processes and their modelling is discussed. It starts with an explanation of the water quality parameters as well as the interactions among them and floating structures. It further continues with a presentation of floating structures and research on their impact on water quality, followed by an introduction to water quality numerical modelling, the importance it has and the existing modelling approaches.

2.1 Water Quality

2.1.1 Water quality parameters and interactions

Water quality is described by chemical, physical and biological properties and the interactions among them and the surrounding environment. For example, meteorological conditions, inflows and outflows from the system can be predominant factors in determining the water quality [Ji, 2008]. Some of the most important parameters are:

- Turbidity
- Temperature
- Dissolved Oxygen
- pH
- Electro conductivity
- Nutrient Loads

Turbidity is related to the existence of sediment and phytoplankton in the water. High turbidity is responsible for the scattering of light into the water body [Wilson, 2010]. By scattering the light, photosynthesis and subsequently the oxygen production will decrease.

If the oxygen is not enough for the support of the ecosystem of the water body the organisms that depend on oxygen will start to decay. Activities that increase the turbidity of water are for example urban runoff, recirculation of bottom sediment from flooding or bottom feeding animals and excessive algal growth [Ji, 2008].

Temperature is an important parameter since it has a major influence on the biological activity and growth, defines which organisms can live as well as influences the rate of chemical reactions. Moreover, temperature influences the hydrodynamics of a water body [Ji, 2008]. For example, stratification, which is the result of vertical profile temperature differences, hinders vertical mixing.

Oxygen in water is the oxygen that dissolves from the atmosphere into the water and since it is necessary for the survival of most aquatic plants and organisms, it is an indicator of the health status of the water body. The quantity of Dissolved Oxygen (DO) is influenced by the temperature of the water, for example the higher the temperature the lower is the Dissolved Oxygen quantity [Williams, 2007]. Another source of oxygen in the water is the production of oxygen by photosynthesis. The primary energy source for photosynthesis is sunlight. Therefore, the blockage of sunlight can have a negative impact in the photosynthesis mechanism [Kutty, 1987].

Electro conductivity is an indicator of the ability of the water to conduct electricity. The more ions the water has the more it can conduct electricity. Salt dissolved in water separates into ions. Therefore electro conductivity is a measure of the salinity content in the water.

pH determines the solubility and biological availability of chemical constituents such as nutrients and heavy metals. For example, the pH affects which form of phosphorus will be abundant and also determines whether or not it will be available for the aquatic life [Hupfer and Lewandowski, 2008].

Nutrients concentrations define the trophic state of water. A high nutrient concentration is described as eutrophic state. Eutrophication can lead to algal blooms in the open water [Ji, 2008] and may have negative health impacts as well as deteriorate the aesthetic of living close to or over water [Paerl et al., 2001].

Finally, the dead organic material that settles to the *sediment* continues to decompose. Although sediment is not directly a water quality parameter it influences the oxygen levels. Since oxygen levels are lower at the bottom of a water body the amount of oxygen needed by bacteria to decompose the organic material has to be transferred from overlying water. This consumption of Dissolved Oxygen is described as Sediment Oxygen Demand (SOD) [Chapra, 1997]. Also, sediment can be regarded as a phosphorus transient storage [Ekka et al., 2006]. Particulate forms of phosphorus settle to the bottom and can later mineralize and form orthophosphate, which in turn is slowly diffused in the overlying water.

2.1.2 Potential Effect of floating houses

The installation of floating houses directly produces the following effects: blockage of sunlight and shadow, reduction of the air-water interface area (open surface), wind stress, change of water flow and sedimentation [De Graaf, 2012, Hartwich, 2014]. The blockage

of sunlight and shadow not only affects the temperature of the upper layer of the water body but also reduces the production of oxygen by photosynthesis [Burdick and Short, 1999]. On the other hand, the reduction of the available air-water interface reduces the oxygen that is transferred from the air to the water. Furthermore, the floating houses can influence the water flow and the stratification structure [Kitazawa et al., 2010], the vertical circulation [Ji, 2008] and the sediment transport [Hartwich, 2014].

Lower oxygen levels can eventually result in dead organic material that contributes to the turbidity, which in turn influences sunlight penetration. In addition, the dead organic material will settle to the sediment increasing the nutrients concentration as well as the sediment oxygen demand. This can result in the development of a low Dissolved Oxygen zone below the floating houses [Kitazawa et al., 2010], [Penning et al., 2003].

The underwater surface of floating houses or other floating structures is suitable for the development of sessile organisms. This is something that can influence water quality, even more in cases where the water state is more eutrophic and stagnant [Kitazawa et al., 2010]. Finally, part of the floating houses penetrates the water column and the underwater faade creates a no flow boundary. The distance between two floating houses can be critical since they create a partially confined water column. Since the water in a pond has limited flow the oxygen transfer by diffusion or dispersion can be slower and eventually can create bad conditions for the aquatic life.

Wind, as a major mechanical energy source, can influence the circulation and turbulent mixing of a water body. Wind is characterized by temporal and spatial variations therefore its influence on the water body will not be homogeneous. The presence of floating houses can influence the wind pattern since air is compressed as it passes between two adjacent houses. As it is compressed it is accelerated, resulting in an increased wind speed. The magnitude of this increase depends on how much the air is compressed. Furthermore, wind can also be blocked by the presence of the floating houses. The facade opposite to the one facing the wind experiences lower winds.

2.1.3 Importance of Dissolved Oxygen in Water Quality

In Annex V section 1.1.3 of the Water Framework Directive (WFD), Dissolved Oxygen (DO) is considered as one of the five general chemical and physicochemical elements supporting the biological elements [Directive 2000/60/EC, 2000]. Oxygen is important for the survival of the aquatic life and is needed for many chemical reactions. Therefore, monitoring the fluctuations of the oxygen levels as well as the factors that affect these fluctuations is important for assessing the ecological status of the water body.

Main sources of oxygen in water are the exchange of atmospheric oxygen across the air water interface and photosynthesis. The oxygen concentration in the atmosphere is 298.9mg/L while the oxygen concentration in water at equilibrium with air is 8.64mg/L (at 25^{o}C and 1atm). Typically the oxygen levels in natural water are below this equilibrium, therefore these concentration differences cause oxygen molecules to be dissolved in water. On the other hand, when oxygen levels in water are above this equilibrium, oxygen is transferred to the atmosphere. These exchanges of oxygen between the air and the water are intensified when there is turbulence generated by the wind [Michaud, 1991]. Photosynthesis is carried out by aquatic plants, algae and photosynthetic eubacteria. The

basic source of energy for photosynthesis is light, which is used to split water molecules and release oxygen [Best et al., 2007]. Because of the nature of these sources it is expected that the oxygen levels will present variations in time due to varying weather conditions. Finally, turbidity and water clarity are two parameters that influence the penetration and scattering of light in the water column and consequently influence the production of photosynthesis.

The main consumption of oxygen in water is due to decomposition of organic matter, the respiration from fish, microorganisms and aquatic plants, the nitrification and sediment. Decomposition and respiration are processes that take place during the day and night. Therefore, when oxygen production by photosynthesis does not compensate the consumption from decomposition and respiration, the oxygen budget of the aquatic ecosystem is at stake. Nitrification occurs when certain nitrogen compounds enter the water body and break down into ammonia. Nitrifying bacteria (nitrosomonas) oxidize ammonia (NH_3) into nitrite (NO_2^-), which in turn oxidizes into nitrate (NO_3^-). For every mole of ammonia that is oxidized two mole of oxygen are consumed. Finally, dead organic material settles to the bottom sediment. The surface of the sediment is in direct contact with water and undergoes aerobic decomposition. The oxygen required for this process is transferred from the overlying water column.

The key natural physical factors that influence oxygen levels are temperature and salinity. The relation between them is inversely proportional: the higher the temperature and salinity, the lower the saturated Dissolved Oxygen content in the water column. Furthermore, the warmer the water temperature, the higher the metabolism and respiration become [Addy and Green, 1997]. In some water bodies, temperature or salinity stratification can occur. This effect prevents mixing and it can further contribute to the development of hypoxia and anoxia, especially during the summer months [Best et al., 2007].

Stratification occurs mainly in deeper lakes, more than 5m deep and is the result of the density variations of water with different temperatures [Addy and Green, 1997]. Stratification occurs mainly in warmer months when the water of the surface warms up faster than the deeper water. Since warm water is lighter (less dense) than the cold water, the water column separates in three thermal layers: epilimnion, metalimnion and hypolimnion. Stratification can occur also during colder months, in this case the upper layer is colder than the deeper one. In addition, the formation of ice on the surface can also prevent sunlight and reduce oxygen exchange with the atmosphere, consequently reducing oxygen levels in water. Shallow ponds do not develop thermal stratification due to complete mixing of water by wind and waves. However, they may experience stratification in summer, during days with no wind, and winter, when they are covered by ice [Addy and Green, 1997].

Finally, the importance of oxygen levels and the effect of stratification on the water body can be described by the following example. If the oxygen levels at the bottom of the lake are less than 1mg/L nutrients are released from the sediment by a chemical reaction. When stratification finishes, in the beginning of autumn, these nutrients are available to algae and, as a result, algal blooms occur [Addy and Green, 1997].

Table 2.1 shows the proposed Dissolved Oxygen standards of the Water Framework Directive for transitional water. The values represent the 5 percentile, meaning that they should be exceeded 95% of the time [Best et al., 2007].

Table 2.1: Proposed Dissolved Oxygen WFD standards for naturally ventilated layers of transitional water [Best et al., 2007].

Status	Freshwater 5%ile
High	DO $\leq$ 7mg/L
Good	5mg/L $\leq$ DO $<$ 7mg/L
Moderate	3mg/L $\leq$ DO $<$ 5mg/L
Poor	2mg/L $\leq$ DO $<$ 3mg/L
Bad	DO $<$ 2mg/L

2.2 Floating Structures and Water Quality

Nowadays, floating urbanization is becoming an active field of research. Although most of the discussion and research done is related to the technical, economical and policy feasibility, the effect in water quality due to floating objects has been less addressed in the literature.

In Japan, a large floating object, initially intended to be used as an offshore runaway for the Tokyo airport, was assessed by the environmental impact produced [Kitazawa et al., 2010], see Figure 2.2 centre. Two monitoring stations were placed in different positions such that they would give data corresponding to the conditions below the floating structure and the open water. The monitored parameters were physical (current velocity, salinity and temperature) and chemical-biological conditions (Dissolved Oxygen, chlorophyll-a and nutrients concentration). The results showed that the variations between the two monitored locations within the first 5m of water column, out of 16m, can be attributed to the impedance of photosynthesis by sea covering and the activity of the sessile organisms that developed on the bottom of the floating platform, while the effects on the direction of flow and the stratification structure are negligible [Kitazawa et al., 2010].

In 2005 the realization of the first floating greenhouses drew global attention to the Netherlands. Two years prior to the floating greenhouses implementation, a feasibility study was conducted over three aspects: economical, institutional and spatial-environmental. In this study 70% of a seasonal water storage is occupied by greenhouses [Silvis et al., 2003]. The impact on water quality was investigated by a simple model set-up which included the degree of mixing of rainwater with seepage water, the dispersive and advective mixing and the assumptions for the mineralization and oxygen consumption. The results indicated that indeed a difference will emerge in the oxygen concentration below the greenhouses and the open surface. However, an absolute conclusion could not be drawn as a result of the dependency of the assumptions and boundary conditions on the location [Penning et al., 2003].

In a more recent study, in the municipality of Boskoop, The Netherlands, a floating field installed on a ditch was monitored in order to evaluate the effect of the floating field on the ditchs water quality [Pieters and Aendekerk, 2013], see Figure 2.2 left. The monitoring campaign took place during one year and the oxygen levels were measured in 15 minutes intervals in three different points, north and south of the floating field and in the middle

of it. Hardly any difference was noticed in the results, therefore it was concluded that the floating field did not influence the Dissolved Oxygen levels in the ditch [Pieters and Aendekerk, 2013]. However, this is not a complete conclusion since the conditions below the floating field was not measured neither simulated.

Figure 2.1: Floating greenhouses in the Netherlands. (Source: Dura Vermeer)

Apart from the big floating structures like the ones mentioned above, there are also residential types of floating structures, such as house boats and more recently floating houses. Up to this moment, there are no published results related to the effect of floating houses on water quality. However, there is an ongoing project by DeltaSync and Tauw in The Netherlands focusing on this, [DeltaSync, 2014, Tauw, 2014]. Already in the United States, United Kingdom, Australia and The Netherlands a number of regulations exist for floating structures. A part of these regulations is dedicated to the interactions of the floating houses and houseboats with the aquatic environment. For example, in the United Kingdom, instructions and suggestions are given regarding the type of drainage and waste water treatment the inhabitants should consider for their residence [Adur District Council, 2007].

Although the principles of developing over water are the same, the difference between these types of floating structures is related to the distribution of the floating houses over the water surface. Floating houses are characterized by relatively small floating structures separated from each other and distributed over a larger area, see Figure 2.2 right, as opposed to large single structures as in the previously reported studies. Figure 2.2 helps to visualize this difference.

2.3 Numerical Modelling

2.3.1 Numerical modelling and water quality

In order to be able to analyse the water quality and make further steps in decision making regarding measures and policies, the following steps must be considered:

1. Observation

Figure 2.2: Scale difference between floating projects (Left: Floating field; Centre: Floating runaway; Right: Floating houses. (Source: [Pieters and Aendekerk, 2013, Kitazawa et al., 2010] and Deltasync)

2. Theoretical Analysis

3. Numerical modelling

Observations are useful but they are not enough for making water quality management plans, particularly when they concern large and complex water bodies. Additionally, measured data can include errors that can lead to a misunderstanding of the physical, chemical and biological processes that take place in the water body. At this point, theoretical analysis is necessary for understanding the processes that take place in the water body and explain what has been observed with the measurements. Finally, numerical modelling allows to set up a simulation that will be able to represent the hydrodynamic, biological and physical processes that are involved in water quality [Ji, 2008].

Numerical modelling is a useful tool since it is used to evaluate water quality management measures and techniques, clarify the behaviour of the water body towards a certain action and they are cheaper and faster than the actual implementation and monitoring [Wang et al., 2013]. Thus, modelling provides flexibility.

On the other hand, however, water quality modelling is not a simple task as it may seem. It depends on the type of problem to solve and the type of water body to be applied, therefore many different water quality models exist.

In order to address the research question of the current thesis and evaluate the measured data, it is important to understand the hydrodynamic, physical and biological processes that are involved. Therefore, a model of the evolution of the Dissolved Oxygen will assist in this task since it can provide a higher spatial and temporal resolution.

2.3.2 Types of water quality modelling

Water quality modelling involves processes which can be studied independently as well as together with other ones. Additionally, temporal and spatial variations are important for the physical, chemical and biological activities of the water quality parameters (Ji 2008). Thus, a water quality model is composed of hydrodynamic and chemical-biological expressions while the type of problem that is simulated defines the spatial and temporal discretization.

The way water circulates can affect the temperature, nutrients or Dissolved Oxygen distribution but can influence the distribution of biota and water productivity as well. Therefore, the type of water body also determines the dominant hydrodynamic expressions [Ji, 2008]. For example, in a stream, the main driving force is gravity and the main resisting force is bed friction. On the other hand, in lakes and ponds, where the water movements are more restricted the main driving forces are wind, solar radiation, heat exchange, inflows and outflows [Stefan et al., 1989].

Even though we leave in a three dimensional world, when it comes to modelling we have to choose with how many dimensions we want to simulate the given problem. A water quality modeller should choose the dimensions in which the water quality is expected to be significantly influenced [Ji, 2008]. By reducing the number of dimensions in the problem, the computational effort is significantly reduced. The number of dimensions to be modelled defines the type of modelling. A description of the different types of modelling is given below:

Zero-dimensional (0D): This type of modelling relies in a control volume that represents the entire water body. The water body is assumed to be well mixed, and the concentrations will be averaged concentrations [Stefan et al., 1989]. In these types of models, conservation of mass is the applied equation. Therefore these models are also known as Input-Output models. Zero dimensional modelling is suitable for preliminary evaluation of the water quality condition of a lake.

One-dimensional (1D): A one dimension model simulates the water quality changes along a single dimension. In case of a river we can simulate longitudinally downwards its length. Vertical simulation can be also considered in the case of lakes, especially if they are small and well stratified. This type of modelling is very useful if we are interested in the thermal stratification of a lake or the Dissolved Oxygen distribution [Ji, 2008].

Two-dimensional (2D): Two dimensional models consist of spatial variations on the lateral-longitudinal direction or the vertical-longitudinal direction while the state variable is averaged on the third dimension. Vertically averaged models are suitable for shallow lakes that develop strong mixing, while lateral averaged models are suitable for narrow and deep rivers, lakes and reservoirs [Ji, 2008].

Three-dimensional (3D): This type of modelling is the most detailed one, since it can describe the changes that occur in all the three directions.

2.3.3 Review of water quality modelling

Once we know the problem to be modelled, we can choose from an existing water quality model or create our own. In the construction of a model we should take into consideration the following criteria pointed by [Riley and Stefan, 1988]:

i. The model should incorporate the driving physical, chemical and biological processes that occur in the surface water body;

ii. The physical, chemical and biological processes should be modelled with similar orders of detail to reduce the possibility of a weak link in the modelling process;

iii. The model should be general such that it can be used in different surface water bodies with a minimum of changes;

iv. The model should be computationally economical to serve as a management tool.

In the literature there are several studies related to the numerical modelling of Dissolved Oxygen in a variety of surface water bodies. [Mwegoha et al., 2011] presented a mathematical model that predicts the effects of wind, solar radiation, temperature, pH, dissolved carbon dioxide (CO_2) and chemical oxygen demand (COD) on the Dissolved Oxygen in fish ponds. [Ginot and Hervé, 1994] developed a model to predict the dynamics of Dissolved Oxygen in shallow ponds. In both these models it is assumed a complete mixing of the water body, therefore no spatial variability is included (zero dimensional model, 0D). [Rucinski et al., 2010] developed a model that accounts for the vertical profile of temperature (one dimensional model, 1D), mixing and Dissolved Oxygen in a lake. The scope of their model was to determine the effect of climate change on the vertical profile of Dissolved Oxygen. [Riley and Stefan, 1988] implemented a one dimensional (1D) model that was intended to study lake eutrophication. This model is capable of simulating lake stratification and water quality given time a varying weather, inflow, outflow, exchange processes at the water-sediment interface, advective and diffusive transport, settling, chemical and biological kinetics.

Finally, a case similar to the one of the floating houses can be considered the ice cover of a lake. In [Fang and Stefan, 1994] a winter Dissolved Oxygen sub-model was developed based on the deterministic simulation models of water temperature and Dissolved Oxygen of [Stefan et al., 1993]. The model includes biological and physical activities, such as photosynthesis and water column oxygen demand, but the parameters and coefficients used are representative of the winter period. Furthermore, the reaeration process is considered to be zero in the case of ice cover. Thus, the effect of ice cover is similar to the effect of the presence of floating houses, although we expect that photosynthesis will be more influenced from the less transparent surface of the floating houses.

Chapter 3

Case Study

The need of an adaptive sustainable solution for the increased land scarcity, increased urbanization, climate change and flood risks resulted in the concept of the floating urbanization. In The Netherlands the implementation of the program "Living with Water" gave a dual role to the open water surface [Nilessen and Jeroen, 2011]. This role is related to water storage and housing. This new type of housing attracted the interest of local authorities (municipalities and water boards) and there are already plans to incorporate floating houses in the urban planning. A small floating houses project in Delft will serve as a case study for addressing the environmental-ecological knowledge gap discussed in the introduction and literature review, Section 1.3 and Section 2.1.2. Below a description of the area and the project is presented.

3.1 Area description and information

In 2009 the Water Board of Delfland and the Municipality of Delft gave permission for the construction of small scale floating houses at the Voordijkhoornsepolder. This is part of the newly built area of Harnaschpolder in Delft, located on the Western part of The Netherlands between the cities of Rotterdam and The Hague, see Figure 3.1. The climate in the area of Delft is influenced by the coast and is characterized as temperate oceanic. The winter and summer temperatures are milder than the ones further inland. Figure 3.2 shows the annual overview of the climate conditions in Delft, [KNMI, 2010]. Harnaschpolder is a former greenhouse land converted to urbanization and is planned to accommodate 1300 residents. The floating houses are located on the southern part of this new neighbourhood. This area is at -0.1m NAP and the ground consists of clay.

The pilot project consists of six floating houses in a shallow pond of approximately 1.5m mean depth and deepest depth of 2.5m, at the location of the floating houses. The floating houses have an immersion depth of approximately 1.6m. At the time of writing this thesis, three floating houses were already deployed on water and two were under construction, see Figure 3.3. The total surface of the pond is 5.800 m^2 while the estimated occupation

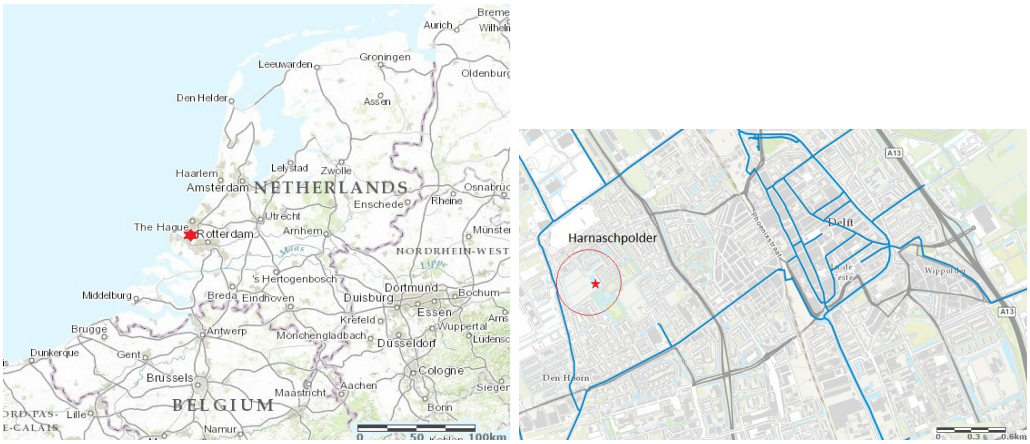

Figure 3.1: Location of the floating houses in Harnaschpolder (Source: Hoogheemraadschap Delfland).

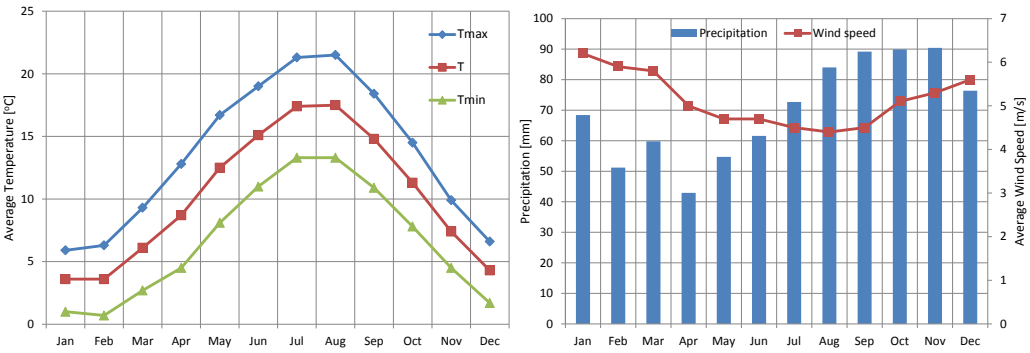

Figure 3.2: Average meteorological conditions in Delft. (source: [KNMI, 2010])

of floating houses is set by the Water Board of Delfland at 10%. Water is flowing into the pond from the surrounding drainage ditches, see Figure 3.4. These ditches have a water level target of -1.45m NAP, while the flow is approximately 0.027m/s. There are two discharge points in the northeast part of the area with a discharge rate of 4.38 m^3/s, see Figure 3.4.

Figure 3.3: Floating houses in Harnaschpolder.

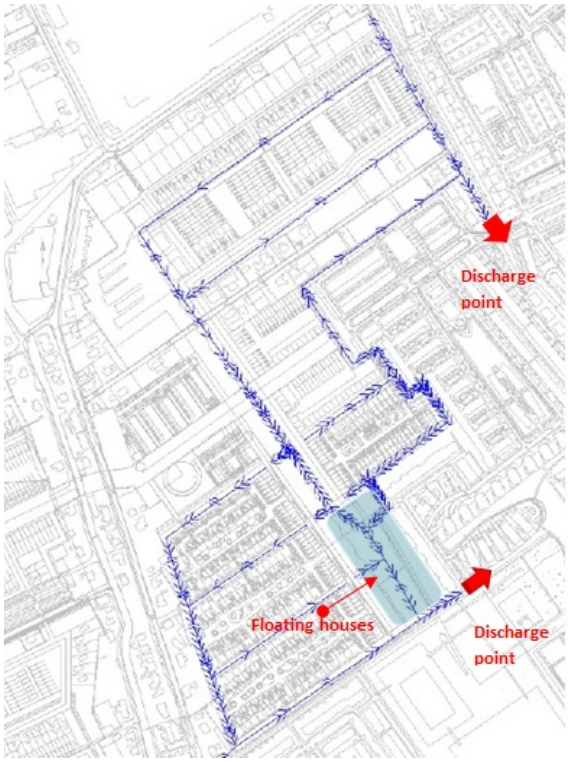

Figure 3.4: Water flow directions and discharge points at floating houses in Harnaschpolder, (Source: [Gielen and de Kwaadsteniet, 2009]).

In 2012, the Water Board of Delfland ran a measurement campaign on the site of the case study. The following parameters were measured on a monthly basis: Electro conductivity, Acidity (pH), Oxygen, Turbidity, Chloride, Nitrogen, Phosphorous, Chlorophyll-a and Macro-ions. These results were presented and analysed in the "Nulrapportage drijvende woningen Harnaschpolder", [Hoefnagel and Raaphorst, 2013]. In this report it is emphasized that the water body was recently dug, therefore a number of years should pass until the water quality becomes stable. The chemical analysis of the water body indicated that the water quality is at a moderate to reasonable level, with chlorine and oxygen levels being within the desired levels. A higher level of phosphorus was observed during the summer months, but this is expected for this period of the year.

Chapter 4

Methodology

As mentioned before, the main objective of this thesis is the study of the potential effect of the floating houses on the Dissolved Oxygen levels of a water body. This work is based on two complementary approaches: measurements and numerical simulation. The measurements can fully capture the oxygen budget variations. However they lack spatial and temporal resolution as a result of their local character. On the other hand, numerical simulation although a simplified Dissolved Oxygen budget, has the advantage of a higher spatial and temporal resolution and therefore more data are available for statistical interpretation. Furthermore, numerical simulation gives a better insight into the fundamental processes since the terms that contribute to the Dissolved Oxygen budget can be evaluated. With this complementary approach we intend to use the measurement data to improve the accuracy of the numerical model, in other words, calibrate the model.

This chapter starts by introducing the reader to the monitored parameters, the measurement equipment and the strategy undertaken for the data collection and is followed by a discussion over the methodology of data analysis. Finally, the mathematical model implemented for the numerical simulation of the Dissolved Oxygen budget processes will be presented in the last part of this chapter.

4.1 Field measurements

4.1.1 Monitored Parameters

Dissolved Oxygen is one of the most important parameters that define the water quality of surface water, as it was discussed above, Section 2.1.3. Other parameters that influence Dissolved Oxygen levels and can be easily measured are temperature and water transparency.

In order to evaluate the influence of floating houses we need to take measurements in a water body where floating houses as well open spaces exist. In this way, the effect of, for example, the shadow created by the floating houses can be analyzed. Furthermore,

measuring Dissolved Oxygen on the vertical profile can give insight of the distribution of Dissolved Oxygen along the water column.

Parallel to the Dissolved Oxygen, it is informative to measure the water temperature. This enables us to estimate the oxygen saturation state of the water and study if the water body is subjected to temporal stratification. Furthermore, measuring the temperature in the vertical orientation and at different locations can help to evaluate the mixing state of the water body. Finally, measuring the water transparency will indicate the depth were photosynthesis is active, as well as monitor the possible development of algal blooms.

For the measurement campaign of the current thesis two measurement types were performed, namely instantaneous and continuous. For the instantaneous measurements a Hydrolab MS5 water quality multi-probe (Figure 4.1 left) and a Secchi disk depth (Figure 4.1 right) were used. The MS5 probe is a portable instrument used for long-term monitoring or profiling applications. The MS5 has four configurable ports that can include a combination of sensors [Hydrolab, 2006]. The sensors used were: Dissolved Oxygen, Temperature, pH, salinity, and electro conductivity. Table 4.1, gives the specifications of the sensors used in the MS5 multi-probe.

Table 4.1: Hydrolab MS5 water quality multi-probe specifications.

Sensor	Range	Accuracy	Resolution
Temperature	-5 to 50°C	±0.10°C	0.01°C
Electro conductivity	0 to 100 mS/cm	±1% of reading: ±0.001 mS/cm	0.0001 units
pH sensor	0 to 14	±0.2	0.01
Dissolved Oxygen	0 to 50 mg/L	±0.2 mg/L at ≤20 mg/L ±0.6 mg/L at >20 mg/L	0.01 mg/L

The Secchi disk is a circular disk with a pattern, e.g. a black and white colour, attached to a rope with length indication. The disk is inserted in the water and lowered. The depth at which the pattern of the disk is no longer visible is recorded as the Secchi disk depth.

Figure 4.1: Measurement equipment: probe (left), diver (middle) and Secchi disk (right).

For the continuous measurements, five divers (see Figure 4.1, middle) were installed in different locations and water depths. The available divers from Schlumberger Water Services were: (i) One Baro Diver, which measured the air temperature and air pressure, (ii) two CTD-Divers, which measured temperature, pressure and electro-conductivity, and finally (iii) two Mini-Divers, which measured temperature and pressure. The specifications of the divers are presented in Table 4.2.

Table 4.2: Divers Specifications.

Sensor		Range	Accuracy	Resolution
Temperature		-20 to 80°C	±0.2°C	0.01°C
Pressure	Baro diver	150 cmH_2O	±2 cmH_2O	0.1 cmH_2O
	CTD diver	10 mH_2O	±0.2% Full Scale	0.2 cmH_2O
	Mini diver	50 mH_2O	±0.25% Full Scale	0.2 cmH_2O
Electro conductivity		10 μS/cm to 120 mS/cm	±1% of reading	

4.1.2 Criteria for choosing measurement locations

For the collection of the necessary data to answer the research question of the current thesis, four measurement points (A, B, C, D) were chosen as indicated in Figure 4.2. The point where the water board was measuring in 2012 is indicated with WB. At the time of the measurement campaign three of the floating houses were already deployed in the water and two of them were inhabited. Two other floating houses were under construction and their future position is indicated in red.

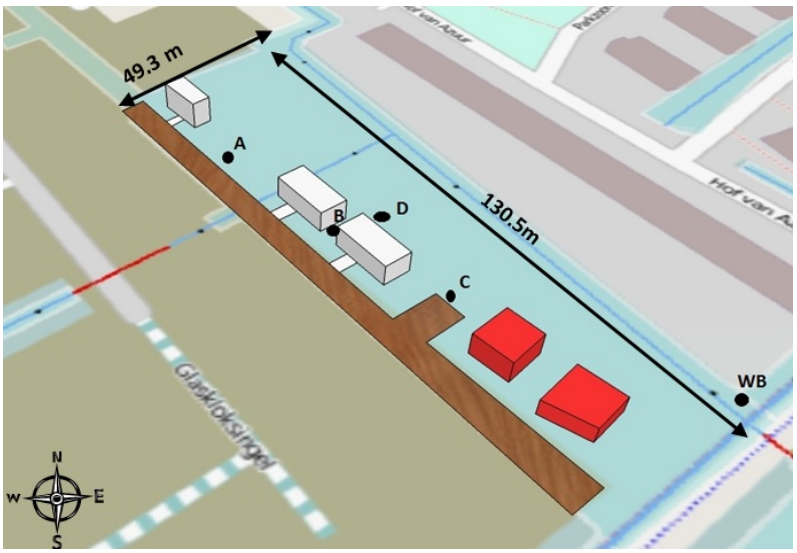

Figure 4.2: Location of the measurement points (the coloured floating houses were not deployed during the measurement campaign, no scale).

The measurement positions were chosen according to the following criteria:

Accessibility, these points are easily accessed from the deck and the floating construction platforms around the houses.

Depth, the deeper points of the pond are more suitable to give a detailed vertical profile of the Dissolved Oxygen and temperature

Shadow point (point B), this point is expected to be the most influenced by the shadow created by the two houses as well as the wind effect.

Open space (points A and C), these locations will be in the future occupied or be close to floating houses and can serve as reference values for comparing the changes in the water in a more open space and in a more confined one, like point B.

Mixed point (point D), this point is close to the floating house and an open surface.

By following these criteria, the chosen positions of measurement are suitable to make a comparison between the open surface and the locations that are close to the floating houses.

For the vertical profile, we chose to measure at the following depths from the surface: 0.0m, 0.5m, 1m, 1.5m, 2m[1]. For each point we measured for 2 minutes with a time step of 10 seconds. The Water Board measured at 0.5m below the surface and used a time step of 10 seconds. Point A is the shallowest one, 1.40m depth, and will serve as a comparison with the deeper measurement locations (B, C and D).

Finally, between the 4$^{\text{th}}$ and 23$^{\text{rd}}$ of September, a pair of CTD and Mini divers where installed in positions B and C at depths 0.7 and 2.0m. A baro diver was placed outside the water and close to position B. The time step of the measurements was set to 5 minutes.

4.1.3 Weather conditions

The measurement campaign took place between the 31$^{\text{st}}$ of July and 23$^{\text{rd}}$ of September 2013. The closest available weather data for the area of Delft were obtained from a private weather station located in Tanthof, Delft, approximately 5km South-East from the measurement location. The type of weather station is a Vantage Pro 2 by Davis Instruments, see Figure 4.3. Information for Temperature, Humidity, Wind speed and Direction, Pressure and Rainfall were recorded every one minute. From these raw data the averaged 5 minutes and 1 hour Temperature (T_{a} [$^{\text{o}}$C]), Global Radiation (G_0 [W/m^2]), Wind Speed (U_{w} [m/s]) and Wind Direction (U_{D} [degrees]) were computed, as well as the total rainfall (Q_{r}, [mm]).

[1]The measuring depths were measured from the point at which the head of the multi-probe was sufficiently immersed in the water. This accounts for 13cm, which is the distance from the water surface up to the head of the multi-probe.

Figure 4.3: Vantage Pro 2 Wireless Weather Station (Source: Davis Instruments).

4.2 Numerical model

In Section 2.1.3, the processes involved in the Dissolved Oxygen budget in the surface water are analyzed. These processes can be represented in a conceptual box model as shown in Figure 4.4.

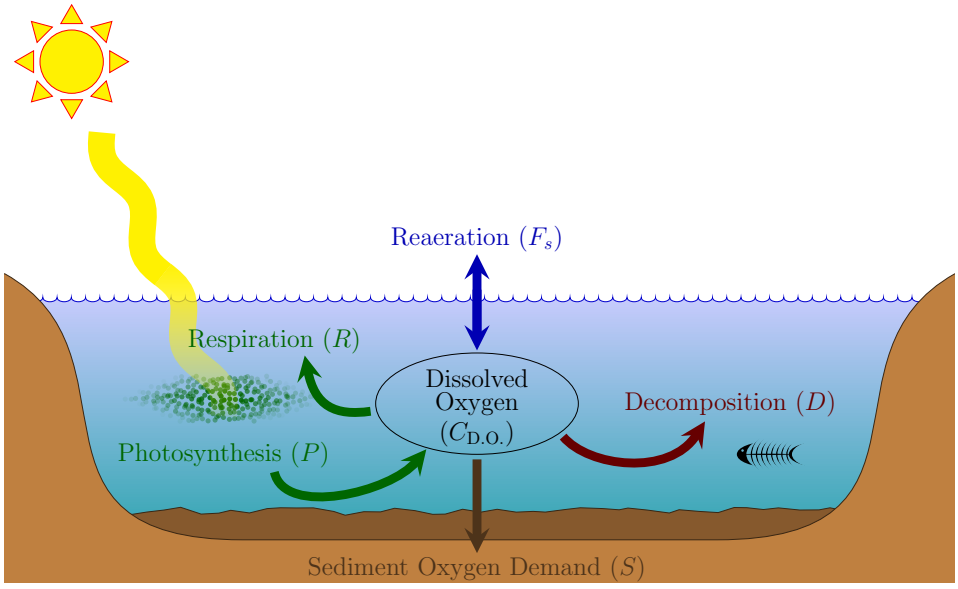

Figure 4.4: Conceptual model of the Dissolved Oxygen budget.

Water quality modelling includes two parts: the *hydrodynamic processes* which describe the way a certain parameter or pollutant is transported in the water body and the *chemical/biological processes*, which describe how this parameter or pollutant is produced (introduced) and consumed in the water body. At this point, we need to introduce the hydrodynamic and the chemical/biological processes involved and how these can be described in a single equation.

The governing equations of a hydrodynamic model include: momentum, continuity, temperature, salinity, turbulence equations, boundary and initial conditions. On the other hand, a water quality model is based on conservation of mass, laws governing chemical/biological processes, boundary and initial conditions. Recalling Figure 4.4, the processes that affect the Dissolved Oxygen levels can be summarized in the following:

1. Dissolved Oxygen is diffused and dispersed within the water column.
2. Reaeration adds Dissolved Oxygen in the system.
3. Biochemical reactions produce or consume Dissolved Oxygen according to a diurnal pattern and the aquatic environment status.
4. Dissolved Oxygen exchanges across the water bed interface.

Apart from the processes described above, there are also others that influence the Dissolved Oxygen levels in the surface water. Such processes are related to the presence of nutrients in water. This however would require a study of the phosphorus and nitrogen cycle as well, which would make our problem more complex. In addition, nutrient analysis requires more detailed measurements than the ones available at the time of this master thesis.

All these processes can be expressed mathematically by a set of coupled mass conservation equations. These equations account for the material that enters/leaves the water body, the transport of material within the water body and all the biochemical interactions that are responsible for the transformations of the material [Ji, 2008], see Figure 4.5. All these can be expressed in the following compact equation [Park et al., 2005]:

$$\frac{\partial C}{\partial t}+\frac{\partial (uC)}{\partial x}+\frac{\partial (vC)}{\partial y}+\frac{\partial (wC)}{\partial z}=\frac{\partial}{\partial x}\left(k_x\frac{\partial C}{\partial x}\right)+\frac{\partial}{\partial y}\left(k_y\frac{\partial C}{\partial y}\right)+\frac{\partial}{\partial z}\left(k_z\frac{\partial C}{\partial z}\right)+S_t\,. \quad (4.1)$$

Where C is the Dissolved Oxygen concentration, [kgm^{-3}], u, v and w are respectively the velocity components on the x, y and z directions, [m/s], k_x, k_y and k_z are the turbulent diffusivities m^2/s], and S_t represents the internal and external sources and sinks per unit volume.

The three last terms on the left hand side (LHS) of (4.1) account for the transport due to advection and the first three terms on the right hand side (RHS) account for diffusion transport. Advection is the result of flow and the properties of the transport substance do not change, see Figure 4.6 (a) and (b). On the other hand, diffusion is the transport of mass due to random water motion or mixing, see Figure 4.6 (a) and (c). Depending on the scale we focus our study on, there are two types of diffusion: (i) molecular diffusion (microscopic scale), which results from the random motion of water molecules and (ii) turbulent diffusion or dispersion (larger scale), which is the result of eddies [Chapra, 1997].

The last term on the RHS of (4.1) represents the kinetic processes and external loads for each of the state variables, in our case the Dissolved Oxygen. It is often that empirical formulations are used to approximate the model sources and sink terms [Ji, 2008]. As a result, there is a variety of mathematical descriptions for the same process. Regarding the Dissolved Oxygen model, a description of the sources and sinks is depicted in Figure 4.7 and is followed by a presentation of their expressions.

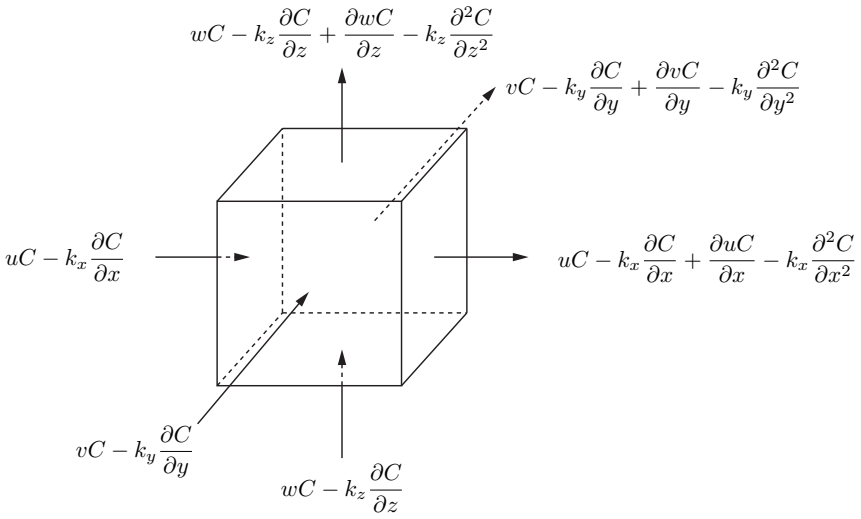

Figure 4.5: Control volume for equation (4.1).

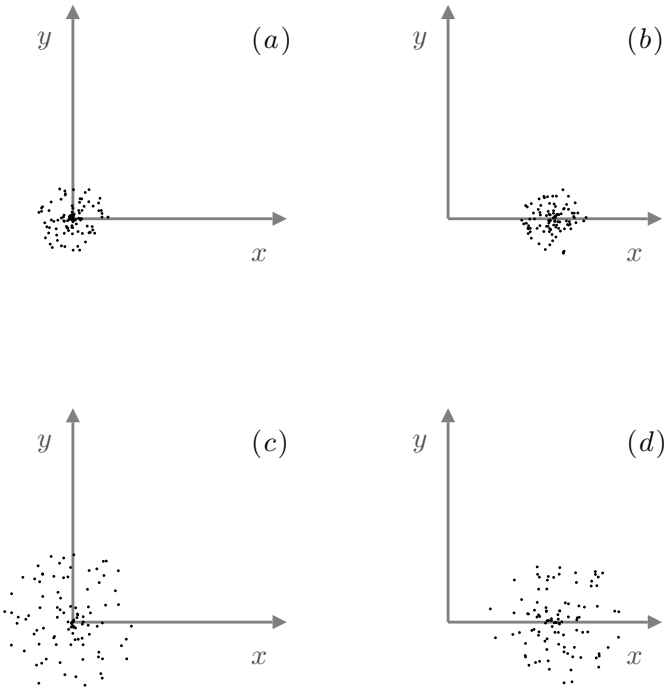

Figure 4.6: Advective and diffusive processes. (a) Initial state, (b) advection, (c) diffusion and (d) advection and diffusion (Source: [Chapra, 1997]).

4.2.1 Introduction of the Source/Sink Terms

4.2.1.1 Photosynthesis (P)

Photosynthesis is an important source of Oxygen in the aquatic ecosystem. It is a metabolic process through which plants convert carbon dioxide (CO_2) and water (H_2O)

Figure 4.7: Sources (blue) and sinks (orange) of Dissolved Oxygen

into carbon compounds and Oxygen (O_2), as can be seen in the simplified equation below:

$$6CO_2 + 6H_2O + \text{light energy} \rightarrow C_6H_{12} + 6O_2\,. \tag{4.2}$$

Photosynthesis depends on temperature, solar radiation and nutrients. In the current model we do not include nutrient limitation. In order to estimate the amount of oxygen produced by photosynthesis the following expression is used, assuming that photosynthesis is a first order kinetic process [Chapra, 1997]:

$$P = r_{\text{oa}} G_{\max} 1.066^{T_{\text{w}}-20} \phi_\ell Chla\,. \tag{4.3}$$

Where r_{oa} is the oxygen production per unit mass of plant biomass, $[\text{mg}O_2(\text{mg}Chla)^{-1}]$, $G_{\max}$ is the maximum plant growth rate for optimal light conditions and excess nutrients, $[\text{d}^{-1}]$, ϕ_ℓ is the attenuation of growth due to light, [-], $Chla$ is the concentration of plant biomass, $[(\text{mg}Chla)\,\text{L}^{-1}]$ and T_{w} is the water temperature, [°C].

The attenuation of growth due to light limitation (ϕ_ℓ) is an important factor in this equation as it indicates the amount of available sunlight at each depth of the water column, ranging between 0 and 1. Light levels determine the maximum depth at which algae can grow. The upper water column portion where light levels are sufficient for algae growth is called euphotic zone. A general rule of thumb says that the depth of this zone is the double of the Secchi disk depth. Therefore, water transparency influences the extent of sunlight penetration, and therefore photosynthesis.

The attenuation of growth due to light limitation can be estimated by the following expressions introduced by [Henderson-Sellers, 1984]:

$$\begin{cases} \phi_\ell = \exp\left(-\dfrac{\tau^2}{2\sigma^2}\right) \\ \tau = \dfrac{\eta z}{\log 2} \\ \eta = \dfrac{\omega}{SD} \\ \sigma = \dfrac{\log I_0 - \log\left(0.5 I_k\right)}{\log 2}\sqrt{\dfrac{2}{\pi}} \\ I_k = 1.5625 T_{\text{w}} \end{cases}. \tag{4.4}$$

Where τ is the optical depth, [m], related to the extinction coefficient η, [m^{-1}], and the depth z, [m], ω is a constant with a range 1.7-1.9 [−] [Chapra, 1997], SD is the Secchi disk depth, [m], T_w is the water temperature, [°C], I_0 is the solar radiation at subsurface depth [$W\,m^{-2}$] and I_k is the limit radiation, [$W\,m^{-2}$]. For water, the subsurface solar radiation is approximately 50% less than the solar radiation at the surface [Medrano, 2008].

The concentration of plant biomass (Chlorophyll-a, $Chla$) can be either measured or given according to the trophic state of the water body. The trophic state of a lake depends on the surface area, the maximum depth and the Secchi disk depth [Stefan et al., 1993]. Table 4.3 presents the range and variety of plant biomass concentrations based on different studies.

Table 4.3: Plant biomass ($Chla$ [$\mu g\,L^{-1}$]) concentrations based on water body trophic state [Henderson-Sellers, 1984].

Trophic State	[Sakamoto, 1966]	[National Academy of Sciences, 1972]	[Dobson et al., 1974]	[USEPA, 1974]	[Rast and Lee, 1983]
Oligotrophic	0.3-2.5	0-4	0-4.3	<7	0-2
Mesotrophic	1-15	4-10	4.3-8.8	7-12	2-6
Eutrophic	5-140	>10	>8.8	>12	>6

4.2.1.2 Reaeration (F_s)

Reaeration is the second major source of oxygen in the water body and corresponds to the transfer of oxygen across the water surface. Compared to photosynthesis, this process takes place throughout the day. The rate of diffused oxygen in the water body depends on the oxygen levels of the water body and the saturated oxygen levels. Typically, natural water oxygen levels are below saturation. However, when photosynthesis takes place during the daytime, pure oxygen is produced and the oxygen levels can be above the saturation levels. In that case, oxygen is transferred to the atmosphere by the water body. The equation used for the reaeration is given by the following equation, [Riley and Stefan, 1988, Stefan and Fang, 1994, Chapra, 1997]:

$$\begin{cases} F_s = k_a\,(C_{sat} - C) \\ k_a = \dfrac{k_l}{\Delta z_s} \\ C_{sat} = 14.652 - 0.4102\,T_w + 7.99 \times 10^{-3}\,T_w^2 - 7.774 \times 10^{-5}\,T_w^3 \end{cases} . \tag{4.5}$$

Where k_a is the reaeration rate, [d^{-1}], k_l is the oxygen transfer coefficient, [$m\,d^{-1}$], Δz_s is the thickness of surface layer, [m], C_{sat} is the saturated oxygen concentration, [$mg\,L^{-1}$], C is the current oxygen concentration, [$mg\,L^{-1}$], and T_w is the water temperature, [°C]. Note that for a 0D model, Δz_s is the whole water depth, H. For a 1D model, Δz_s corresponds to the thickness of the top discretization cell Δz.

The oxygen transfer coefficient for lakes can be estimated as a function of wind speed by a number of formulas. A widely used formula for the determination of the reaeration coefficient is the one introduced by [Banks and Herrera, 1977], see equation below.

$$k_l = 0.728\, U_{\mathrm{w}}^{0.5} - 0.317\, U_{\mathrm{w}} + 0.0372\, U_{\mathrm{w}}^2\,. \tag{4.6}$$

Where U_{w} is the wind speed measured at 10m height [m/s].

This expression includes various wind dependencies in order to characterize the different turbulence regimes that take place at the air-water interface [Chapra, 1997]. For high wind speed the second order expression becomes dominant as can be seen in Figure 4.9.

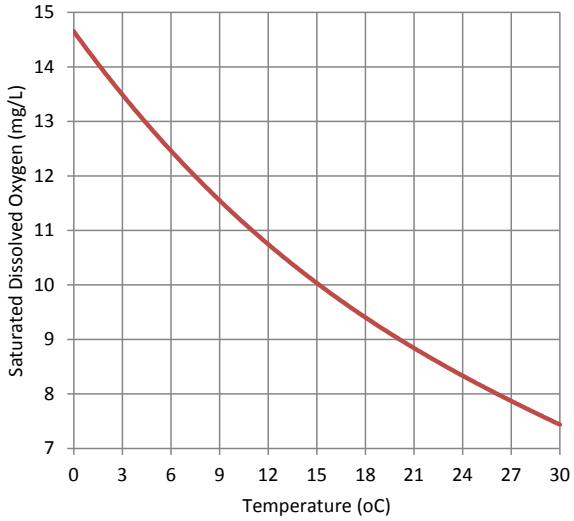

Figure 4.8: Relation of oxygen saturation and temperature.

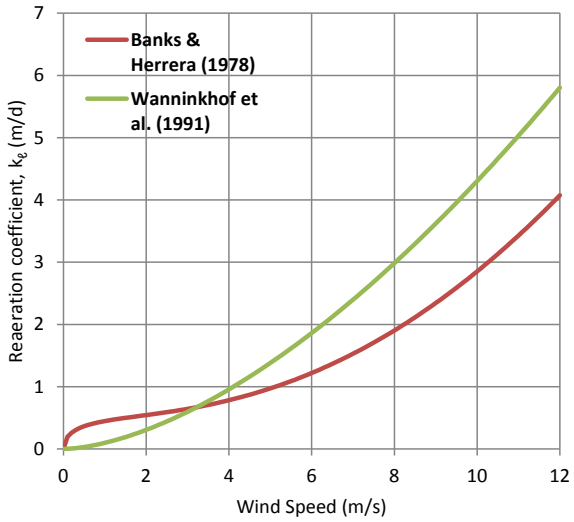

Figure 4.9: Comparison of wind dependant reaeration coefficient formulas.

Lake oxygen transfer formulas have both theoretical and empirical expressions. An empirical expression based on gas tracer experiments in lakes by [Wanninkhof, 1992] is given

by:

$$k_l = 0.108\, U_{\mathrm{w}}^{1.64} \left(\frac{S_{\mathrm{c}}}{600} \right)^{0.5} . \tag{4.7}$$

Where S_{c} is the Schmidt number[2], [-], which for oxygen transfer in lakes is taken as 500 [Chapra, 1997].

As can be seen from Figure 4.9, for wind speeds up to 5m/s the two formulas show small differences but for higher wind speeds they diverge.

4.2.1.3 Respiration (R)

Respiration can be considered as the reverse process of photosynthesis, by which the organic matter in the water body is transformed into inorganic matter by consuming oxygen (O_2) and releasing carbon dioxide (CO_2). Respiration occurs during day and night. Assuming that respiration is a first order kinetic process and that it is related only to the concentration of plant biomass ($Chla$) and water temperature (T_{w}), the following expression gives the consumption of oxygen by respiration [Stefan and Fang, 1994].

$$R = \frac{1}{\mathrm{YCHO2}}\, k_{\mathrm{rs}} \theta_{\mathrm{rs}}^{(T_{\mathrm{w}}-20)} Chla\,. \tag{4.8}$$

Where $YCHO2$ is the ratio of mg of plant biomass to mg of oxygen used in respiration, [-], k_{rs} is the respiration rate coefficient, [d^{-1}], θ_{rs} is the temperature adjustment coefficient [-], $Chla$ is the concentration of plant biomass, [(mg$Chla$)/L], and T_{w} is the water temperature, [$^{\mathrm{o}}$C].

4.2.1.4 Decomposition (D)

Decomposition is a diurnal process and indicates the amount of oxygen that is required for the degradation of organic matter. Decomposition is assumed to be a first order kinetic process and is expressed as [Stefan and Fang, 1994]:

$$D = k_{\mathrm{b}} \theta_{\mathrm{b}}^{(T_{\mathrm{w}}-20)} BOD\,. \tag{4.9}$$

Where k_{b} is the first order decay coefficient, [d^{-1}], θ_{b} is the temperature adjustment coefficient, [-], BOD is the Biological Oxygen Demand, [mg/L], and T_{w} is the water temperature, [$^{\mathrm{o}}$C].

[2]The Schmidt number, S_{c}, is a dimensionless parameter representing the ratio of diffusion of momentum to the diffusion of mass in a fluid.

4.2.1.5 Sediment Oxygen Demand (S_{d})

The Sediment Oxygen Demand (SOD) is the amount of oxygen that the organic matter in the benthic sediment consumes, is given by [Stefan and Fang, 1994]:

$$S = \left(\frac{1}{\Delta z_{\mathrm{b}}}\right) S_{\mathrm{b}} \theta_{\mathrm{s}}^{T_{\mathrm{w}}-20}. \tag{4.10}$$

Where Δz_{b} is the thickness of the bottom water layer, [m], S_{b} is the sediment oxygen demand at 20°C, [gO_2 m^{-2} d^{-1}], θ_s is the temperature adjustment coefficient, [-], and T_{w} is the water temperature, [°C]. Note that for a 0D model, Δz_{b} is the whole water depth, H. For a 1D model, Δz_{b} corresponds to the thickness of the bottom discretization cell Δz.

4.2.1.6 Range of rates and constants for kinetic equations

The ranges for the rates and constants for the kinetic Equations 4.3, 4.8, 4.9 and 4.10 are given in Table 4.4 [Bowie and Tech, 1985, Stefan and Fang, 1994, Chapra, 1997, Ji, 2008, D-Water Quality, 2013]. As we can see, the parameters that are related to the consumption ($YCHO2$, k_{rs}, k_{b} and S_{b}) and production (r_{oa} and $G_{\max}$) have the largest ranges of values. This happens because these values are established by measurements in lakes with various trophic states and morphology.

4.2.1.7 Water temperature

Water temperature plays an important role in the Dissolved Oxygen budget by regulating the oxygen saturation levels and the rate of biochemical reactions. Furthermore, it regulates the development of stratification, which is discussed in Section 2.1.3. Throughout the measurement campaign (31$^{\mathrm{st}}$ of July to 23$^{\mathrm{rd}}$ of September), water temperature was measured with the Hydrolab multi-probe and the divers. However, the continuous water temperature monitoring (divers) was only available for the month of September.

Continuous data are a useful input parameter for the mathematical model described above. Therefore, it is essential to introduce a method for obtaining continuous water temperature data also for the month of August. The one dimensional heat equation in the vertical direction given by [Henderson-Sellers, 1984, Antonopoulos and Gianniou, 2003] shows that an increase in the net heat flux corresponds to an increase to the water temperature:

$$A\frac{\partial T_{\mathrm{w}}}{\partial t} = \frac{\partial}{\partial z}\left(Ak_z\frac{\partial T_{\mathrm{w}}}{\partial z}\right) - \frac{1}{\rho c_p}\frac{\partial (Aq)}{\partial z}. \tag{4.11}$$

Where T_{w} is the water temperature, [°C], A is the surface, [m^2], q is the internal distribution of solar radiation, [cal m^{-2}d^{-1}], k_z is the coefficient for diffusivity, [m^2/d], ρ is the water density, [kg/m^3], and c_p is the specific heat of water, [cal °C^{-1}kg^{-1}].

Table 4.4: Range of rates and constants for kinetic equations.

Parameter	Description	Values	Unit
r_{oa}	Oxygen production per unit mass of plant biomass	40.0-300.0	mgO_2/mg$Chla$
$G_{\max}$	Maximum plant growth rate for optimal light conditions and excess nutrients	1.5-3	d^{-1}
$YCHO2$	Ratio of mg of Chlorophyll-a to mg of oxygen used in respiration	0.003-0.01	mg$Chla$/mgO_2
k_{rs}	Respiration rate coefficient	0.02-0.6	d^{-1}
θ_{rs}	Temperature adjustment coefficient for respiration	1.08, 1.045, 1.047	-
k_{b}	Decomposition rate coefficient	0.02-3.4	d^{-1}
θ_{b}	Temperature adjustment coefficient for decomposition	$\begin{cases} 1.047, & T > 20^{\text{o}}\text{C} \\ 1.130, & 4^{\text{o}}\text{C} < T < 20^{\text{o}}\text{C} \end{cases}$	-
BOD	Biological Oxygen Demand	1-3	mg/L
S_{b}	Sediment oxygen demand at $T = 20^{\text{o}}\text{C}$	0-8.4	gO_2m^{-2}d^{-1}
θ_{s}	Temperature adjustment coefficient	$\begin{cases} 1.065, & T \geq 10^{\text{o}}\text{C} \\ 1.130, & T < 10^{\text{o}}\text{C} \end{cases}$	-

A simpler empirical approach to the heat equation is presented by [Kettle and Thompson, 2004]. In their model they assume the lake surface temperature is predominately controlled by the local air temperature and therefore is described by:

$$\frac{\mathrm{d}T_\mathrm{w}}{\mathrm{d}t} = k\left(T_\mathrm{a} - T_\mathrm{w}\right) . \tag{4.12}$$

Where T_w is the lake water surface temperature, [°C], k is a constant heat exchange coefficient [d^{-1}], and T_a is the local air temperature, [°C].

This equation can be numerically solved after time integration, resulting in an exponentially smoothed water temperature ($T_{\mathrm{w},t}$):

$$T_{\mathrm{w},t} = \left(1 - e^{-k\Delta t}\right) T_{\mathrm{a},t} + e^{-k\Delta t} T_{\mathrm{w},t-\Delta t} . \tag{4.13}$$

Comparing Equations 4.11 and 4.12 we see that the second one is a zero dimensional approximation, therefore it does not account for the diffusion of temperature, and furthermore it does not account for variations of internal distribution of heat fluxes and temperature. The fact that the internal distribution of net heat fluxes is considered to have a constant value limits the daily variation of the water temperature. Later on, in the results sections, we will see that the vertical profile of the water temperature did not have large variations. Therefore, the estimated water temperature from (4.12) can be applied. Appendix A presents the calibration and validation of the air to water temperature conversion.

4.2.2 Zero dimensional model

Zero dimensional models assume that the water body is well mixed, no water fluxes exist and the output of the model is the averaged Dissolved Oxygen evolution in time. Based in these assumptions, the general equation for the Dissolved Oxygen, see (4.1), is simplified:

i. The three terms on the LHS of (4.1), page 24, which represent the advection transport are zero, since advection does not exist due to the assumption of no spatial variation.

ii. The three terms that represent the diffusion are also zero because we have no spatial variation, the system is assumed to be well.

Therefore, the temporal variation of Dissolved Oxygen in a zero dimensional model is equal to the sources/sink terms. The general expression of the zero dimensional model is given by:

$$\frac{\mathrm{d}C}{\mathrm{d}t} = P + F_\mathrm{s} - D - R - S_\mathrm{d} . \tag{4.14}$$

Where P is the photosynthesis term, [mg/(Ld)], F_s is the reaeration term, [mg/(Ld)], D is the decomposition term, [mg/(Ld)], R is the respiration term, [mg/(Ld)], and S_d is the sediment oxygen demand term, [mg/(Ld)].

The advantages of working with a zero dimensional model were analyzed in Section 2.3.2, page 11. In this case, we work with a control volume in which the average values over the water column are calculated. This is the initial step of our methodology in order to obtain a preliminary understanding of the physical and biochemical processes involved in the Dissolved Oxygen budget.

4.2.3 One dimensional model

In order to evaluate the evolution of Dissolved Oxygen in space and the effect of the floating houses, we need to consider a more elaborate model than the zero dimensional. In the one dimensional model the term associated to the vertical component of the diffusion transport is included. Therefore the advantage of the one dimensional model is that it combines the transport of Dissolved Oxygen within the water column with the production and consumption of Dissolved Oxygen by the biochemical equations described above. In the current thesis we chose to work on the vertical direction, which enables studying:

i. The stratification effect of Dissolved Oxygen.

ii. The dispersion of Dissolved Oxygen within the water column by the influence of wind.

Therefore, the general (4.1) is rewritten as:

$$\frac{\partial C}{\partial t} = \frac{\partial}{\partial z}\left(k_z \frac{\partial C}{\partial z}\right) + P + F_\mathrm{s} - D - R - S_\mathrm{s}\,. \tag{4.15}$$

Where k_z is coefficient of vertical diffusivity on the vertical profile [m^2/d], and the remaining quantities are as in (4.14).

Vertical diffusion accounts for both molecular and turbulent diffusion (dispersion). The diffusion in the vertical direction is directly related to the stratification of the water body [Bella, 1970], and it is larger at the epilimnion where wind mixing is more effective [Stefan and Fang, 1994]. Although the molecular diffusion is smaller than the thermal diffusivity in water ($2.1 \times 10^{-9}\mathrm{m}^2/\mathrm{s}$ to $1.43 \times 10^{-7}\mathrm{m}^2/\mathrm{s}$, at 25°C) [Cussler, 2009] the waves, seiches induced by the wind as well as the natural convention, result in a turbulent diffusion much larger than the molecular one [Stefan et al., 1993]. The mechanisms of heat transfer and turbulent diffusion are therefore similar [Geankoplis, 1984] and it is usual that the diffusion coefficient of the Dissolved Oxygen models is considered to be identical to the thermal diffusivity [Antonopoulos and Gianniou, 2003].

[Stefan et al., 1993] estimate the vertical diffusion coefficient k_z by the expressions:

$$\begin{cases} k_z &= 7.59 A^{0.56} \left(N^2\right)^{-0.43} \\ N^2 &= -\dfrac{g}{\rho}\dfrac{\mathrm{d}\rho}{\mathrm{d}z} \end{cases}. \tag{4.16}$$

Where A is the surface of the lake, [m^2], N^2 is stability frequency of stratification, [d^{-2}], g is the standard acceleration due to gravity, [m/d^2], and ρ is the density of water, [kg/m^3]. Typical maximum values for the lake hypolimnion of 0.0864 to 1.728 m^2/d were used in the one dimensional model by [Stefan and Fang, 1994].

Chapter 5

Field Measurement Results

This chapter presents the results from the measurements. The collected data from the field measurements will be used to give a preliminary answer to the main research question, i.e., *Do the floating houses have an effect on Dissolved Oxygen levels* and to which processes can we attribute these changes. Although in the measurement plan we indicated four measuring locations, the data analysis mainly refers to the positions that represent the open space (measuring location C) and the floating houses (measuring locations B and D).

The field measurements data are treated in different ways. The vertical profile of the raw data (daily and averaged) of the field measurements is used for estimating the variation of Dissolved Oxygen and water temperatures. We focus in particular on the depth profiles and on the differences between the locations. Finally, in order to establish a relation between the Dissolved Oxygen levels at the measurement locations, a linear correlation is implemented.

After establishing the differences in Dissolved Oxygen at the different measurement locations, a primary investigation on the reasons underlying these differences is done. The influence of the available solar radiation, sun trajectory and wind speed on the diurnal Dissolved Oxygen pattern, the Dissolved Oxygen levels and water temperature differences between the floating houses (locations B and D) and open space (location C), and the differences between the Dissolved Oxygen at the surface and the bottom will be investigated.

5.1 Field Measurements

5.1.1 Weather conditions in Harnaschpolder

The summer of 2013 in the Netherlands was characterized as dry and sunny, see Figure 5.1, however the spring was the coldest since 1970. In the beginning of the measurement campaign there was a heat wave (21^{st} -27^{th} of July), see Figure 5.2. September continued

to be warm and dry in the first third of the month. The total average rainfall in The Netherlands in 2013, was 106 mm less than the average of 827mm [KNMI, 2013]. An overview of the monthly averaged temperature, wind speed and total rainfall is given in Table 5.1. The prevailing wind orientation for the measurement period was West for July and SouthWest for August and September, see Figure 5.3.

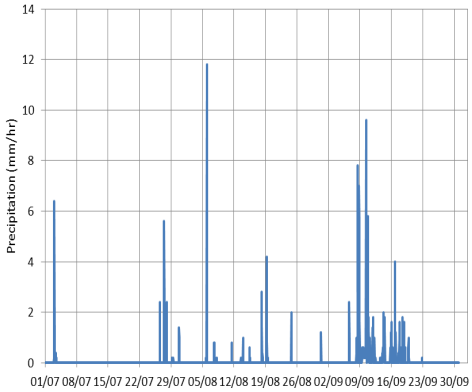

Figure 5.1: Precipitation during the measurement campaign.

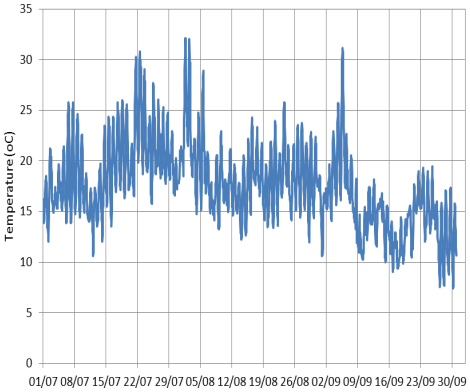

Figure 5.2: Air temperature during the measurement campaign.

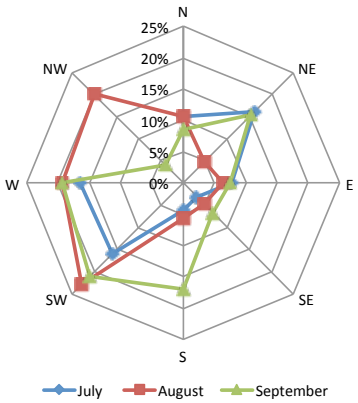

Figure 5.3: Wind Direction during measurement campaign.

Furthermore, the collected weather conditions, namely the air temperature, solar radiation and wind speed will be used as input parameters for the numerical simulation of the Dissolved Oxygen budget. This information is important because it influences the processes involved in the Dissolved Oxygen budget, i.e. the photosynthesis and reaeration.

5.1.2 Dissolved Oxygen

The distribution of Dissolved Oxygen across the vertical profile is homogeneously distributed in most of the measurement days. However, days with Dissolved Oxygen stratification did occur (2^{nd} of August, 5^{th} and 23^{rd} of September), see Figure 5.4. As a

Table 5.1: Weather conditions during the measurement campaign.

Month	Temperature (°C)			Wind Speed Average (m/s)	Total Rainfall (mm)
	Minimum	Average	Maximum		
July	10.3	19.4	31	2.9	29.4
August	11.8	18.7	32.5	2.6	36.4
September	7.3	14.8	31.4	3.0	123.2

result of the water body morphology, a shallow pond with a maximum depth of 2.5m, the developed stratifications did not last for a long period

Furthermore, days with large Dissolved Oxygen differences between the top and bottom layer were observed in the 6th, 21st and 23rd of August. These differences are due to a rapid drop of Dissolved Oxygen levels in the lower 1m of the water column, as can be seen in seen in Figure 5.4. Since Dissolved Oxygen production is a process directly influenced by solar radiation, the Dissolved Oxygen stratification is mainly attributed to the diurnal process of photosynthesis. Finally, the measurement point located at the shallowest region (location A) is the only one that did not develop low Dissolved Oxygen levels (less than 2 mg/L) and has the smallest differences between the Dissolved Oxygen on the top and bottom. This occurs because at location A the depth of the water column is only 1.4m as opposed to the 2.5m at locations B, C and D.

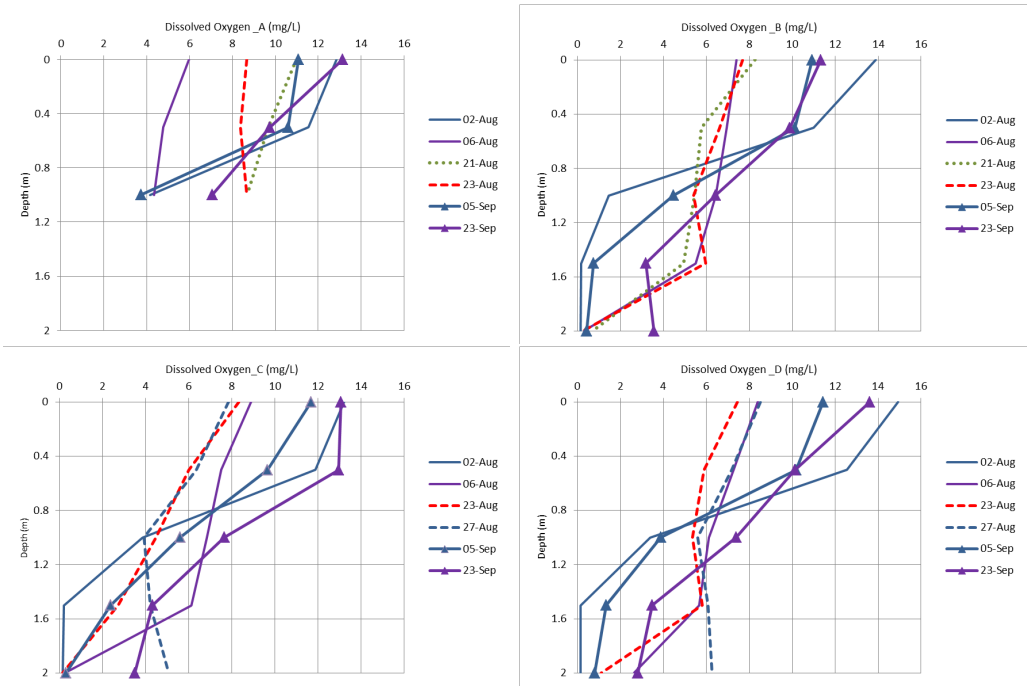

Figure 5.4: Dissolved Oxygen vertical profiles.

The following remarks can be identified by analysing the averaged vertical profile of Dissolved Oxygen, see Figure 5.5:

- The average values of the vertical profile show that during the measurement period the location situated between the floating houses (location B) showed the lowest values up to the first 1m.
- The levels of Dissolved Oxygen between the floating houses (location B) show a reduction of 10% (1 mg/L) in comparison to the open space (location C)
- The rate of change of Dissolved Oxygen with depth (gradient) can be up to 60% ($2.5 mgL^{-1}m^{-1}$, location C).

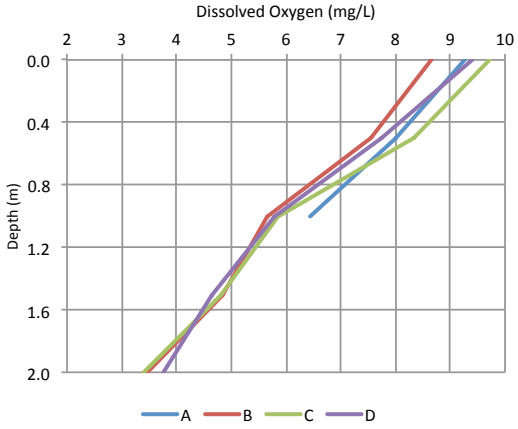

Figure 5.5: Averaged vertical profile of Dissolved Oxygen.

The differences observed, especially regarding the Dissolved Oxygen, show that the floating houses generate an effect, but this effect is low (∼10%). Moreover, we observe that the Dissolved Oxygen has vertical variations. Therefore, modelling the vertical profile will give us essential information regarding the effect of the floating houses on the Dissolved Oxygen levels.

As seen above, there are differences in the Dissolved Oxygen between the locations close to the floating houses (B and D) and the open space (C). A better demonstration of these differences is shown in Figure 5.6. In this figure we show the correlation between the measure data of two locations (B vs C, D vs C and D vs B) for two depth intervals (0-1.0 m and 1.5-2.5m). The fitting curves indicate lower oxygen levels close to the floating houses (locations B and D) compared to the open space (location C). Moreover, these differences in the oxygen levels are more obvious in the upper part of the water column (0.0m to 1.0m) than in the lower part (1.5m to 2.0m). Nevertheless, the oxygen difference in the upper layer of the water column are not significant and are more recognisable for the position between the two floating houses (B), which is the most enclosed one.

5.1.3 Temperature

The distribution of temperature across the vertical direction was homogeneously distributed and the observed trends were similar for all the measurement locations, as can

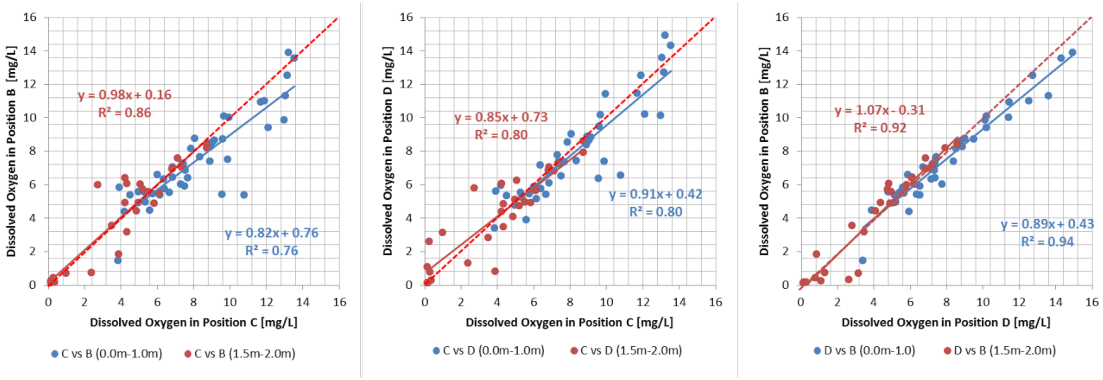

Figure 5.6: Dissolved Oxygen correlations between the positions B, C and D for 0.0m to 1.0m depth and 1.5m and 2.0m depth (left to right).

be seen in Figure 5.7. Thermal stratification was observed on the days of 2nd of August and 5th and 23rd of September. However, as was explained for the Dissolved Oxygen, due to the shallow character of the water body, the developed thermal stratification did not last for a long period. Furthermore, the observed temperature differences between the top and bottom of the measurements points, see Table 5.2, and the average temperature profile, see Figure 5.8, show that during the measurement period the temperature was in most of the days homogeneously distributed.

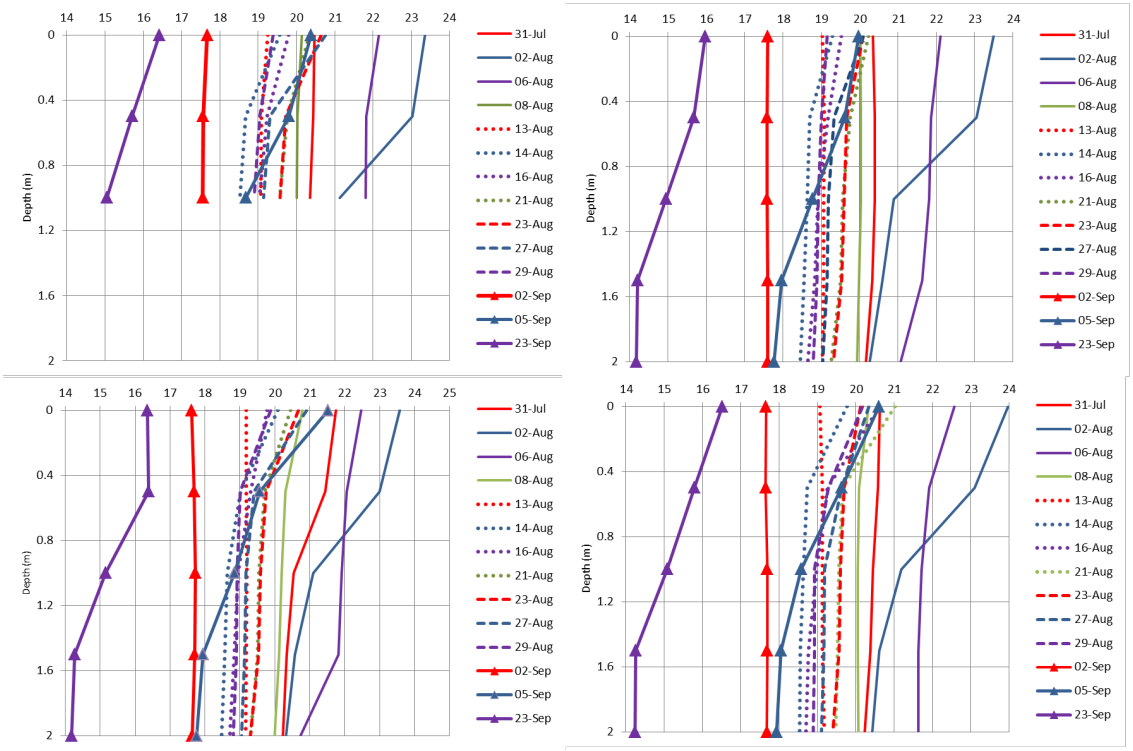

Figure 5.7: Vertical temperature profiles for measurements points A, B, C and D (right to left, top to bottom).

Analysing the average temperature vertical profile, see Figure 5.8, the following are

Table 5.2: Temperature differences [°C] between the top and bottom layer.

Date	A	B	C	D
31-Jul	0.12	0.19	1.52	0.40
02-Aug	2.23	3.22	3.26	3.54
06-Aug	0.35	1.05	1.74	0.94
08-Aug	0.14	0.09	0.78	0.26
13-Aug	0.19	0.00	0.02	-0.13
14-Aug	1.03	0.84	1.61	1.24
16-Aug	0.77	0.88	1.07	1.93
21-Aug	0.78	0.98	1.15	1.54
23-Aug	1.08	0.78	1.37	0.72
27-Aug	1.61	1.06	1.86	1.23
29-Aug	0.48	0.36	1.08	1.28
02-Sep	0.12	-0.01	-0.01	-0.03
05-Sep	1.71	2.22	3.77	2.67
23-Sep	1.36	1.79	2.17	2.27

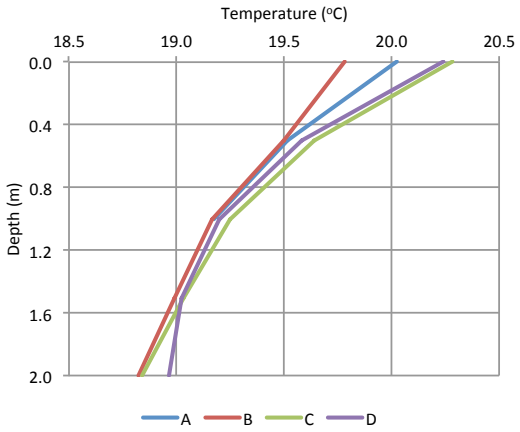

Figure 5.8: Averaged vertical profile of Temperature.

important to remark:

- The average values of the vertical profile show that during the measurement period the location situated between the floating houses (location B) showed the lowest temperatures up to the first 1m.
- The average water temperature between the floating houses (location B) is 2.5% (0.5°C) lower than the open space (location C).

- The maximum rate of change of water temperature with depth (gradient) is 5% (0.4°C/m, location C).
- The average temperature difference in depth is 1.25°C and per location 0.5°C, which correspond to saturated Dissolved Oxygen differences of 0.21mg/L and 0.09mg/L, respectively.

We see that the temperature of the water is not characterized by a large variation in depth and differences between the measuring locations. Therefore, we can assume that the water temperature is the same for the whole depth and the different measuring locations. Thus, we can apply the simple empirical equation (4.13), page 32, to estimate the water temperature from air temperature for the days we have no available water temperature data.

More detailed temperature data were obtained by the installation of the divers at the final part of the measurement campaign. These data give a better insight to the temperature profile because they measured temperature continuously for 19 days. The temperature measured by the divers was corrected using the probe temperature as the reference measurement. The procedure is explained in the Appendix C.

In general, the divers temperature measurements show that location B has lower values than location C, see Figure 5.9 where the negative temperature differences are predominant. Particularly, the upper part of the water column shows a larger difference between location B and C than the bottom part. However, in the first period of the measurements (4^{th} to 8^{th} of September) we can identify the opposite behaviour, where location B has higher temperatures than location C. This can be explained by taking into account the ambient temperature during this period. As can be seen in Figure 5.2, page 36, the ambient temperature starts to increase on the 1^{st} of September, reaches a peak on the 5^{th} of September (8.9°C higher) followed by a steady decrease up to the 9^{th} of September (11.6°C lower). The starting date of the measurements with the divers (4^{th} of September) coincides with the peak and captures the quick drop of the ambient temperature. This positive difference in temperatures between the position B and C is due to the fact that the water in position C adjusts faster to the changes of the ambient temperature than position B. A possible reason behind this slower temperature adaptability of point B can be the fact that it is situated between the two floating houses, a more confined area than position C. The much faster drop in temperature differences that we observe in Figure 5.9 after reaching the peak, can be attributed to the rain that occurred in that period, see Figure 5.1, page 36.

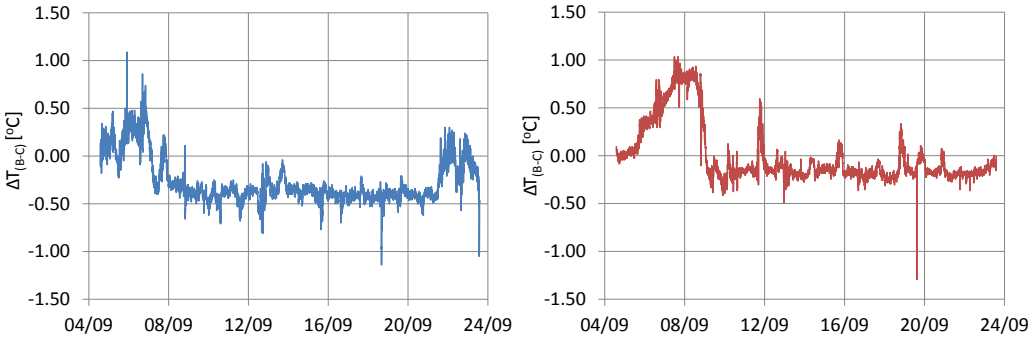

Figure 5.9: Corrected temperature differences for the divers between points B and C for depths 0.7m (left) and 2.0m (right).

5.1.4 Secchi disk depth

Throughout the measurement period the water transparency (Secchi Disk depth) ranged between 28 and 32cm, with an average value of 28cm, see Figure 5.10. This value is used to estimate the approximate depth up to which light penetration occurs, and consequently photosynthesis is active. As a rule of thumb, this penetration depth is equal to the double of the water transparency depth [Hasadsri and Maleewong, 2012]. Therefore, it is expected that the upper 56cm of the water column will be influenced by light penetration.

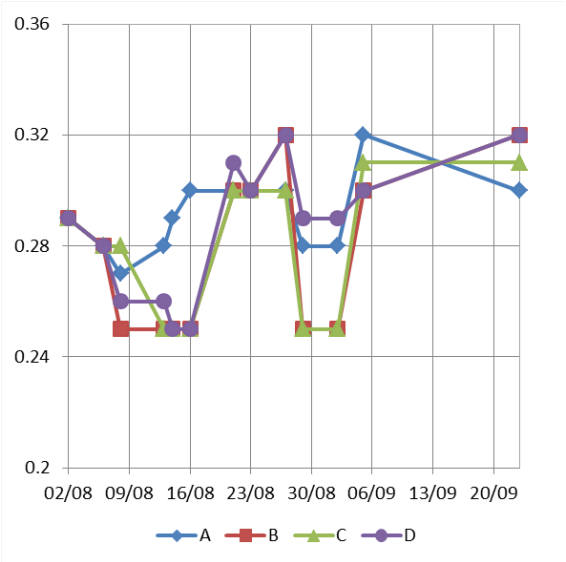

Figure 5.10: Secchi disk depth measurements.

5.1.5 Discussion of field measurements

This part analyses which physical property (temperature) or weather conditions (solar radiation and wind) may be responsible for the observed Dissolved Oxygen differences.

5.1.5.1 Temperature

Temperature is the first cause to be analysed. As it was mentioned before, temperature is important for water quality because it regulates the biochemical reactions and determines the ability of water to withhold the available Dissolved Oxygen. As we observed in the vertical temperature profile, Figure 5.8, the temperature variations in depth and between locations are small. A relation between the temperature differences and the Dissolved Oxygen differences between the floating houses and the open space are presented in Figure 5.11. From this correlation we see that the temperature differences are mostly zero while the Dissolved Oxygen differences range from approximately -5 to 3mg/L. It is clear that the cause of these Dissolved Oxygen differences lies in a different physical property or weather condition. Given the fact that the majority of the measurements took place during daytime, the differences in Dissolved Oxygen can be attributed to the contribution of photosynthesis.

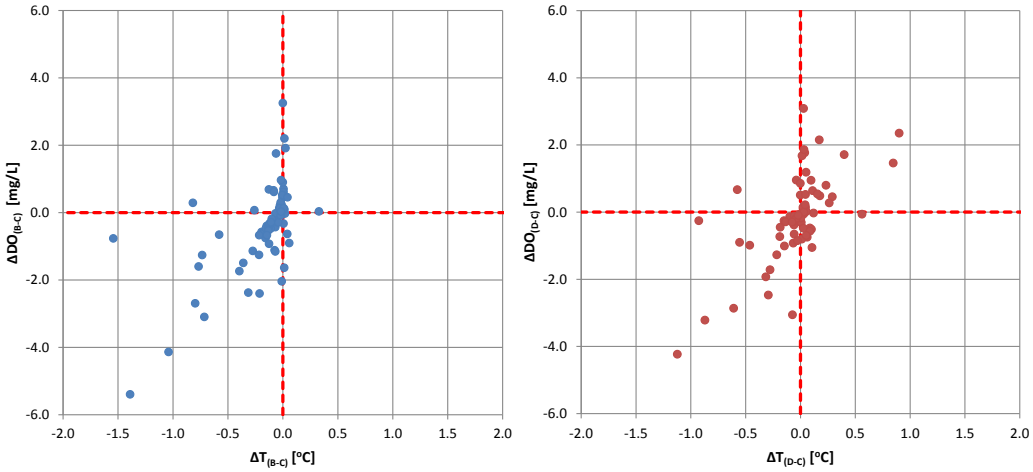

Figure 5.11: Dissolved Oxygen and Temperature differences correlation, B-C (left) and D-C (right).

5.1.5.2 Solar Radiation

On the 31st of July and 2nd of August four measurements were performed in each day. With these results the diurnal pattern of Dissolved Oxygen and temperature was plotted, see Figure 5.12. On the 31st of July temperature stratification took place. On the other hand, Dissolved Oxygen was initially equally distributed along the vertical profile and began to deviate during the day. The first 0.5m of the water column displays more diurnal variation than the deeper points. This behaviour coincides with the fact that light penetration, therefore photosynthesis, is predominant in the first 0.56m of the water column, which is the double of the measured Secchi disk depth. The largest Dissolved Oxygen deviation occurred at 14:00pm. This difference can be attributed to the fact that the open space (location C) was more exposed to solar radiation than the floating houses (location B). Finally, at the end of the day (18:00pm and 21:00pm) the Dissolved Oxygen content did not differ significantly, apart from the lower part of the water column where the Dissolved Oxygen content was less than the one at 10:00am.

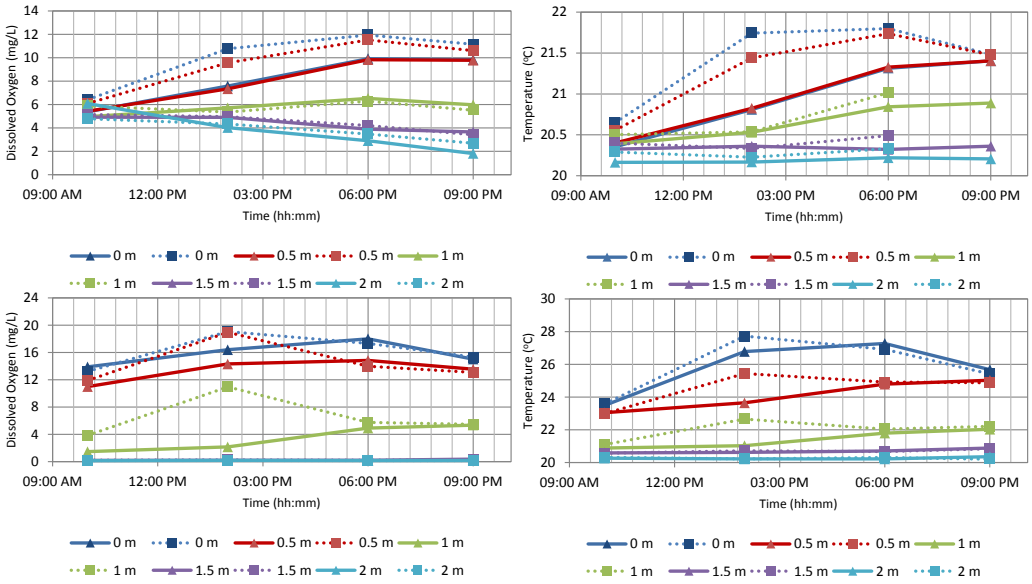

Figure 5.12: Diurnal Patterns of Dissolved Oxygen and temperature 31st of July (top) and 2nd of August (bottom), (solid line: floating houses, dotted line: open space).

On the 2nd of August, thermal and Dissolved Oxygen stratification occurred, with a large deviation on the upper layers of the water column but almost no changes on the lower layers. Also here we observe the largest differences to occur at 14:00pm. However, after 18:00pm the two locations have similar Dissolved Oxygen contents, especially below the 0.5m. Furthermore, it is interesting to see that although the initial temperature distributions in the two locations (open surface and between floating houses) are almost equal, the Dissolved Oxygen distribution exhibits different concentrations, especially for the depth of 1m, see Figure 5.12.

The observations regarding the diurnal pattern of Dissolved Oxygen and temperature can be summarized as follows:

- The lower parts (1.5 and 2.0m) of the water column at locations B and C have similar behaviour.
- The upper parts (0.0 and 0.5m) of the water column start with approximately the same Dissolved Oxygen concentration and temperature but in the course of the day the open space location gains more oxygen than the floating houses location.
- In the end of the day, the two locations have approximately the same Dissolved Oxygen and temperature.

This shows that there is an impact from the sunlight or lack of it.

5.1.5.3 Wind Speed

Wind speed is a factor that can affect the Dissolved Oxygen of the water column. This occurs mainly by two processes, firstly by reaeration and secondly by turbulence (mixing).

The study of the influence of wind speed on Dissolved Oxygen mixing within the water column is presented in Figure 5.13. In these figures we can see that the Dissolved Oxygen gradient ([mgO_2/(Lm)]) becomes smaller with higher wind speeds. However, due to the small amount of data, a concrete conclusion cannot be drawn from this plot. A general remark is that the floating houses (location B) show a smaller gradient than the open space (location C) on the first 0.5m, Figure 5.13 left, which indicates better mixing.

Additionally, it is expected that the presence of floating houses will result in two phenomena: wind tunnel and wind blocking. Based on the orientation of the floating houses (SW, 225 degrees) and the location of the measuring point B, it is expected that wind tunnel effect occurs for SW (225 degrees) and NE (45 degrees) wind directions. On the other hand, wind blocking will appear for SE (135 degrees) and NW (315 degrees) wind directions. Figure 5.14 shows the relation of the Dissolved Oxygen gradient and wind orientation. Due to the small amount of the available data a concrete conclusion cannot be made also in this case.

Finally, in both cases, the measurements took place during the daytime where photosynthesis is the major contributor of Dissolved Oxygen production and interferes with the Wind effect. This increases the difficulty of isolating the impact of these two factors.

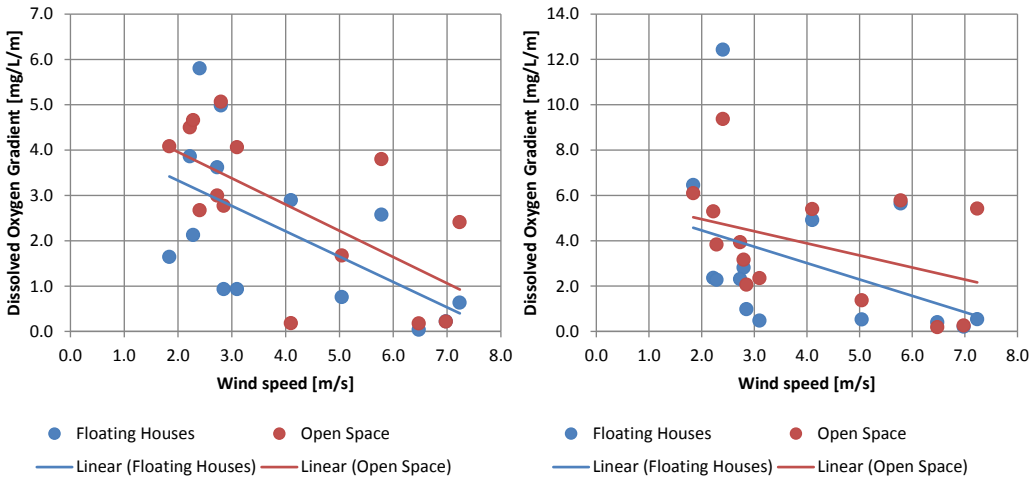

Figure 5.13: Dissolved Oxygen differences on the first 0.5m (left) and 1.0m (right) of the water column with respect to wind speed.

Additionally, during the measurement period it was observed that in the area between the floating houses the wind was creating turbulence on the water and therefore we think that in that position we have a better mixing. In order to check this assumption the vertical temperature differences in the two positions, floating houses and the open space, are plotted against wind speed, see Figure 5.15.

As can be observed in Figure 5.15, for the higher wind speeds we have a smaller dispersion of temperature differences. Regarding the different positions and the mixing, we observe that the location between the floating houses has more clustered results in the lower wind speeds. Therefore, it appears that the latter is experiencing more mixing by the wind compared to the open water surface. For example, for a wind speed of 6m/s, the maximum temperature differences are 2°C and 2.8°C for the floating houses and the open space respectively.

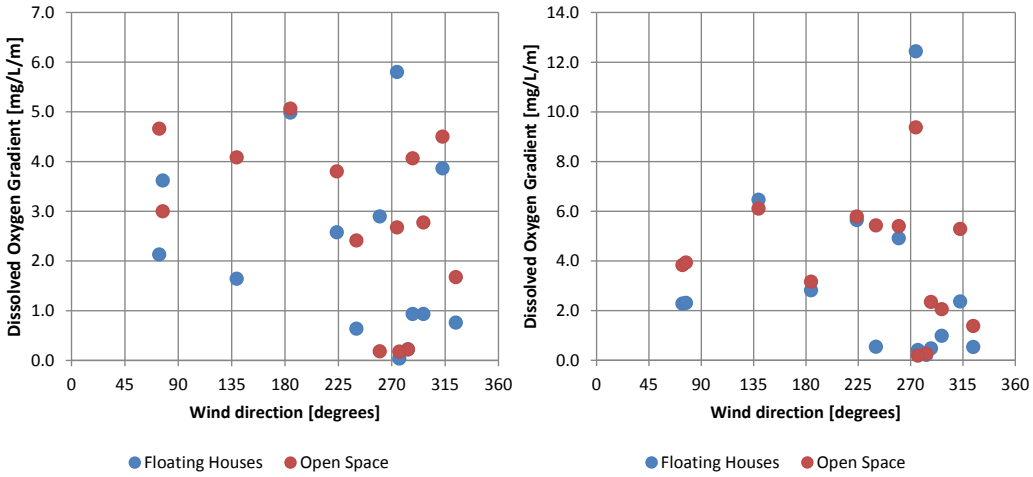

Figure 5.14: Dissolved Oxygen differences on the first 0.5m (left) and 1.0m (right) of the water column with respect to wind direction.

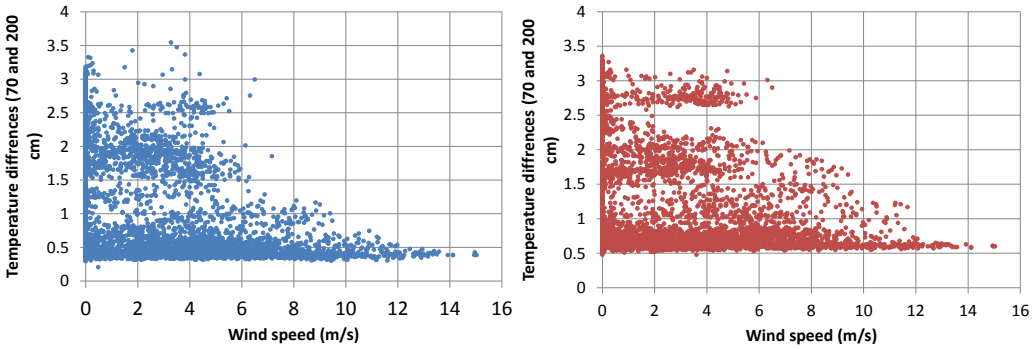

Figure 5.15: Correlations between wind speed and temperature differences between 70 and 200cm in the two measuring locations (Floating left, Open Space right).

Chapter 6

Numerical Results

In this work, the advantage of numerical modelling is the ability to model the oxygen budget evolution with a high temporal and spatial resolution. Moreover, the numerical model enables us to have an insight into the causes that can influence the levels of Dissolved Oxygen in the water body under discussion. The current research focuses on two numerical models which will be used to simulate the Dissolved Oxygen budget of the water body in Harnaschpolder:

- A time dependent zero dimensional model, which gives a first estimation of the causes for the observed Dissolved Oxygen differences between the open and floating houses locations.
- A time dependent one dimensional model in the vertical direction, which gives an estimation of the causes for the observed Dissolved Oxygen differences on the vertical profile between the open and floating houses locations.

The inputs for the numerical model are the measured meteorological conditions (wind speed and solar radiation), the water temperature, estimated by the local air temperature, and the parameters involved in the kinetic processes and external loads of equations (4.3)-(4.10). Additionally, the diffusion coefficient is an input parameter for the one dimensional model.

The second step is the determination of the initial and boundary conditions. For both cases the initial conditions are given by the first measurement of Dissolved Oxygen (31^{st} of July). The upper and lower boundary conditions are given by the reaeration and the sediment oxygen demand (SOD), respectively. In the zero dimensional model, the boundary conditions are included into the physical model as sources/sinks.

As can be seen in Table 6.1, page 49, the parameters for the kinetic equations are either fixed, measured, determined by equations or free parameters. The free parameters are characterised by a range of values stated in a number of literature sources [Bowie and Tech, 1985, Stefan and Fang, 1994, Chapra, 1997, Ji, 2008, D-Water Quality, 2013]. The

values of these free parameters are determined within these ranges such that the output of the numerical models best fit the field measurement data.

Although the temperature adjustment coefficient for respiration (θ_{rs}) is reported with three different values, see Table 4.4, page 31, in the models described here we treat it as a fixed parameter. The value of this value is chosen based on the one used in [Stefan and Fang, 1994, D-Water Quality, 2013]. The output of the numerical simulations will be evaluated by statistical tools of least squares error and regression coefficients of Pearson and Spearman, see Appendix B.

6.1 Zero Dimensional model

6.1.1 Set up

For the zero dimensional model we need to consider a box model, therefore we work with average values. For this reason a number of assumptions need to be taken into account. These assumptions are:

- Due to the absence of plant biomass ($Chla$) data during the measurement campaign, we chose to use the measurements of the previous year. Therefore, we assume that there is no change in plant biomass from one year to the other and during the simulation period. The value for the plant biomass is 51μg/L.
- The available plant biomass ($Chla$) is homogeneously distributed in the water column.
- The available solar radiation (I_0) is reduced by 50% just below the water surface.
- Photosynthesis is a process directly related to the light intensity in the water column, therefore it varies with depth. For this reason, in the zero dimensional model the depth integrated photosynthesis will be used.
- When the oxygen level is below 2mg/L there is no consumption by the sediment, $SOD = 0$, as in (D-Water Quality 2013).
- The average wind speed during the measurement campaign was 2.86m/s. Therefore, the two formulas for the Oxygen transfer coefficient, k_l, presented in Section 4.2.1.2, page 27, give similar results. We chose to work with the formula (4.7), page 29.
- Due to the low vertical variation of temperature, shown in Figure 5.8 and Figure 5.7, page 39, and the absence of detailed water temperature data for the simulation period, the water temperature will be estimated from air temperature using equation (4.13), page 32.

The model is applied in hourly time steps using the hourly values of air temperature, solar radiation and wind speed, which are available from a private weather station in Tanthof. The numerical solution of equation (4.14), page 32, is based on the finite difference method. As discussed before, the kinetic processes and external loads consist of

Table 6.1: Parameter characterization for kinetic equations.

Fixed Parameters	Measured Parameters	Given by equations	Free Parameters
$\boldsymbol{\theta_{rs}}$: Temperature adjustment coefficient for respiration	$\boldsymbol{SD}$: Secchi disk depth	$\boldsymbol{\phi_\ell}$: Attenuation of growth due to light	$\boldsymbol{r_{oa}}$: Oxygen production per unit mass of plant biomass
$\boldsymbol{\theta_b}$: Temperature adjustment coefficient for decomposition	$\boldsymbol{Chla}$: Concentration of plant biomass	$\boldsymbol{k_\ell}$: Oxygen transfer coefficient	$\boldsymbol{G_{max}}$: Maximum plant growth rate for optimal light conditions and excess nutrients
$\boldsymbol{\theta_s}$: Temperature adjustment coefficient for sediment oxygen demand	$\boldsymbol{H}$: Water depth	$\boldsymbol{C_{sat}}$: Saturated Oxygen Concentration	$\boldsymbol{YCHO2}$: Ratio of mg of Chlorophyll-a to mg of oxygen utilized in respiration $\boldsymbol{k_{rs}}$: Respiration rate coefficient $\boldsymbol{k_b}$: Decomposition rate coefficient $\boldsymbol{BOD}$: Biological Oxygen Demand $\boldsymbol{S_b}$: Sediment oxygen demand at T=20°C $\boldsymbol{k_z}$: Turbulent diffusivity

various parameters, see Table 6.1. Therefore, the first step of the numerical modelling is the calibration of the free parameters. The range of values of the free parameters is given in Table 4.2.1.6, page 30. As can be seen, the number of free parameters is large compared to the available measured data, seven free parameters towards seventeen measurement data. Thus, reducing the free parameters will simplify the process. For the current case standard BOD and SOD values were chosen such that they are representative of the Dutch water systems. This added two more assumptions:

- Due to the highly eutrophic state of the majority of surface waters in the Netherlands the value of 2.8mg/L for BOD is chosen.
- The value for SOD is based on a study of a small Dutch meso-eutrophic lake [Jean-Pierre and Sweerts, 1991] and is equal to 27 mmolO_2m^{-2}d^{-1}, or 0.864 gO_2m^{-2}d^{-1}.

6.1.2 Determination of free parameters

The determination of the free parameters of equations (4.3)-(4.10) is done by minimizing the error between the output of the numerical model and the measured data. In this work, this process of determining the optimal parameters is referred to as *calibration*. For the calibration, the data from the first three days of the measurement campaign were used. These data were chosen because during these days more frequent measurements took place in order to capture the diurnal pattern of the measurement locations.

The set of parameters with the best fit is presented in Table 6.2. As can be seen in Figure 6.1, the numerical model shows a good agreement with the daily Dissolved Oxygen variations, the modelled values are close to the averaged measurement data. However, it appears to be unable to obtain the peak of Dissolved Oxygen of the 2nd of August. The above is also identified in the high root mean squares error (RMSE), 1.01, and a strong Pearson and Spearman correlation coefficients, $r_P = 0.67$ and $r_S = 0.74$ respectively.

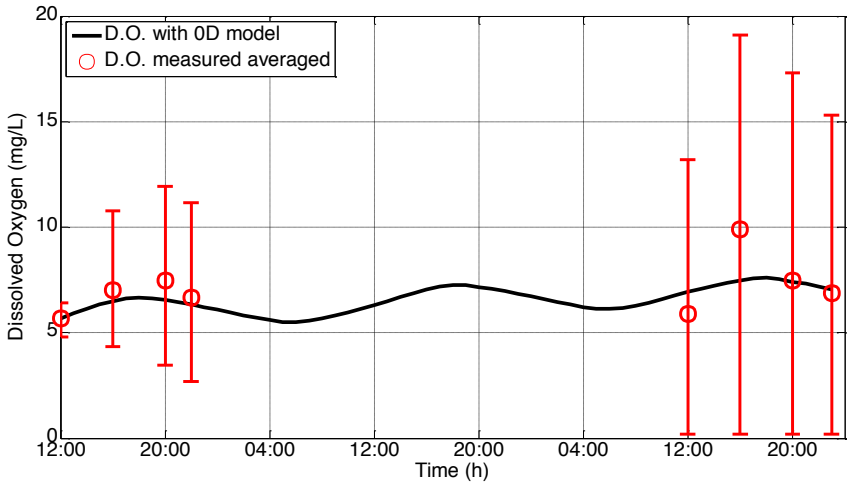

Figure 6.1: Calibration of zero dimensional model (error bars: range of measured values in vertical profile).

Table 6.2: Determined free parameters for zero dimensional model.

Parameter	Description	Range of values	Best fit value	Unit
r_{oa}	Oxygen production per unit mass of plant biomass	40.0-300.0	250.0	$\mathrm{mgO_2/mg}Chla$
$G_{\max}$	Maximum plant growth rate for optimal light conditions and excess nutrients	1.5-3	2.5	d^{-1}
$YCHO2$	Ratio of mg of Chlorophyll-a to mg of oxygen utilized in respiration	0.003-0.01	0.0033	$\mathrm{mg}Chla/\mathrm{mgO_2}$
k_{rs}	Respiration rate coefficient	0.02-0.6	0.15	d^{-1}
k_{b}	Decomposition rate coefficient	0.02-3.4	0.1	d^{-1}

The calibrated parameters were used to assess the validity of the model on a longer simulation period, i.e. one month. The data used for the assessment of the numerical model represent the measurements during the period 31$^{\mathrm{st}}$ of July until 31$^{\mathrm{st}}$ of August. In this work, this assessment process is referred to as *validation*. As can be seen in Figure 6.2, the numerical model depicts the Dissolved Oxygen budget evolution within the range of the measurements. However, the statistical error analysis indicates a moderate correlation between the modelled and the measured data. The obtained root mean squares error for the validation period is 1.22 and the correlation of coefficients of Pearson and Spearman are $r_{\mathrm{P}} = 0.55$ and $r_{\mathrm{S}} = 0.53$ respectively.

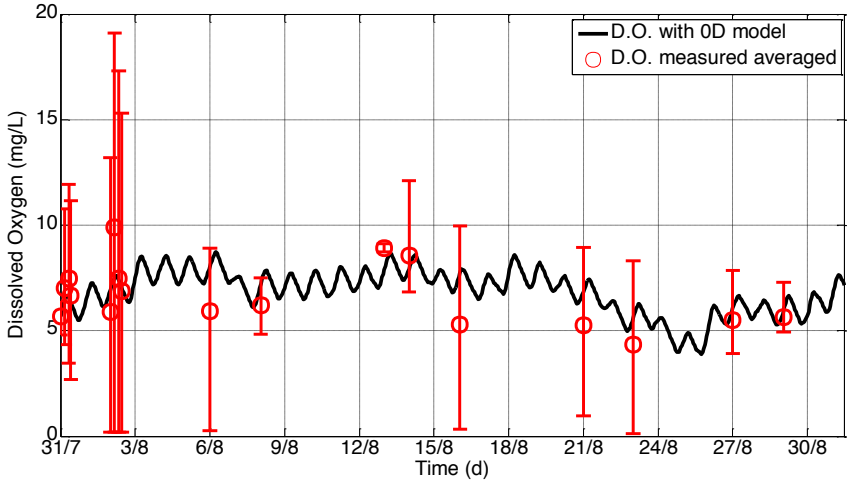

Figure 6.2: Validation of zero dimensional model (error bars: range of measured values in vertical profile).

The cumulative Dissolved Oxygen production and consumption for the simulated period 31st of July to 31st of August is presented in Figure 6.3 and Figure 6.4 respectively indicate that the major contributors in the Dissolved Oxygen budget are the processes of photosynthesis and respiration. Reaeration is also a contributor but in a lower rate.

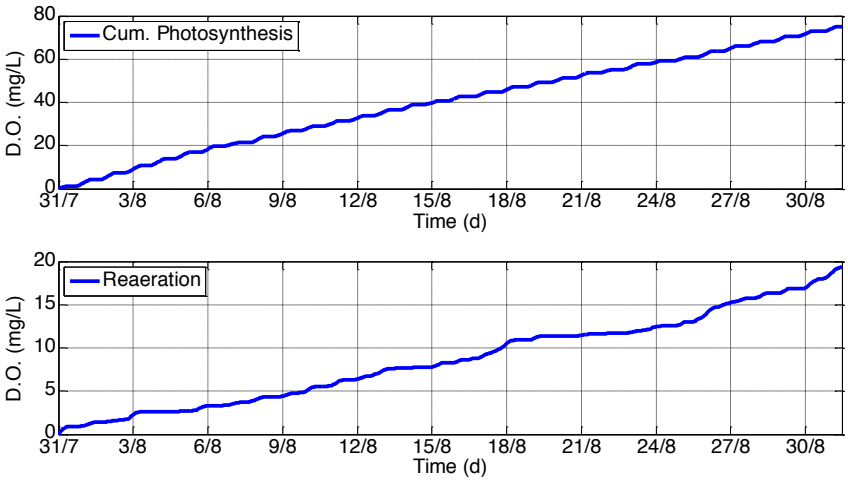

Figure 6.3: Cumulative Dissolved Oxygen production by photosynthesis (up) and reaeration (down) respectively.

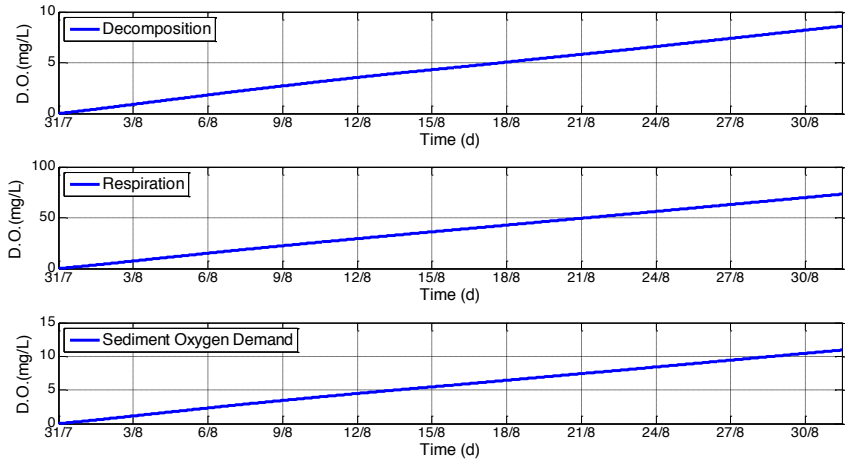

Figure 6.4: Dissolved Oxygen cumulative consumption by decomposition (top), respiration (middle) and sediment oxygen demand (bottom).

6.1.3 Sensitivity Analysis

A sensitivity analysis was performed in order to determine how much the model output is affected by changes in the input parameters. Two types of sensitivity analysis have been applied to the current model. In the first type the obtained parameters were changed and

the model output was evaluated. The variation of the parameters ranged from -75% to 50% such that they fit within the range reported in literature. As it is indicated by the error analysis in Table 6.3, the model output is affected more by changes to the parameters related to oxygen consumption by respiration (k_{rs}, -75%) and the ratio of plant biomass ($Chla$) to oxygen utilized in respiration ($YCHO2$). Furthermore, a decrease of 25% in either the oxygen production, r_{oa}, or in the maximum plant growth $G_{\max}$, which are related to the oxygen production by photosynthesis, indicated a better correlation to the measured data while an increase of 50% in the decomposition rate coefficient, k_{b}, decreased the RMSE and improved the correlation coefficients. Note that these changes refer to the validation process, not the calibration one.

Table 6.3: Error analysis for the calibrated parameters sensitivity analysis.

Parameters	RMSE	r_{p} (Pearson)	r_{s} (Spearman)
Best fit Parameters	**1.22**	**0.55**	**0.53**
r_{oa} (-75%)	3.76	0.44	0.62
r_{oa} (-25%)	1.55	0.64	0.73
$G_{\max}$ (-25%)	1.55	0.64	0.73
k_{b} (-75%)	1.52	0.38	0.35
k_{b} (+50%)	1.13	0.62	0.59
k_{rs} (-75%)	5.21	-0.24	-0.50
k_{rs} (+50%)	2.49	0.61	0.63
$YCHO2$ (+50%)	2.78	-0.03	-0.17

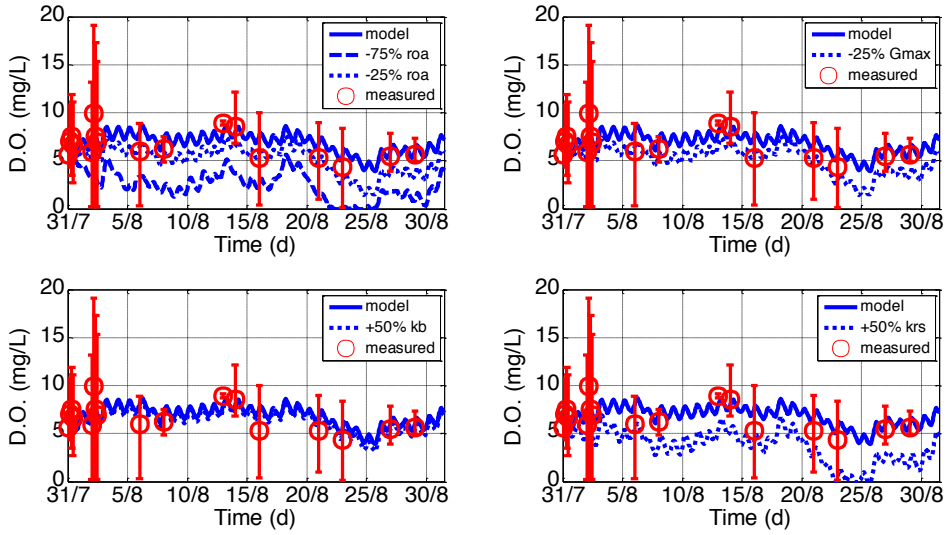

Figure 6.5: Sensitivity analysis for optimized parameters r_{oa}, k_{rs} and $YCHO2$.

The second type of sensitivity analysis was done to evaluate the effect of a change in the

values of the assumptions made for the zero dimensional model set up, see Section 6.1.1. The variation of the assumption values was based on previous and current observations as well as for incorporating measurement errors. The studied parameters are: plant biomass ($Chla$), Secchi disk depth, Water Temperature, Sediment and Biological Oxygen demand. Based on the error analysis in Table 6.4, the model output is sensitive to a change in the parameters that are related to the abundance of Dissolved Oxygen in the water column, for example a decrease in the water temperature makes the system to hold more Dissolved Oxygen. However, plant biomass ($Chla$) which is present in both photosynthesis and respiration expressions, has a different behaviour. The model output is more sensitive to a decrease of the plant biomass, therefore to less Dissolved Oxygen available in the water column.

Table 6.4: Error analysis for the assumptions sensitivity analysis.

Parameters	RMSE	r_{p} (Pearson)	r_{s} (Spearman)
Best fit Parameters	**1.22**	**0.55**	**0.53**
$Chla$ (-50%)	1.31	0.41	0.41
$Chla$ (+50%)	1.24	0.59	0.59
SD (-10%)	1.13	0.64	0.62
SD (+10%)	1.56	0.39	0.35
T (-10%)	1.55	0.36	0.33
T (+10%)	1.10	0.65	0.67
S_{d} (-50%)	1.47	0.41	0.40
S_{d} (+50%)	1.11	0.63	0.61
BOD (-50%)	1.41	0.44	0.42
BOD (+50%)	1.13	0.62	0.59

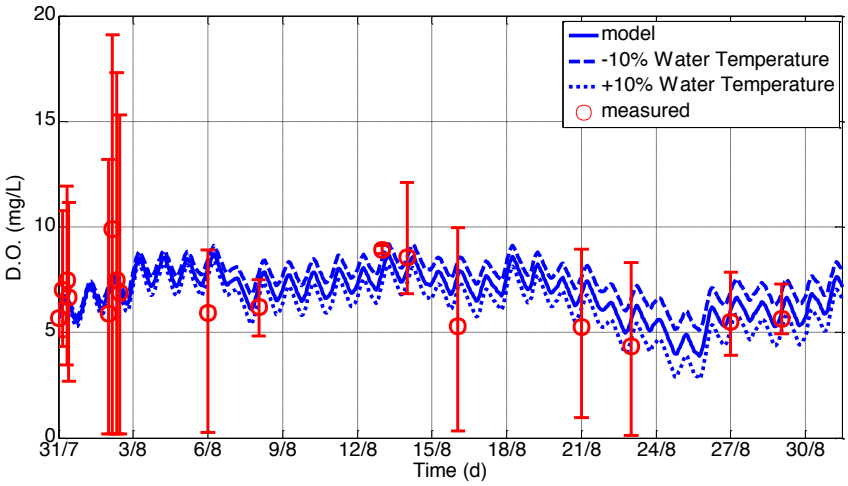

Figure 6.6: Sensitivity analysis for water temperature in the zero dimensional model.

6.1.4 Floating Houses Effects: Shade Factor

During the measurement campaign it was observed that the measurement point between the floating houses, position B, was under the shadow created by the adjacent floating houses, see Figure 6.7. In the diurnal pattern from the measurement, see Figure 5.12, it is observed that the position between the floating houses has lower levels of Dissolved Oxygen compared to the open space. This difference is predominant in the top layer, where photosynthesis is mainly active. Since floating houses cast a shadow over the measurement location B, we decided to investigate the influence of sunlight blockage in Dissolved Oxygen levels.

Figure 6.7: Shadow from the floating house during measurements at location B.

In order to include the shadow effect in the numerical model we need to identify the period during which shade was present. To do this we have to consider not only the height and

placement of the floating houses but also the sun path, see Figure 6.8. Taking this into account it is possible to determine that location B is in the shade between 7:00am and 15:00pm.

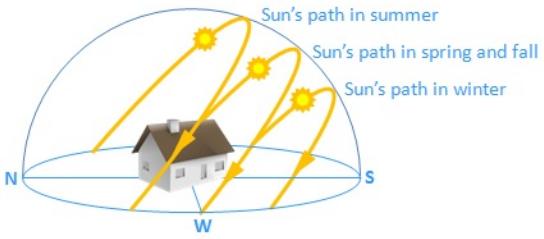

Figure 6.8: Sun path for the northern hemisphere.

The shadow effect was then modelled by a shade factor that reduces the available sunlight during the period in which location B was under shade. Given the typical values for the percentage of beam radiation (direct sunlight), see [Heisler, 1986], and the fact that location B is close to a large reflecting surface (the wall of the adjacent floating house), we chose a value of 0.6 for the shade coefficient. This means that the shade blocks 40% of the total available solar radiation at the water surface.

Figure 6.9 shows the Dissolved Oxygen budget evolution for the open space and the floating houses with shadow effect. As can be seen, the Dissolved Oxygen budget of the floating houses becomes lower than the one in the open space, especially after the 20^{th} of August, as observed in the measurements.

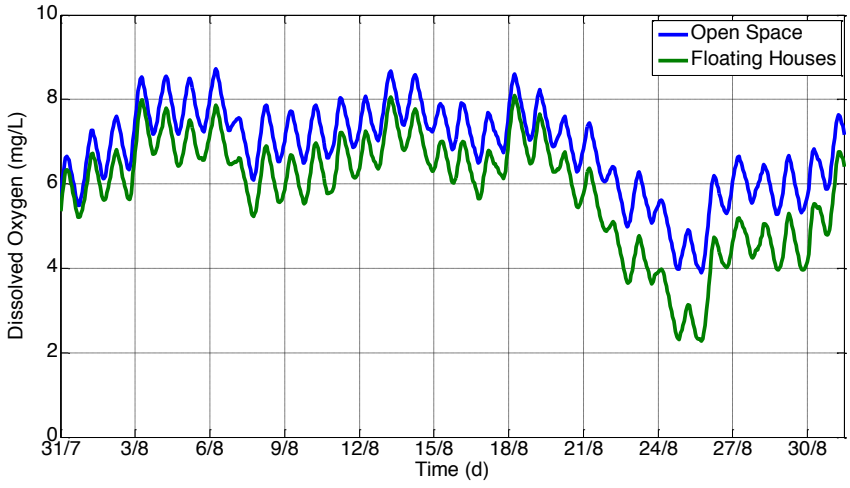

Figure 6.9: Dissolved Oxygen Budget for the open space and floating houses (shadow effect-zero dimensional).

6.1.5 Floating Houses Effects: Wind factor

Another observation during the measurement campaign was related to the wind speed. During the measurements, the area between the floating houses was more influenced by

the wind. Furthermore, the orientation of the houses (southwest) and the prevailing wind orientation (southwest), see Figure 5.3, page 36, creates a wind barrier which results in a wind tunnel effect between the floating houses, see Figure 6.10. In addition, the area between the floating houses also experienced increased turbulence at the surface layer. However, in the zero dimensional model we can partially model the wind factor effect, increased wind speed, because only the reaeration factor is included.

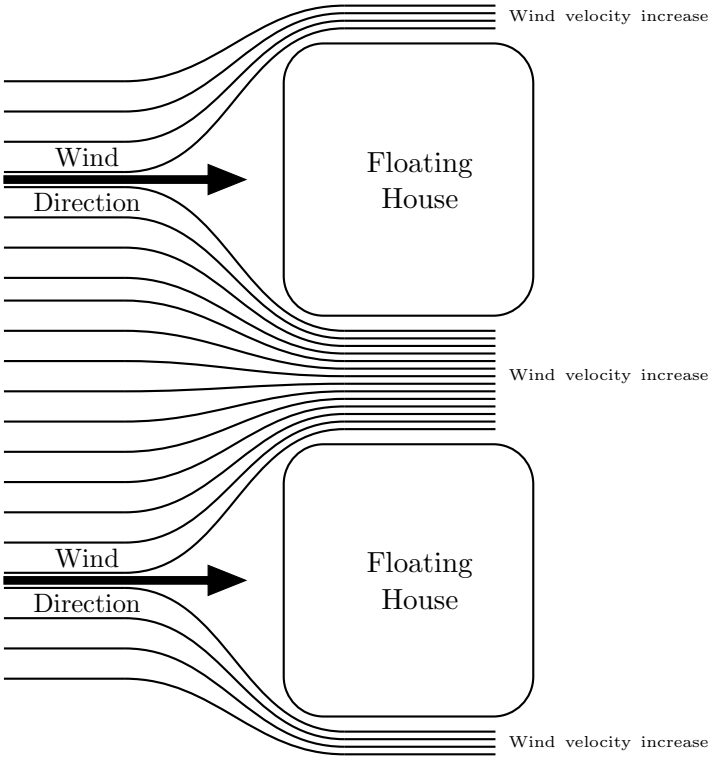

Figure 6.10: Wind effect in a building.

A simulation with an increased wind speed, 50% increase [Asfour, 2010], was tested in order to simulate the above mentioned observation. For this simulation the shadow effect was not taken into account in order to separate the two effects. As we can see from the results, see Figure 6.11, an increased wind speed results in higher Dissolved Oxygen levels, which comes in contradiction with the measured data.

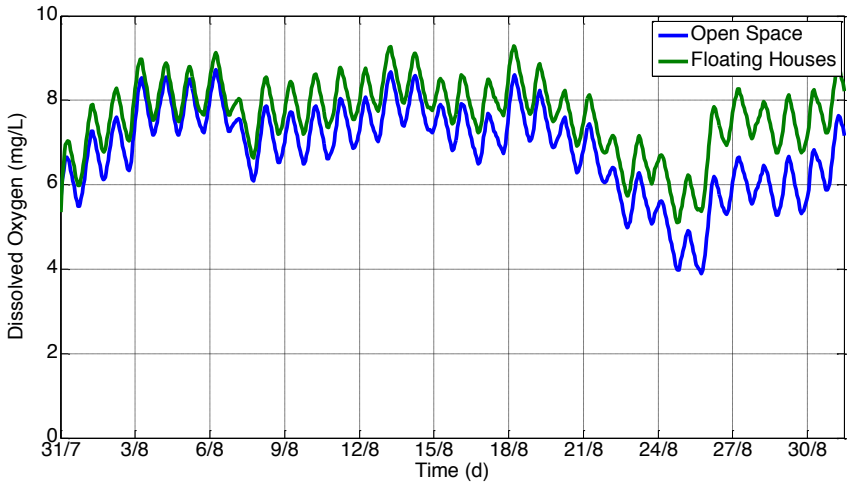

Figure 6.11: Dissolved Oxygen budget for the open space and floating houses (wind effect-zero dimensional).

6.2 One Dimensional Model

6.2.1 Set up

The one dimensional model is based upon the general idea and assumptions of the zero dimensional model but includes also variation in the vertical direction and diffusion effects. The diffusion coefficient, k_z, includes both molecular and dispersion diffusion and was calibrated within the range mentioned in [Stefan and Fang, 1994]. For the one dimensional model, the water column is divided into vertical cells in order to evaluate the vertical distribution of Dissolved Oxygen. The simulated Dissolved Oxygen concentration is associated to the middle of each cell, while the diffusion fluxes are associated to the interfaces between the cells. The boundary conditions are reaeration only on the top boundary and the sediment oxygen demand at the lower bottom boundary. The time and spatial discretization are set to 0.1 hour and 0.1m (25 cells), respectively, in order to have stability in the numerical model. Since we work on the vertical direction, photosynthesis is calculated at each depth and is not averaged, as in the zero dimensional model. Finally, water temperature is estimated from the air temperature using equation (4.13), page 32. Based on the field measurements, it is assumed that water temperature has no variation with depth.

The same procedures employed in the 0D model for the determination of the free parameters (calibration) and assessment of the model (validation) were used for the 1D model as well. Initially, during the calibration of the model, the obtained results showed a low correlation with the observed data. Moreover, the model was unable to capture the variations in the upper 1m of the water column, while it overestimated the Dissolved Oxygen concentration in the lower part (1.5 and 2m), as presented in Figure 6.12. Furthermore, during the validation process, the results of the numerical in the lower part of the water column showed minimum Dissolved Oxygen concentrations and were not able to follow the variations observed in the measurements, see Figure 6.13. For that reason it was

important to redefine the assumptions.

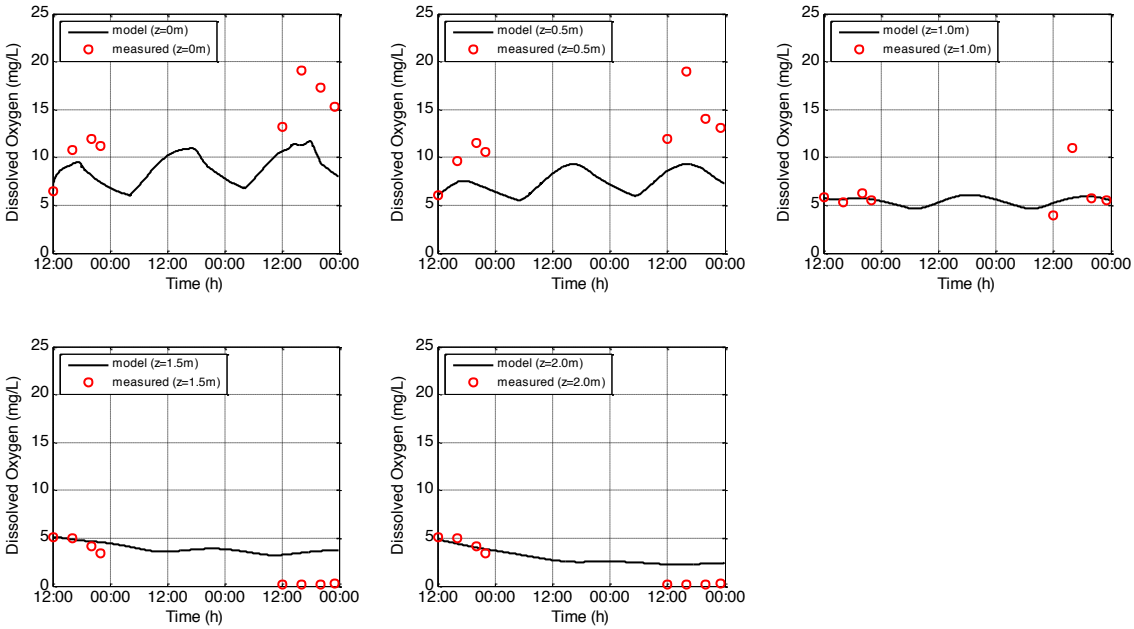

Figure 6.12: First calibration results of one dimensional model.

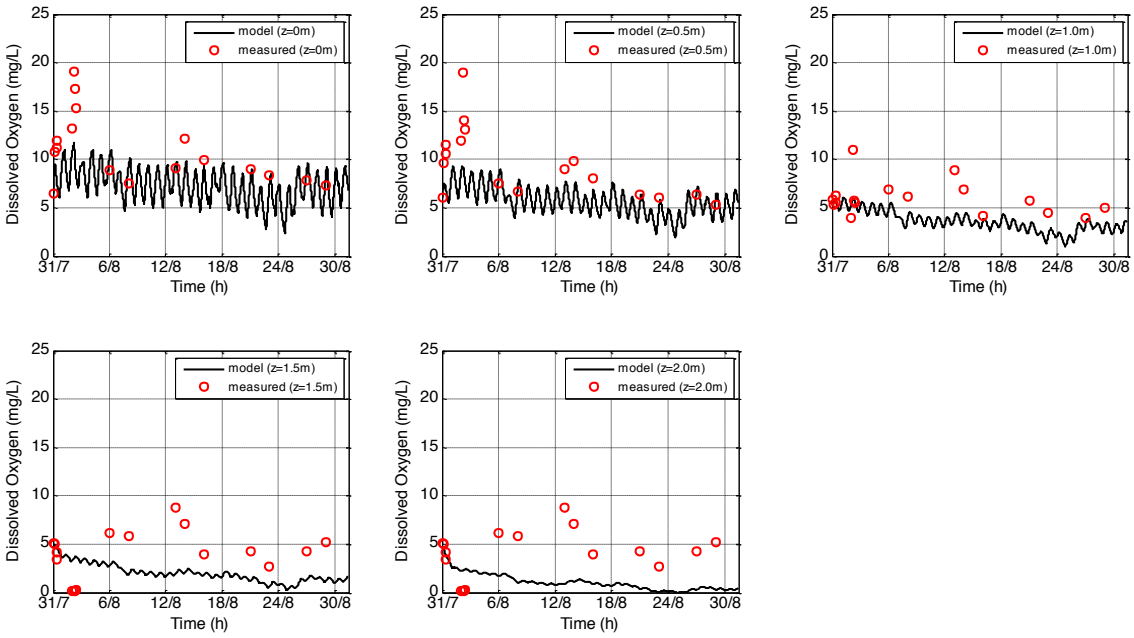

Figure 6.13: First validation results of one dimensional model.

The first step for the construction of the new assumptions was to reconsider the measured parameters. One of the parameters that needed to be reassessed was the one representing the concentration of plant biomass, *Chla*. The value of this parameter was based on measurements of the previous year on the same period. However, the plant biomass is a parameter that is characterised by variations throughout the year and from year to year, as

can be seen by the measurements in the year prior to the installation of the floating houses, see Figure 6.14. In addition, the other measured parameter, Secchi disk depth, contains a possible error since it is a measurement based on subjective observation. Finally, in the zero dimensional model we assume that the plant biomass is homogeneously distributed in the water column. However, in reality plant biomass is heterogeneously distributed and, depending on the depth, can be functional or non-functional, see Figure 6.15.

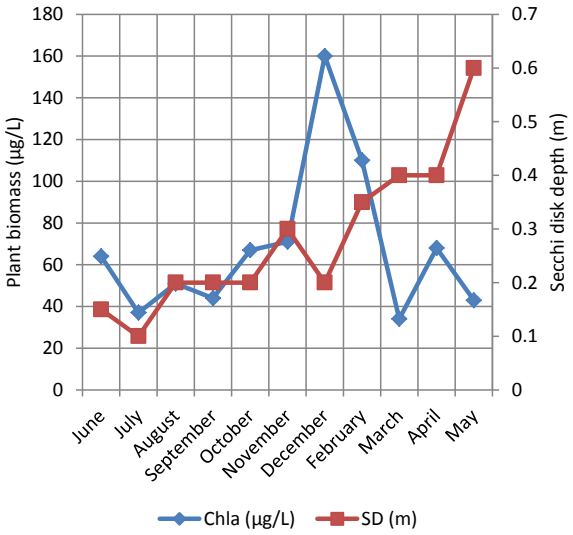

Figure 6.14: Plant biomass and Secchi disk depth measurements by the Water board of Delfland (June 2012-May 2013, no measurements in January due to ice cover).

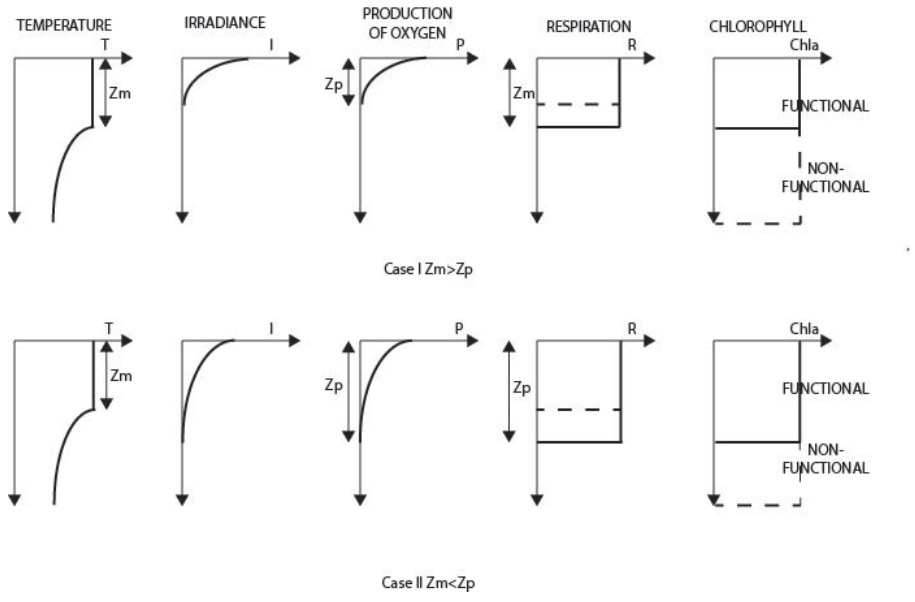

Figure 6.15: Schematic figures for temperature, irradiance, production of oxygen (photosynthesis), respiration and Chlorophyll-a distributions in the regional Dissolved Oxygen model by [Stefan and Fang, 1994]. (z_{m}: surface mixed layer depth, z_{p}: photic depth).

At this point it was important to find a way to estimate the amount of plant biomass. Since

Secchi Disk depth was more representative of the measurement campaign and contains less uncertainty than the plant biomass, we decided to use it to estimate the plant biomass. [Carlson and Simpson, 1996] used the measured plant biomass, Secchi Disk depth and phosphorus in order to find a relation and ultimately define a trophic state index. A non-linear relation between secchi disk depth and plant biomass is defined by:

$$\log(SD) = 2.04 - 0.68 \log(Chla) \ . \tag{6.1}$$

Where SD is the Secchi Disk depth, [m], and $Chla$ the concentration of plant biomass, [μg/L].

As mentioned above, Secchi Disk depth is a subjective measurement, therefore a modification was applied for minimising this measurement error. An increase of the Secchi Disk depth from 28cm to 32cm improved the variations observed on the top water layer (up to 1m depth). By using the modified Secchi Disk depth in equation (6.1) the obtained plant biomass was 107μg/L, while by using the original Secchi Disk depth of 28cm the obtained plant biomass was 130μg/L. Thus, an increase of 14.3% in the Secchi Disk depth results in a 17.7% reduction of the plant biomass.

Finally, the Dissolved Oxygen consumption in the lower water column (1.5 to 2.0m) is high and the measured variations are not captured by the numerical model, see Figure 6.13. In addition, based on Figure 6.15, the lower part of the water column corresponds to the non-photic zone and consequently the plant biomass in that part is non-functional. Therefore, respiration was considered to be zero at the lower water column.

For all the above reasons the revised assumptions for the one dimensional numerical modelling are summarised as follows:

- The functional plant biomass is homogeneously distributed on the upper 1.5m of the water column.
- The concentration of plant biomass is estimated by the expression introduced by [Carlson and Simpson, 1996], equation (6.1) above, resulting in a value of 100μg/L.
- The Secchi Disk depth is set to 0.32m in order to capture the variations in the top water layer, up to 1m depth.
- The available solar radiation (I_0) is reduced by 50% just below the water surface.
- Photosynthesis is calculated for each cell. The value used in the simulation is the representative value at the middle of each cell.
- Respiration is considered to be zero at the lower part of the water column, due to the non-functionality of plant biomass in that region.
- When the oxygen level is below 2mg/L there is no consumption by the sediment, $SOD = 0$, as in [D-Water Quality, 2013].
- In order to minimize the free parameters, the biological and sediment oxygen demand were set to 2.8mg/L and 0.864gO_2m^{-2}d^{-1}, respectively, representing conditions observed in The Netherlands.

- The average wind speed during the measurement campaign was 2.86m/s. Therefore, the two formulas for the Oxygen transfer coefficient, k_l, presented in Section 4.2.1.2, page 27, give similar results. We chose to work with the formula (4.7), page 29.
- Finally, due to the observed low vertical variation of temperature, see Figure 5.8, page 40, and Figure 5.7, page 39, the water temperature in all measurement depths was estimated by the air temperature using equation (4.13), page 32.

6.2.2 Calibration and Validation

With the above mentioned changes and adjustments, the free parameters of the one dimensional numerical model were calibrated, see Table 6.5, and later validated. The procedure was the same as for the zero dimensional model, with the only difference being that for the one dimensional model we have an extra free parameter to calibrate, the diffusion coefficient, k_z.

Table 6.5: Calibrated free parameters for one dimensional model.

Parameter	Description	Range of values	Best fit value	Unit
r_{oa}	Oxygen production per unit mass of plant biomass	40.0-300.0	300.0	mgO_2/mg$Chla$
$G_{\max}$	Maximum plant growth rate for optimal light conditions and excess nutrients	1.5-3.0	3.0	d^{-1}
$YCHO2$	Ratio of mg of Chlorophyll-a to mg of oxygen utilized in respiration	0.003-0.01	0.003	mg$Chla$/mgO_2
k_{rs}	Respiration rate coefficient	0.02-0.6	0.27	d^{-1}
k_{b}	Decomposition rate coefficient	0.02-3.4	0.06	d^{-1}
k_z	Diffusion coefficient	0.0864-1.728	0.96	m^2/d

The set of free parameters with their best fit is presented in Table 6.5. As we can see from Figure 6.16, the numerical model shows a good representation of the daily Dissolved Oxygen variations on the upper 1m of the water column. However, the lower part of the water column does not seem to have an improvement compared to the initial assumption simulation, see Figure 6.13. The corresponding root mean squares error (RMSE) and the correlation coefficients are given at Table 6.6.

The validation results are presented in Figure 6.17. If we compare Figure 6.13 with Figure 6.17 we can see that the new assumptions resulted in a better representation of the Dissolved Oxygen evolution, especially regarding the lower part of the water column.

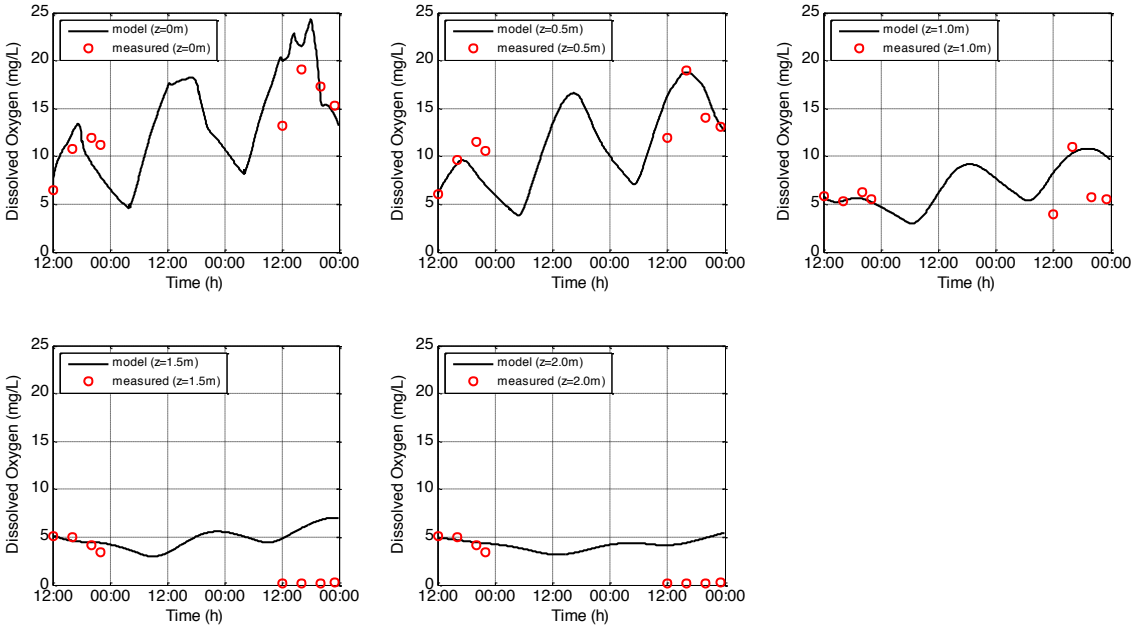

Figure 6.16: Calibration of the one dimensional model.

However, the statistical analysis, see Table 6.6, indicates a weaker correlation between the modelled and measured results compared to calibration period.

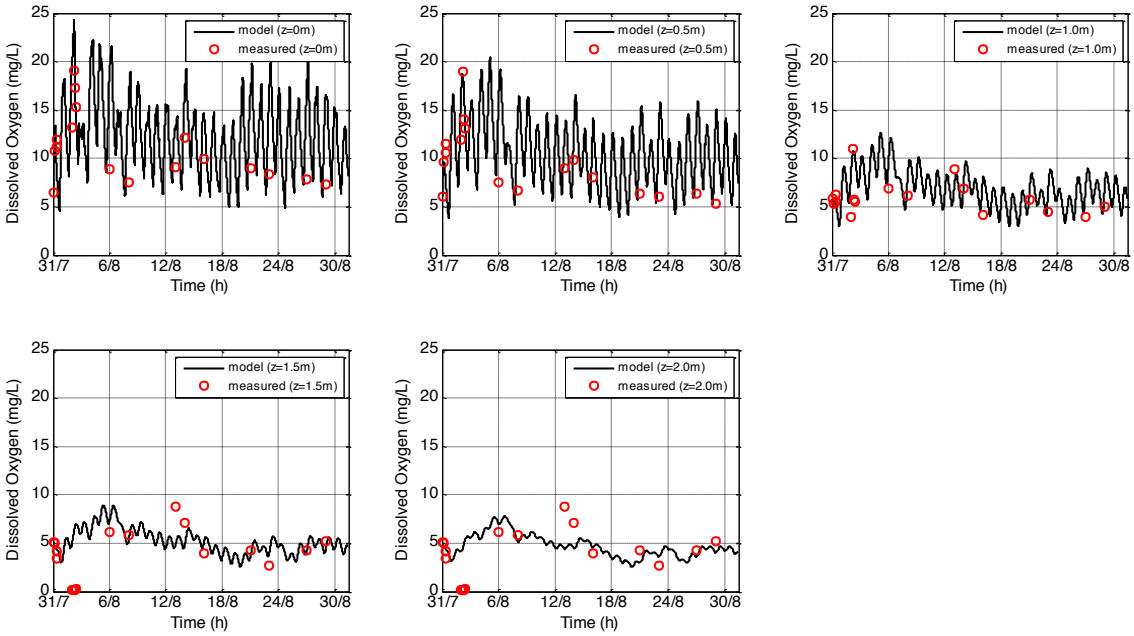

Figure 6.17: Validation of the one dimensional model.

The one dimensional cumulative fluxes indicate that reaeration is the most important source/sink of Dissolved Oxygen followed by photosynthesis and respiration. Comparing to the zero dimensional we can distinguish the following behaviour:

Table 6.6: Error analysis for the calibration and validation of the one dimensional model.

		$z = 0.0$m	$z = 0.5$m	$z = 1.0$m	$z = 1.5$m	$z = 2.0$m
Calibration	RMSE	3.06	2.53	2.89	4.23	3.28
	r_p	0.82	0.84	0.34	-0.69	-0.06
	r_s	0.86	0.90	0.24	-0.44	0.06
Validation	RMSE	5.84	5.08	2.52	3.18	3.38
	r_p	0.35	0.38	0.31	-0.33	-0.14
	r_s	0.23	0.32	0.14	-0.10	-0.05

i. The reaeration flux is mainly a sink of Dissolved Oxygen, which indicates that on the upper boundary Dissolved Oxygen is mainly released back to the atmosphere, see Figure 6.18.

ii. The upper layers of the water column are the ones producing the majority of Dissolved Oxygen.

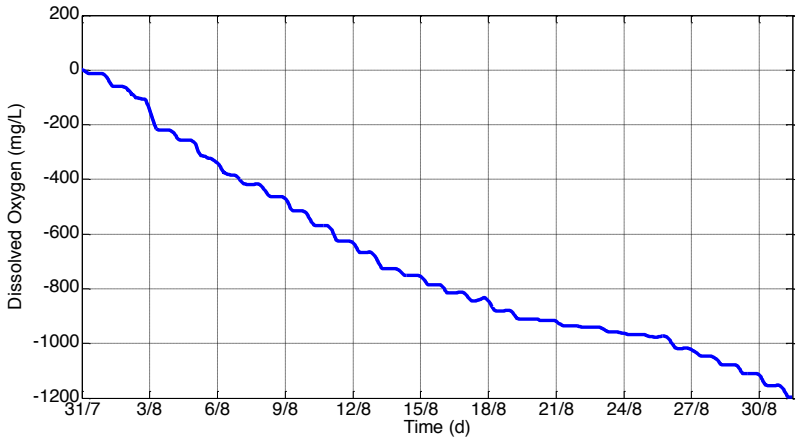

Figure 6.18: Cumulative reaeration, one dimensional model.

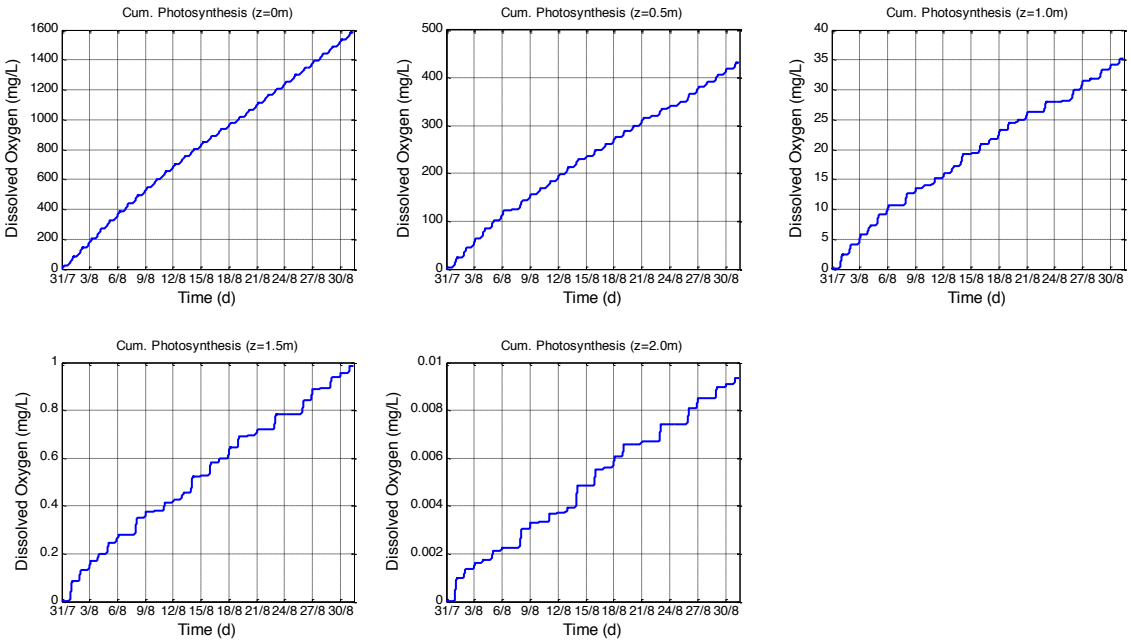

Figure 6.19: Dissolved Oxygen cumulative production by photosynthesis per layer, one dimensional model.

6.2.3 Sensitivity Analysis

A sensitivity analysis similar to the one described for the zero dimensional model was also performed for the one dimensional model. One new free parameter was added into the analysis. For the sake of visual simplicity, only the vertical profiles of three specific dates will be plotted. These dates indicate the beginning, middle and end of the numerical simulation and correspond to the 31$^{\text{st}}$ of July, 8$^{\text{th}}$ and 29$^{\text{th}}$ of August respectively.

Regarding the sensitivity analysis of the best fit parameters it can be seen that apart from the case of the decomposition rate coefficient (k_{b}) the model output is sensitive to changes of the parameters, see Figure 6.20 and Figure 6.21, Figure 6.22 and Figure 6.23. The sensitivity analysis of the diffusion coefficient, k_z, shows that this parameter affects particularly the lower part of the water column, especially when this parameter is decreased, see Figure 6.24.

Finally, regarding the sensitivity analysis on the assumptions, we can say that the model output is more sensitive to the parameters of Secchi disk depth and plant biomass, see Figure 6.25 and Figure 6.26, and less to the rest of the assumptions, e.g. water temperature, see Figure 6.27.

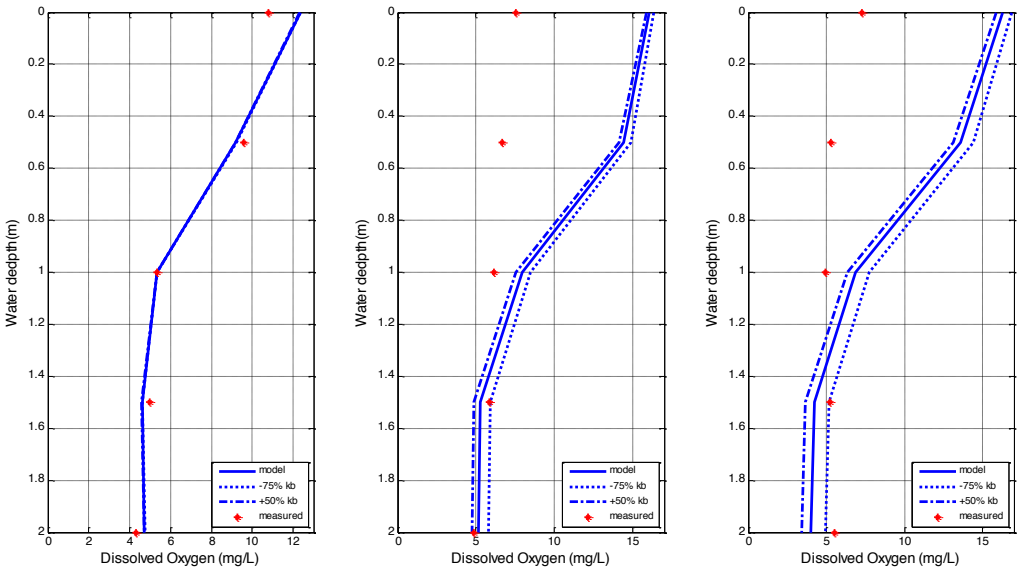

Figure 6.20: Sensitivity analysis for optimised parameters k_{b} (31$^{\mathrm{st}}$ of July (left), 8$^{\mathrm{th}}$ of August (middle) and 29$^{\mathrm{th}}$ of August (right)).

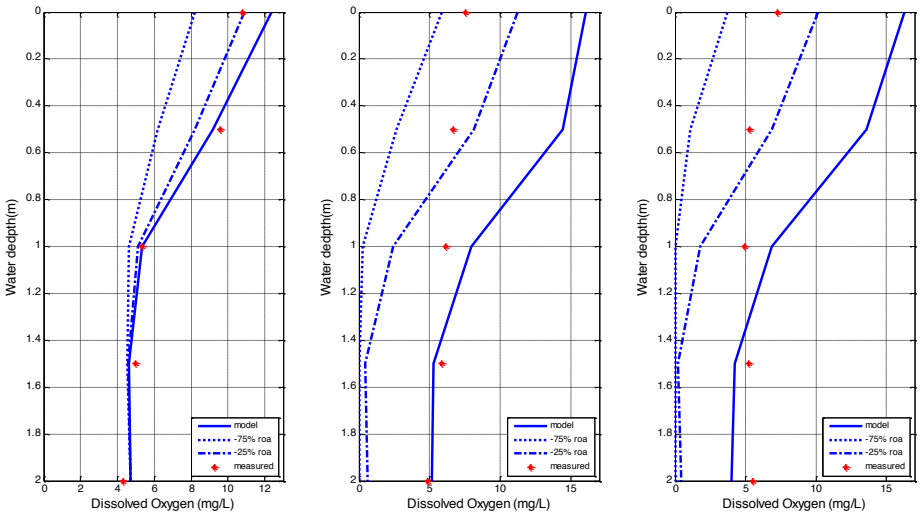

Figure 6.21: Sensitivity analysis 1D for parameter r_{oa} (31$^{\mathrm{st}}$ of July (left), 8$^{\mathrm{th}}$ of August (middle) and 29$^{\mathrm{th}}$ of August (right)).

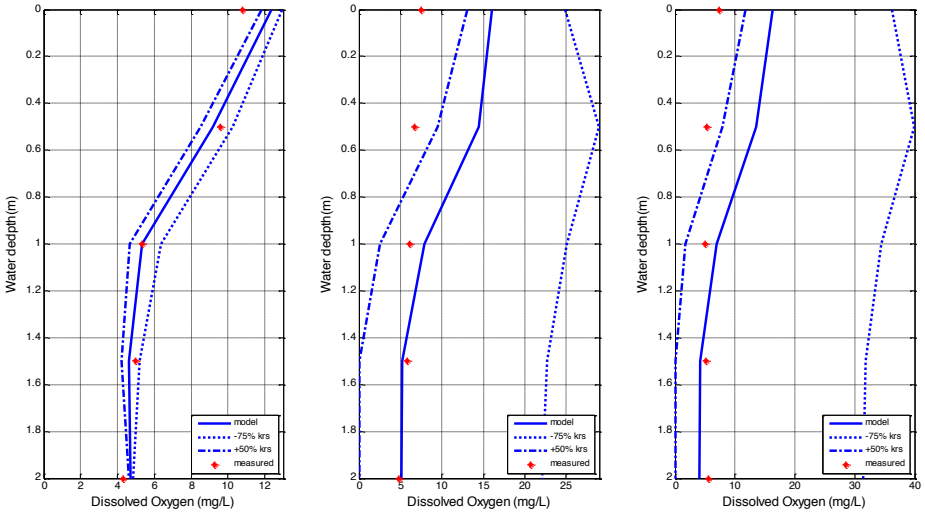

Figure 6.22: Sensitivity analysis 1D for parameter k_{rs} (31$^{\mathrm{st}}$ of July (left), 8$^{\mathrm{th}}$ of August (middle) and 29$^{\mathrm{th}}$ of August (right)).

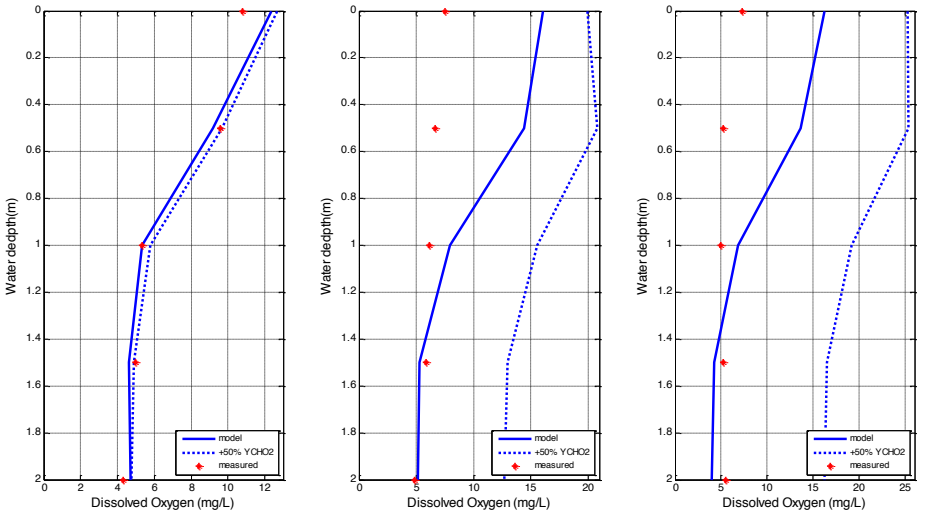

Figure 6.23: Sensitivity analysis 1D for parameter $YCHO2$ (31$^{\mathrm{st}}$ of July (left), 8$^{\mathrm{th}}$ of August (middle) and 29$^{\mathrm{th}}$ of August (right)).

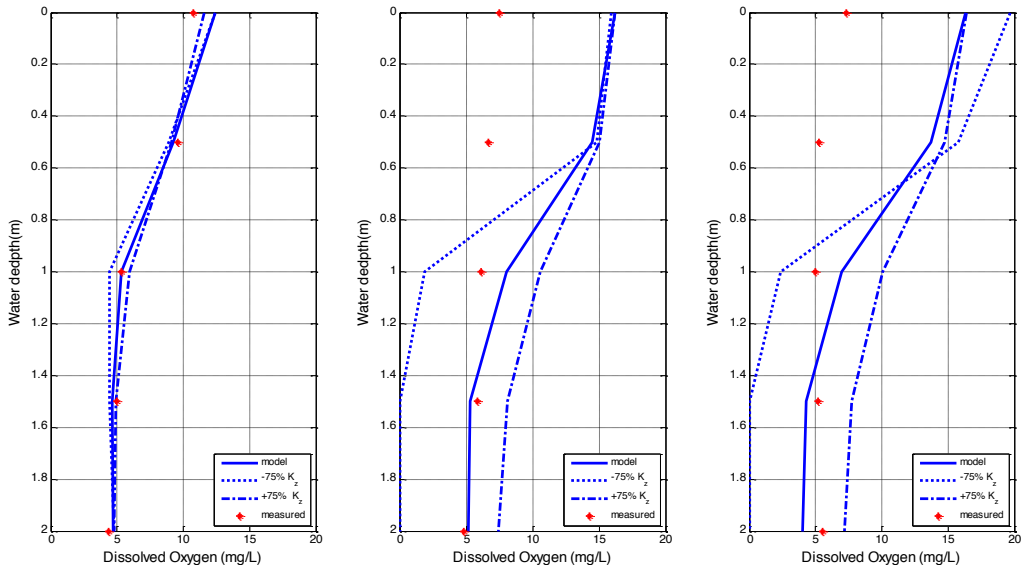

Figure 6.24: Sensitivity analysis 1D for k_z (31st of July (left), 8th of August (middle) and 29th of August (right)).

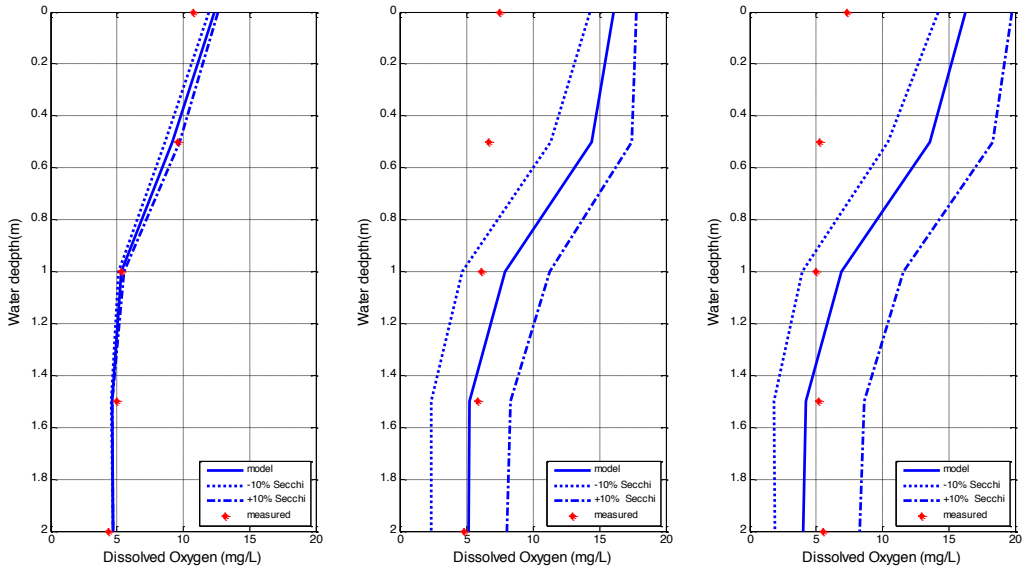

Figure 6.25: Sensitivity analysis 1D for Secchi disk parameter (31st of July (left), 8th of August (middle) and 29th of August (right)).

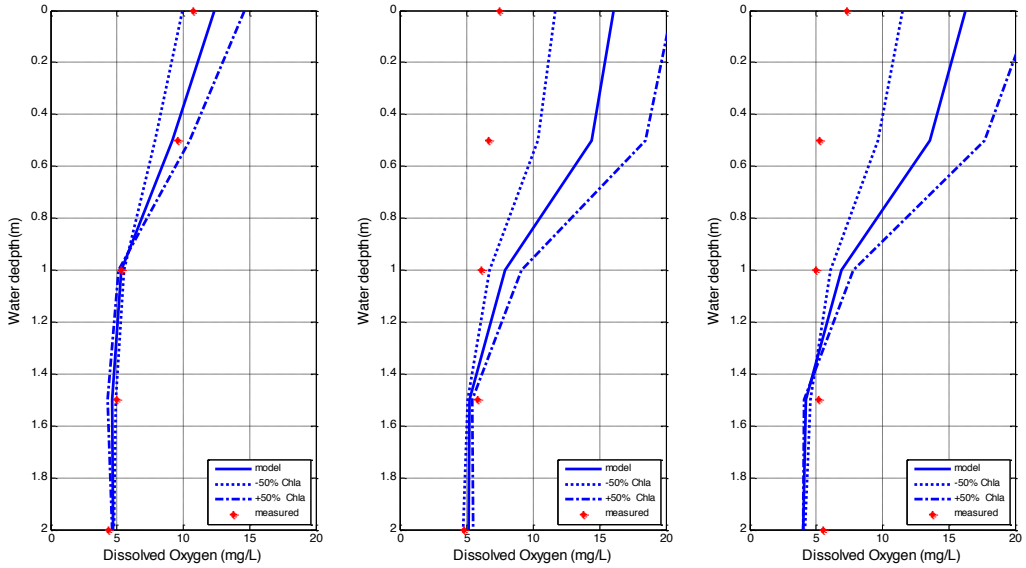

Figure 6.26: Sensitivity analysis 1D for plant biomass (31st of July (left), 8th of August (middle) and 29th of August (right)).

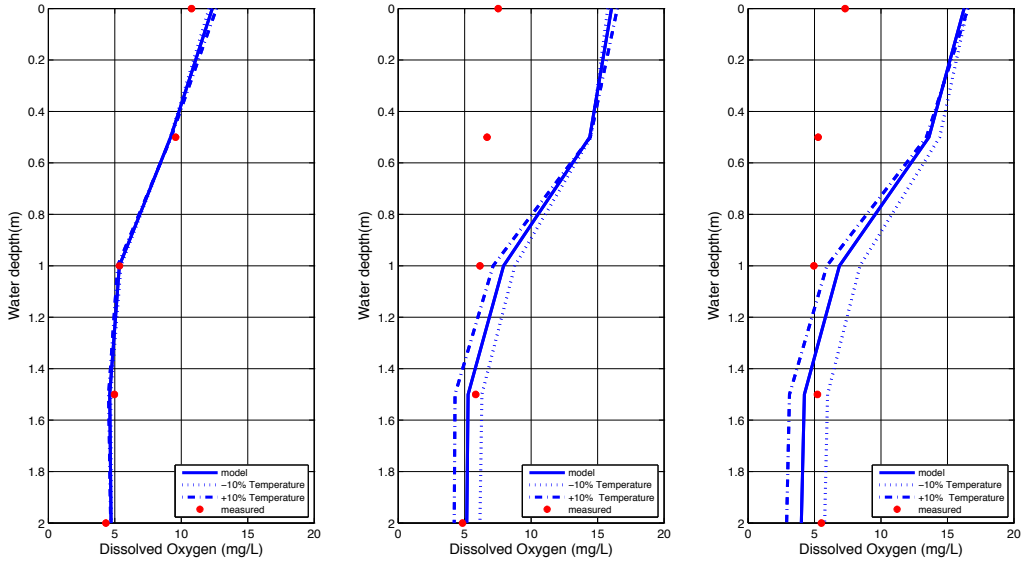

Figure 6.27: Sensitivity analysis 1D for water temperature (31st of July (left), 8th of August (middle) and 29th of August (right)).

6.2.4 Floating Houses Effects: Shade factor

Once having assessed the numerical model for the one dimensional simulation, the effect of the floating houses can be evaluated. The shadow effect is the first factor that will be evaluated in the one dimensional model. Similar to the zero dimensional model, a shade factor was introduced in the model. We chose a value of 0.6 for the shade factor, as explained in section Section 6.1.4, page 55. The error analysis of the simulation for floating houses with and without the shade factor is given in Table 6.7. As can be seen, including the shade effect improved the correlation coefficients, however still a weak correlation is obtained.

Table 6.7: Error analysis for floating houses with and without shade effect.

Floating Houses	z [m]	RMSE	r_p (Pearson)	r_s (Spearman)
No shade	0.0	6.59	0.38	0.27
	0.5	5.43	0.40	0.36
	1.0	3.54	-0.39	-0.44
	1.5	3.45	-0.55	-0.65
	2.0	3.61	-0.06	-0.03
Shade	0.0	5.73	0.45	0.35
	0.5	4.38	0.52	0.50
	1.0	3.33	-0.41	-0.44
	1.5	3.69	-0.55	-0.56
	2.0	3.51	-0.10	-0.07

Figure 6.28, shows the Dissolved Oxygen evolution in time and space for the open space and the floating houses with the shade effect. It can be seen that the floating houses develop lower Dissolved Oxygen concentrations at the bottom part of the water column. The differences between the two locations are displayed in Figure 6.29. One can see that the differences between the two locations are in the range of $\pm$1mg/L, except for some days in which the top part of the water column of the floating houses developed considerably lower Dissolved Oxygen levels compared open space.

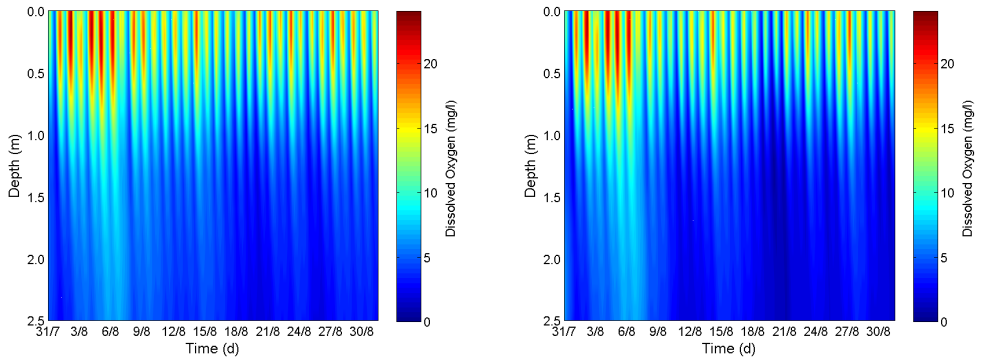

Figure 6.28: Dissolved Oxygen evolution for open space (left) and floating houses (right), for shade effect.

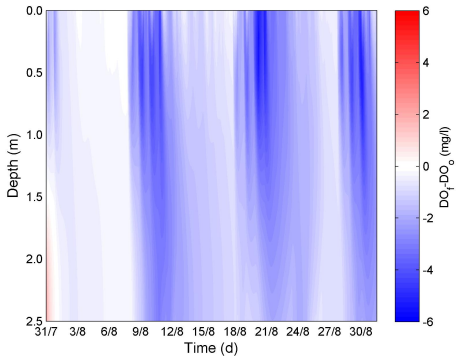

Figure 6.29: Dissolved Oxygen differences evolution between floating houses (DO_f) and open space (DO_o), for shade effect.

6.2.5 Floating Houses Effects: Wind tunnel effect

According to our observations the wind was stronger between the floating houses resulting in a wind tunnel effect. This effect can influence the reaeration rate coefficient and, consequently, the exchange rate of Dissolved Oxygen between the water and the atmosphere. Furthermore, in the case of the one dimensional model, the diffusion coefficient can be influenced as well, and more specifically the turbulence mixing. Therefore, a simulation with a 50% increase in wind speed and a 25% increase in diffusion coefficient was tested in order to simulate the above mentioned observations. For this simulation the shadow factor was kept equal to one, therefore no shade effect. The error analysis of the wind tunnel effect simulation is presented in Table 6.8. As we can see, the correlation coefficients do not improve and an even weaker correlation is established by the implementation of these two factors.

As shown in Figure 6.30 the top part of the water column of floating houses location developed lower Dissolved Oxygen levels. This is because the upper part of the water column is supersaturated. Therefore, an increase in the wind speed increases the reaeration coefficient, which in turn increases the oxygen exchange with the atmosphere. Furthermore, the diffusion coefficient is responsible for the transfer of Dissolved Oxygen from regions

Table 6.8: Error analysis for floating houses with wind tunnel effect.

Floating Houses	z [m]	RMSE	r_{p} (Pearson)	r_{s} (Spearman)
No wind effect	0.0	6.59	0.38	0.27
	0.5	5.43	0.40	0.36
	1.0	3.54	-0.39	-0.44
	1.5	3.45	-0.55	-0.65
	2.0	3.61	-0.06	-0.03
Wind effect	0.0	4.90	0.28	0.13
	0.5	4.18	0.36	0.22
	1.0	3.09	-0.50	-0.42
	1.5	3.56	-0.71	-0.74
	2.0	3.59	-0.22	-0.22

with higher concentrations to the ones with lower, the lower part of the water column. Therefore, since both locations (open space and floating houses) have the same amount of Dissolved Oxygen produced by photosynthesis, we see that the increased turbulence results in a higher flux of Dissolved Oxygen to the lower parts and the only differences between the two locations are limited to the top. These differences are better depicted in Figure 6.31.

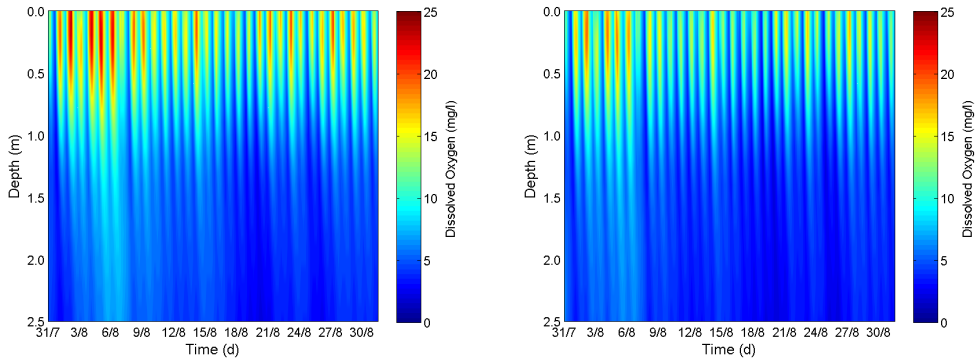

Figure 6.30: Dissolved Oxygen evolution for open space (left) and floating houses (right), for increased wind effect.

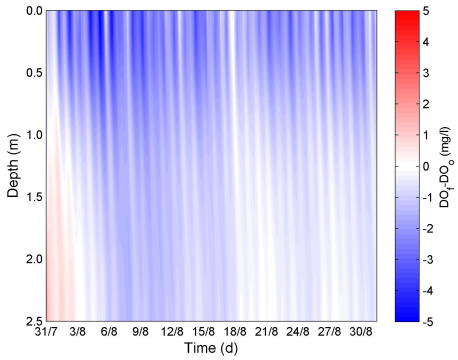

Figure 6.31: Dissolved Oxygen differences evolution between floating houses (DO_f) and open space (DO_o), for increased wind effect.

6.3 Discussion numerical modelling

Lake water quality modelling is a complex problem. This is particularly well expressed in [Loucks et al., 2005]:

> *The development and application of water quality models is both a science and an art. Each model reflects the creativity of its developer, the particular water quality management problems and issues being addressed, the available data for model parameter calibration and verification, the time available for modelling and associated uncertainty, and other considerations. The fact that most, if not all, water quality models cannot accurately predict what actually happens does not detract from their value. Even relatively simple models can help managers understand the real world prototype and estimate at least the relative, if not actual, change in water quality associated with given changes in the inputs resulting from management policies or practices.*

There are numerous water quality models in the market which use complex water quality mechanisms, i.e. DELWAQ by Deltares. However, in the current research a complex mechanistic model would not be beneficial, due to the limited available data. Therefore, the scope of this research was not to accurately model the Dissolved Oxygen variations, but to understand the mechanisms involved in it and estimate the relative changes associated to the presence of floating houses. For this reason a simple model was developed.

On what follows we will discuss and analyse the estimations obtained by the numerical model and compare them with the obtained measurements. We will further discuss which information can be used to improve the existing model in order to better understand the effects of floating houses on water quality.

As can be seen in Figure 6.2, page 51, and Figure 6.17, page 63, the numerical model is able to estimate the behaviour observed in the measurements of Dissolved Oxygen. We can see that the model captures both daily and monthly variations. Nevertheless, by what was mentioned above, the water quality model is not able to exactly reproduce the measured values. This can be seen for example in the low correlation coefficients. The main reasons we attribute to these disparities are the uncertainty in the parameters

and in the model. Therefore, we will first discuss the impact of the uncertainty in the parameters on the output of the model. This will be followed by a similar discussion regarding the uncertainty in the model.

Once the uncertainty of the model has been addressed, we will focus on the performance of the model regarding the effects of the floating houses. This will mainly concern the impact of shade and increased wind.

6.3.1 Parameter Uncertainty

As presented in Section 4.2, page 23, the driving terms that characterize our system have been taken into account in our model. The effects of the simplifications and assumptions used are discussed in the following section. In here we focus on the determination of the free parameters. Therefore, for the sake of the analysis, we consider here that the equations used can adequately model the physics.

The first point to note is the limited size of the measurement data relative to the number of free parameters. This means that the free parameters are more sensitive to errors in the measurement data. As an example, consider the least squares fitting of a line to a set of data points. This line is defined by two free parameters. If only two data points are used the curve will pass by the two points. If one of the points has a high measurement error, this error will strongly affect the parameters that define the line. On the other hand, for the same measurement error, the larger the number of data points the more accurately we can obtain the free parameters. The same occurs in this work.

Another point to refer is the fact that the measurements performed were made at most four times in one day and typically once per day. Moreover, they constitute instantaneous measurements of Dissolved Oxygen. For this reason, and in order to compare the model results with the measurements, we had to run the model with a time step of 1hour for the zero dimensional model and 0.1hour for the one dimensional model. In the literature, see [Stefan and Fang, 1994, Antonopoulos and Gianniou, 2003], the measurements are daily averages which are used to calibrate the model that ran with a time step of one day. This averaging is particularly important since the models implemented are not able to capture the fine scale dynamics. Therefore, calibrating the model with instantaneous measurements adds error to the determination of the parameters since they model the system at a coarser scale.

In order to assess the sensitivity of our model to the parameters, we have made a sensitivity analysis. As described in sections 6.1.3, page 52, and 6.2.3, page 65, we have varied the free parameters and compared the output of the model. In both numerical models the sensitivity analysis indicates that the parameters involved in the photosynthesis (r_{oa}, $G_{\max}$) and respiration ($YCHO2$ and k_{rs}) have high sensitivity, see Figure 6.5, Figure 6.21, Figure 6.22 and Figure 6.23. This result was expected since these parameters are associated to the terms with larger contribution to the Dissolved Oxygen budget.

6.3.2 Model structure uncertainty

Having discussed the parameter uncertainty and its impact on the output of the model, we now address the limitations and implications of the assumptions used to construct

our two numerical models. First we discuss the zero dimensional model and then the one dimensional.

As was explained in more detail in Section 6.1, page 48, the zero dimensional model assumes an homogeneous distribution of Dissolved Oxygen (and all other quantities) over the three spatial dimensions. [Stefan and Fang, 1994] applied a similar model to different types of lakes and concluded that the model performed better in deeper lakes than in shallow ones. This is due to the more dynamic behaviour of shallow lakes. This dynamic behaviour was observed in our measurements with the Dissolved Oxygen distribution in the vertical direction changing from a homogeneous profile into one with large variations (6^{th}, 16^{th}, 21^{st} and 23^{rd} of August). Since this model is unaware of the vertical profile it is not able to account for these profile variations.

The one dimensional model adds variability in the vertical direction, see Section 6.2, page 58. Nevertheless, a similar assumption of homogeneity, now only in the horizontal plane, is considered. Therefore, as said before, heterogeneity in the horizontal plane will affect the performance of the model since it is captured by the measurement data but not by the model. Moreover, an important point is the vertical distribution of both the fixed parameters, e.g. plant biomass, water temperature, and some of the free parameters, e.g. the diffusion coefficient, k_z. For example, we verified that if we used a larger concentration of plant biomass in the active photosynthetic region, the model would perform much better. This assumption is reasonable since algae tend to exist where light is abundant. Nevertheless, we were unable to measure the vertical distribution of plant biomass in order to confirm if this assumption is correct.

Another parameter that we considered homogeneous over the depth was the turbulent diffusion. Since this parameter is strongly driven by the wind speed, we expect it to be larger in the top of the water column and smaller in the bottom. The treatment of the diffusion coefficient as a constant with a homogeneous distribution showed high sensitivity, especially in the lower parts of the water column, see Figure 6.24, page 68. In the literature is mentioned that the dispersion mechanisms of heat and Dissolved Oxygen are similar [Geankoplis, 1984, Henderson-Sellers, 1984] and the same coefficients are used in the heat and Dissolved Oxygen transport equations [Antonopoulos and Gianniou, 2003]. This was not implemented in the current model but is an important addition.

In both models the fact that we assume that both the fixed and free parameters do not change in time is a source of error. For example, in Figure 6.14, page 60, we can see that the plant biomass changes considerably during the period of one year. Therefore, it is expected that it changes during the 30 days of the simulation. A more detailed monitoring of the plant biomass would allow including this variation into the simulation.

6.3.3 Floating houses effects

The objective of this work is not confined to identifying if the floating houses have an impact on water quality, namely Dissolved Oxygen levels. We aim also to identify the effects that have a key role in this impact. The motivation for developing a numerical model of the pond under investigation stems precisely from this. As mentioned before, by constructing a numerical model for the lake we are able to identify the main terms that contribute to Dissolved Oxygen production and consumption. With this knowledge we

can isolate the external factors that interfere with these terms. Including these external factors in our model, we can estimate their impacts. In the future, this can help to pinpoint the areas for design improvement of floating houses.

We have identified two external factors: shade produced by the floating houses and increased wind speed due to the wind tunnel effect between two floating houses. We will discuss them and the results obtained with each of the numerical models.

The shadow effect was included in both the zero dimensional and the one dimensional models by reducing the available solar radiation, see Section 6.1.4 and Section 6.2.4, pages 55 and 70, respectively. In the zero dimensional model the results obtained agree with the measurements. In Figure 6.9, page 56, we can see that by introducing the shadow effect the predicted Dissolved Oxygen values are reduced in comparison to the simulation with no shadow effect. The same effect, with similar differences, is observed between the measurements of the open space (C) and floating houses (B). In the one dimensional model a similar behaviour was identified, Figure 6.29, page 71. Nevertheless, as mentioned earlier, the lower layers of the water column showed lower values of Dissolved Oxygen than the measurements.

The higher wind speed was included in the model by directly increasing the wind speed variable, which is one of the parameters of our model, see equations (4.5) to (4.7), pages 27 to 29. As can be seen, wind speed contributes to the reaeration term. By increasing the wind speed, the absolute value of the reaeration flux will increase. If the Dissolved Oxygen concentration is lower than the saturation value, the inflow of oxygen from the atmosphere will be larger. If on the other hand the Dissolved Oxygen concentration is higher than the saturation value, the outflow of oxygen to the atmosphere will be larger. This explains the discrepancy in the behaviour of the zero dimensional model when higher wind speeds are included. Reaeration is a flux that takes place only on the upper layer of the water body. According to our measurements, the upper layer was most of the time oversaturated, which implies that oxygen is transferred out of the system. Since in the zero dimensional model we take the average value of Dissolved Oxygen in the water column, this value will always be smaller than the saturation point. For this reason, in our zero dimensional model the reaeration flux is positive, that is, oxygen is being transferred from the atmosphere to the water. Increasing the wind speed will increase this positive flux, resulting in higher values of Dissolved Oxygen, instead of lower ones as in the measurements. For this reason we decided to extend our model into a one dimensional one. In this way we can simulate the vertical variation of Dissolved Oxygen. Indeed we saw that the reaeration flux became negative, as expected, see Figure 6.18, page 64. This resulted in a better representation of the measurement data. However, also in this case we have an overestimation of the Dissolved Oxygen in the bottom layer.

From this study it was not possible to clearly identify which of the two effects is predominant. First, because our model is characterized with knowledge uncertainty, and secondly because both of these effects take place in the same region of the water column, i.e. the top layers. We think that both effects play similar roles on average, changing from day to day depending on the wind speed and available solar radiation. Further research is needed, involving a better estimation of the parameters and a better description of the local conditions.

Chapter 7

Summary, Conclusions and Recommendations

7.1 Summary

A measurement campaign of Dissolved Oxygen and water temperature took place in the period between July and September 2013 at Harnaschpolder, where three floating houses where deployed over a small pond. The objective of the measurements was to identify whether differences in water quality, namely Dissolved Oxygen and water temperature, occurred and how the floating houses are responsible for these changes.

To better understand and estimate the effects of the floating houses, a numerical model for the Dissolved Oxygen budget was implemented. The Dissolved Oxygen model included photosynthesis, reaeration, respiration, decomposition and sediment oxygen demand as source and sink terms. The model was initially implemented as a box model (zero dimensional) and later extended to one dimensional, in order to include vertical variations. For both models the free parameters were determined and the models assessed against measured data. Finally the effects of floating houses were simulated.

The conclusions and recommendations for improvements and further research are presented on what follows next.

7.2 Conclusions

What are the effects of floating houses on the Dissolved Oxygen levels of the applied water body?

- The average values of the vertical profile show that during the measurement period the location situated between the floating houses showed the lowest values up to the first 1m.

- The levels of Dissolved Oxygen between the floating houses show a reduction of 10% (1mg/L) in comparison to the open space.
- The rate of change of Dissolved Oxygen with depth (gradient) can be up to 60% (2.5 $\text{mgL}^{-1}\text{m}^{-1}$, open space).

The shadow of the floating houses reduces available sunlight. This lowers the Dissolved Oxygen levels in their vicinity.

- The lower parts (1.5 to 2.0m) of the water column at the floating houses and open space showed similar values of Dissolved Oxygen.
- Before sunrise the upper parts (0 to 0.5m) of the water column start with approximately the same Dissolved Oxygen concentrations and temperatures but in the course of the day the open space location gains more oxygen than the floating houses location.
- In the end of the day, the two locations return to the same values of Dissolved Oxygen and temperature.
- In the numerical model, a solar radiation blockage of 40% reproduces the Dissolved Oxygen differences between the floating and the open space.

Wind tunnel effect is produced by the floating houses increasing the turbulence of the water. This increases the mixing in the water column which reduces the Dissolved Oxygen vertical gradient.

- For higher wind speeds the floating houses show a smaller dispersion of temperature differences than the open space, see Figure 5.15, page 46. This indicates that the floating houses experiences more mixing induced by wind compared to the open space. However, these differences are small. For example, for a wind speed of 6m/s, the maximum temperature differences are 2°C and 2.8°C for the floating houses and the open space respectively.
- In the 1D numerical model, an increase of 50% in the wind speed together with an increase of 25% in the diffusion coefficient reproduced the Dissolved Oxygen differences.

Close to the floating houses the water temperature gradient in the vertical direction will decrease.

- The average values of the vertical profile show that during the measurement period the location situated between the floating houses showed the lowest temperatures up to the first 1m.
- The average water temperature between the floating houses is 2.5% (0.5°C) lower than the open space.

- The maximum rate of change of water temperature with depth (gradient) is 5% (0.4°C/m, open space).

Below the floating houses a hypoxic area is created and oxygen is transferred laterally by the adjacent water column. This lowers the Dissolved Oxygen levels in their vicinity.

The averaged profile of Dissolved Oxygen showed that the lower part of the water column did not have any significant differences between the floating houses and the open space. However, no measurements were obtained from the area below the floating houses. Given the limits of the current research, the conditions below the floating houses are unknown. Therefore, it was not possible to assess this hypothesis. For this reason, we present recommendations in order to include this study in the future.

7.3 Recommendations

Based on the conclusions of the current research, the recommendations are divided into three categories. We will focus first on the measurement campaign, indicating additional physical quantities to be monitored and different measurement methodologies (e.g., spatial and temporal resolution, location of the measurements and equipment to use). Afterwards, we will address the recommendations regarding the modelling, pinpointing further applications and improvements. Finally, we will suggest additional environmental factors to be monitored for potential impact due to the installation of floating houses

7.3.1 Measurement campaign

- Continuous measurement of vertical profiles of Dissolved Oxygen concentration throughout the day and for long periods (preferably one year). A large set of measurement data is essential for an adequate calibration of the numerical model. Long-time measurement data allows for capturing the seasonal variability of the system.
- Continuous measurement of vertical profiles of water temperature throughout the day and for long periods (preferably one year). Monitoring of temperature is important since it is an input parameter for the kinetic equations and for the determination of the diffusion coefficient.
- Local wind speed and wind direction measurements between the floating houses and in the open space will assist in identifying the wind tunnel effect. These measurements will help to establish a potential relation between the increase of wind speed and Dissolved Oxygen variations. Additionally, the local wind speed measurements can be used in the estimation of the diffusion coefficient of oxygen in the water.
- Monitoring of the vertical profile of plant biomass. Such data are fundamental for the correct implementation of a numerical model since plant biomass determines one of the main sources of Dissolved Oxygen: photosynthesis.
- Extend the above mentioned measurements to the region below the floating houses.

- Monitor the water quality parameters in places with different water body characteristics, for example less eutrophicated, more flow.

7.3.2 Numerical modelling

- Comparison of the output of the current model with a more complex model such as DELWAQ from Deltares.
- Implementation of techniques of data assimilation (to include the measurement data in a more systematic way) and automated approaches for the determination of the free parameters.
- Implementation the one dimensional model on the horizontal direction and extension to a two dimensional model. This enables the modelling of the effect of the floating houses in the horizontal direction due to the reduction of the free surface, therefore the reaeration. The horizontal model would further enable us to assess the effect of multiple floating houses on the water surface. This would be an important step for the implementation of design guidelines. For example, the spacing between the floating houses without strongly affecting the water quality.
- A long term simulation that would indicate future long term impacts. This would further extend the numerical model as a policy tool.

7.3.3 Further developments

- Due to the future measurement needs outlined above, we recommend the development of a low cost automated water quality measurement system. This system can be assembled from OEM[1] measurement probes and controlled by currently existing integrated computer boards, such as the Raspberry PI, and microcontroller boards, such as the Arduino. This would allow for a considerable cost reduction in comparison with currently available commercial alternatives. Furthermore, it would allow for a continuous measurement and possibly online monitoring through the Internet.
- Investigate over other possible effects of floating houses: sedimentation, noise, light and thermal pollution.

[1] An original equipment manufacturer (OEM) manufactures products or components that are purchased by another company and retailed under that purchasing company's brand name.

References

[Addy and Green, 1997] Addy, K. and Green, L. (1997). Dissolved Oxygen and Temperature.

[Adur District Council, 2007] Adur District Council (2007). Good Practice Guide for Houseboats.

[Antonopoulos and Gianniou, 2003] Antonopoulos, V. Z. and Gianniou, S. K. (2003). Simulation of water temperature and dissolved oxygen distribution in Lake Vegoritis, Greece. *Ecological Modelling*, 160(1-2):39–53.

[Asfour, 2010] Asfour, O. S. (2010). Prediction of wind environment in different grouping patterns of housing blocks. *Energy and Buildings*, 42(11):2061–2069.

[Banks and Herrera, 1977] Banks, R. B. and Herrera, F. F. (1977). Effect of wind and rain on surface reaeration. *Journal of the Environmental Engineering Division*, 103(3):489–504.

[Bella, 1970] Bella, D. A. (1970). Dissolved oxygen variations in stratified lakes. *Journal of the Sanitary Engineering Division*, 96(5):1129–1146.

[Best et al., 2007] Best, M. A., Wither, A. W., and Coates, S. (2007). Dissolved oxygen as a physico-chemical supporting element in the Water Framework Directive. *Marine pollution bulletin*, 55(1-6):53–64.

[Bowie and Tech, 1985] Bowie, G. and Tech, T. (1985). Rates, constants, and kinetics formulations in surface water quality modeling.

[Burdick and Short, 1999] Burdick, D. M. and Short, F. T. (1999). The effects of boat docks on eelgrass beds in coastal waters of Massachusetts. *Environmental Management*, 23(2):231–240.

[Carlson and Simpson, 1996] Carlson, R. E. and Simpson, J. (1996). A coordinators guide to volunteer lake monitoring methods. *North American Lake Management Society*, 96.

[Chapra, 1997] Chapra, S. (1997). *Surface water-quality modeling*. Waveland Press, INC.

[Cussler, 2009] Cussler, E. L. (2009). *Diffusion: mass transfer in fluid systems*. Cambridge university press.

[D-Water Quality, 2013] D-Water Quality (2013). D-Water Quality.

[De Graaf, 2012] De Graaf, R. (2012). *Adaptive urban development*. Rotterdam Unversity Press, Rotterdam, 1st edition.

[DeltaSync, 2014] DeltaSync (2014). http://www.deltasync.nl.

[Directive 2000/60/EC, 2000] Directive 2000/60/EC (2000). Directive 2000/60/EC of the European Parliament and of the Council of 23 October 2000 establishing a framework for Community action in the field of water policy. *Official Journal of the European Communities*.

[Dobson et al., 1974] Dobson, H. F. H., Gilbertson, M., and Sly, P. G. (1974). A summary and comparison of nutrients and related water quality in Lakes Erie, Ontario, Huron, and Superior. *Journal of the Fisheries Board of Canada*, 31(5):731–738.

[Ekka et al., 2006] Ekka, S., Haggard, B., Matlock, M., and Chaubey, I. (2006). Dissolved phosphorus concentrations and sediment interactions in effluentdominated Ozark streams. *Ecological Engineering*, 26(4):375–391.

[Fang and Stefan, 1994] Fang, X. and Stefan, H. (1994). Temperature and dissolved oxygen simulations in a lake with ice cover. *Project Report*.

[Geankoplis, 1984] Geankoplis, C. J. (1984). Molecular mass transport phenomena in liquids. *Mass Transport Phenomena*, pages 124–130.

[Gielen and de Kwaadsteniet, 2009] Gielen, H. and de Kwaadsteniet, M. (2009). Rioleringsen waterstructuurplan Voordijkhoorn te Delft. Technical Report 27114147, Fugro Ingenieursbureau B.V.

[Ginot and Hervé, 1994] Ginot, V. and Hervé, J. (1994). Estimating the parameters of dissolved oxygen dynamics in shallow ponds. *Ecological modelling*, 61:169–187.

[Graaf, 2009] Graaf, R. D. (2009). *Innovations in urban water management to reduce the vulnerability of cities*. PhD thesis, Technische Universiteit Delft.

[Hartwich, 2014] Hartwich, H. (2014). *Preliminary study for an environmental impact assesment of floating cities*. PhD thesis, Universitat Potsdam.

[Hasadsri and Maleewong, 2012] Hasadsri, S. and Maleewong, M. (2012). Finite Element Method for Dissolved Oxygen and Biochemical Oxygen Demand in an Open Channel. *Procedia Environmental Sciences*, 13(2011):1019–1029.

[Heisler, 1986] Heisler, G. M. (1986). Effects of individual trees on the solar radiation climate of small buildings. *Urban Ecology*, 9(3-4):337–359.

[Henderson-Sellers, 1984] Henderson-Sellers, B. (1984). *Engineering limnology*. Pitman Advanced Pub. Program Boston.

[Hoefnagel and Raaphorst, 2013] Hoefnagel, R. and Raaphorst, E. (2013). Waterkwaliteit in de Harnaschpolder bij de waterwoningen. Technical report, Hoogheemraadschap van Delfland.

[Howe et al., 2011] Howe, C., Anton, B., Philip, R., and Morchain, D. (2011). Adapting Urban Water Systems. Technical report, SWITCH.

[Hupfer and Lewandowski, 2008] Hupfer, M. and Lewandowski, J. (2008). Oxygen Controls the Phosphorus Release from Lake Sediments - a Long-Lasting Paradigm in Limnology. *International Review of Hydrobiology*, 93(4-5):415–432.

[Hydrolab, 2006] Hydrolab (2006). Hydrolab DS5X, DS5, and MS5 Water Quality Multiprobes_User Manual. Technical Report 003078, Hach Company.

[Jean-Pierre and Sweerts, 1991] Jean-Pierre, R. and Sweerts, A. (1991). Oxygen-consuming processes at the profundal and littoral sediment-water interface of a small meso-eutrophic lake. *Limnol. Oceanogr*, 36(6):1124–1133.

[Ji, 2008] Ji, Z.-G. (2008). *Hydrodynamics and water quality: modeling rivers, lakes, and estuaries*. John Willey & Sons, Inc.

[Kettle and Thompson, 2004] Kettle, H. and Thompson, R. (2004). Empirical modeling of summer lake surface temperatures in southwest Greenland. *Limnology and ...*, 49(1):271–282.

[Kitazawa et al., 2010] Kitazawa, D., Tabeta, S., Fujino, M., and Kato, T. (2010). Assessment of environmental variations caused by a very large floating structure in a semi-closed bay. *Environmental monitoring and assessment*, 165(1-4):461–74.

[KNMI, 2010] KNMI (2010). Valkenburg, langjarige gemiddelden, tijdvak 1981-2010. Technical report.

[KNMI, 2013] KNMI (2013). Jaaroverzicht van het weer in Nederland,2013. Technical report, Koninklijk Nederlands Meteorologisch Instituut Ministrie Van Verkeer en Waterstaat.

[Kutty, 1987] Kutty, M. (1987). Chemical features of water.

[Loucks et al., 2005] Loucks, D. P., Van Beek, E., Stedinger, J. R., Dijkman, J. P. M., and Villars, M. T. (2005). *Water resources systems planning and management: an introduction to methods, models and applications*. Paris: UNESCO.

[Medrano, 2008] Medrano, E. A. (2008). *Urban Surface Water as Energy Source & Collector*. PhD thesis, TU Delft.

[Michaud, 1991] Michaud, J. (1991). Citizens' guide to understand and monitoring lakes and streams. Technical Report 6295, Washington state department of ecology.

[Mwegoha et al., 2011] Mwegoha, W., Kaseva, M., and Sabai, S. (2011). Mathematical Modeling of Dissolved Oxygen in Fish Ponds. *International Journal of Environmental Research*, 5(2):307–320.

[National Academy of Sciences, 1972] National Academy of Sciences (1972). Water quality criteria. Technical report, Engineering, National Academy of Science and National Academy of.

[Nilessen and Jeroen, 2011] Nilessen, A. L. and Jeroen, S. (2011). *Waterwonen in Nederland*. NAi Uitgevers.

[Paerl et al., 2001] Paerl, H. W., Fulton, R. S., Moisander, P. H., and Dyble, J. (2001). Harmful freshwater algal blooms, with an emphasis on cyanobacteria. *TheScientificWorldJournal*, 1:76–113.

[Park et al., 2005] Park, K., Jung, H.-S., Kim, H.-S., and Ahn, S.-M. (2005). Three-dimensional hydrodynamic-eutrophication model (HEM-3D): application to Kwang-Yang Bay, Korea. *Marine Environmental Research*, 60(2):171–193.

[Penning et al., 2003] Penning, E., Bakkum, R., Holleman, E., and Filius, J. (2003). Drijvende kassen: waterberging in een nieuw kassengebied. *H2O*, 23:39–42.

[Pieters and Aendekerk, 2013] Pieters, B. and Aendekerk, T. (2013). Monitoring waterkwaliteit drijvende teeltvloer. Technical report, Gemeente Boskoop, Grontmij Nederland B.V.

[Rast and Lee, 1983] Rast, W. and Lee, G. F. (1983). Nutrient loading estimates for lakes. *Journal of Environmental Engineering*, 109(2):502–517.

[Riley and Stefan, 1988] Riley, M. J. and Stefan, H. G. (1988). MINLAKE: A dynamic lake water quality simulation model. *Ecological Modelling*, 43:155–182.

[Rucinski et al., 2010] Rucinski, D. K., Beletsky, D., DePinto, J. V., Schwab, D. J., and Scavia, D. (2010). A simple 1-dimensional, climate based dissolved oxygen model for the central basin of Lake Erie. *Journal of Great Lakes Research*, 36(3):465–476.

[Sakamoto, 1966] Sakamoto, M. (1966). Primary production by phytoplankton community in some Japanese lakes and its dependence on lake depth. *Arch. Hydrobiol.*, 62:1–28.

[Silvis et al., 2003] Silvis, L., Diermanse, F., Penning, E., Bakkum, R., Gehrels, J. C., and Swierstra, W. (2003). Haalbaarheidsstudie Drijvende Kassen. Aanvullingen. Technical report.

[Stefan et al., 1989] Stefan, H. G., Ambrose, R. B., and Dortch, M. S. (1989). Formulation of water quality models for streams, lakes and reservoirs: modeler's persperctive. Technical report, US Army Corps of Engineers.

[Stefan and Fang, 1994] Stefan, H. G. and Fang, X. (1994). Dissolved oxygen model for regional lake analysis. *Ecological Modelling*, 71(1-3):37–68.

[Stefan et al., 1993] Stefan, H. G., Hondzo, M., and Fang, X. (1993). Lake Water Quality Modeling for Projected Future Climate Scenarios. *Journal of Environmental Quality*, 22(3):417–431.

[Tauw, 2014] Tauw (2014). http://www.tauw.nl.

[USEPA, 1974] USEPA (1974). Relationships of Phosphorus and Nitrogen to the Trophic State of Northeast and North-Central Lakes and Reservoirs. Technical report, USEPA.

[Wang et al., 2013] Wang, Q., Li, S., Jia, P., Qi, C., and Ding, F. (2013). A review of surface water quality models. *The Scientific World Journal*, 2013:7.

[Wanninkhof, 1992] Wanninkhof, R. (1992). Relationship between wind speed and gas exchange over the ocean. *Journal of Geophysical Research: Oceans*, 97(C5):7373–7382.

[Williams, 2007] Williams, N. (2007). *Modelling Dissolved Oxygen in Lake Powell Using CE-QUAL-W2*. PhD thesis, Brigham Younf University.

[Wilson, 2010] Wilson, P. C. (2010). Water Quality Notes : Water Clarity (Turbidity, Suspended Solids, and Color). Technical report, University of Florida.

Appendix A

Air to water temperature conversion

Water temperature is important for the biological activity in the water column as well as the determination of the Dissolved Oxygen saturation levels. However, water temperatures were only measured continuously in the month of September. On the other hand, in the month of August we have more measurements for Dissolved Oxygen. Therefore we have to find a method to obtain the water temperature in the month of August. The method described in Section 4.2.1.7, page 30, converts the local air temperature into water temperature. However, the local air temperature in Glasloksingel (floating houses site) was only measured during the month of September. Nevertheless, there are available air temperature measurements from a nearby meteorological station (Tanthof). For this reason we need to find a methodology to convert the air temperature in Tanhof to water temperature in Glasloksingel.

Three different approaches have been considered:

i. Use the measured air and water temperatures in Glasloksingel to find the optimal k parameter in (4.13), see top left plot in Figure A.1. Apply (4.13) with the optimal k parameter to the air temperature in Tanthof, see bottom left plot in Figure A.1.

ii. Use the air temperature of Tanthof and the measured water temperature in Glasloksingel to find the optimal k parameter in (4.13), see bottom right plot in Figure A.1.

iii. Use the measured air and water temperatures in Glasloksingel to find the optimal k parameter in (4.13), see top left plot in Figure A.1. Convert the air temperature in Tanthof into air temperature in Glasloksingel using a linear regression, see Figure A.2. Apply (4.13) with the optimal k parameter to the corrected air temperature in Tanthof, see top right plot in Figure A.1.

The summarized results of the different methodologies are presented in Table A.1. As can be seen, the approach with the corrected Tanthof temperature (iii) is the one showing the best results. Therefore in the numerical model we applied this approach.

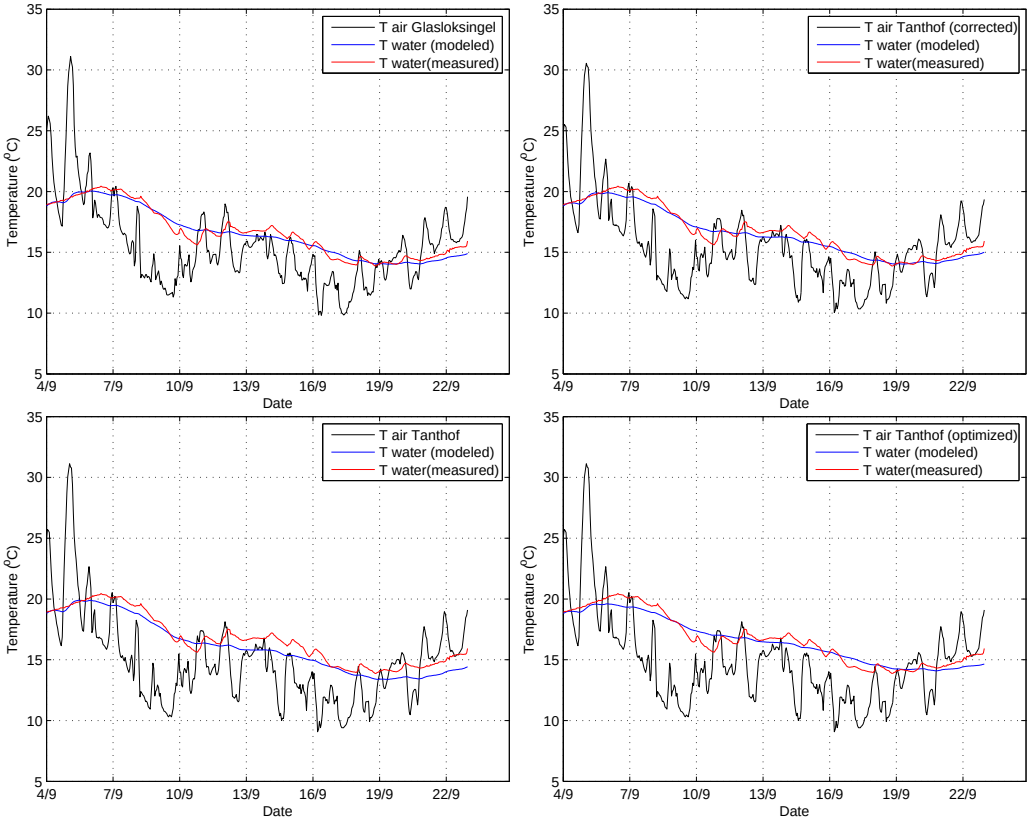

Figure A.1: Modelled and measured water temperature for September for different methodologies.

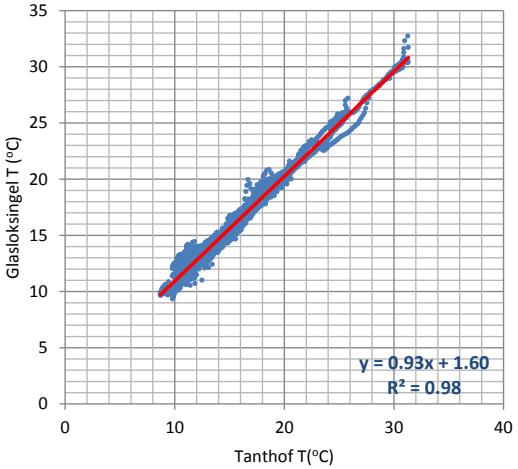

Figure A.2: Tanthof air temperature correction.

Table A.1: Air to water temperature model evaluation results.

Month	Input	RMSE	r
September	$T_{\text{Glasloksingel}}$	0.43	0.98
	T_{Tanthof}	0.73	0.98
	$T_{\text{corrected}}$	0.45	0.98
	$T_{\text{optimized}}$	0.54	0.97
August	T_{Tanthof}	0.84	0.95
	$T_{\text{corrected}}$	0.67	0.95
	$T_{\text{optimized}}$	0.74	0.94

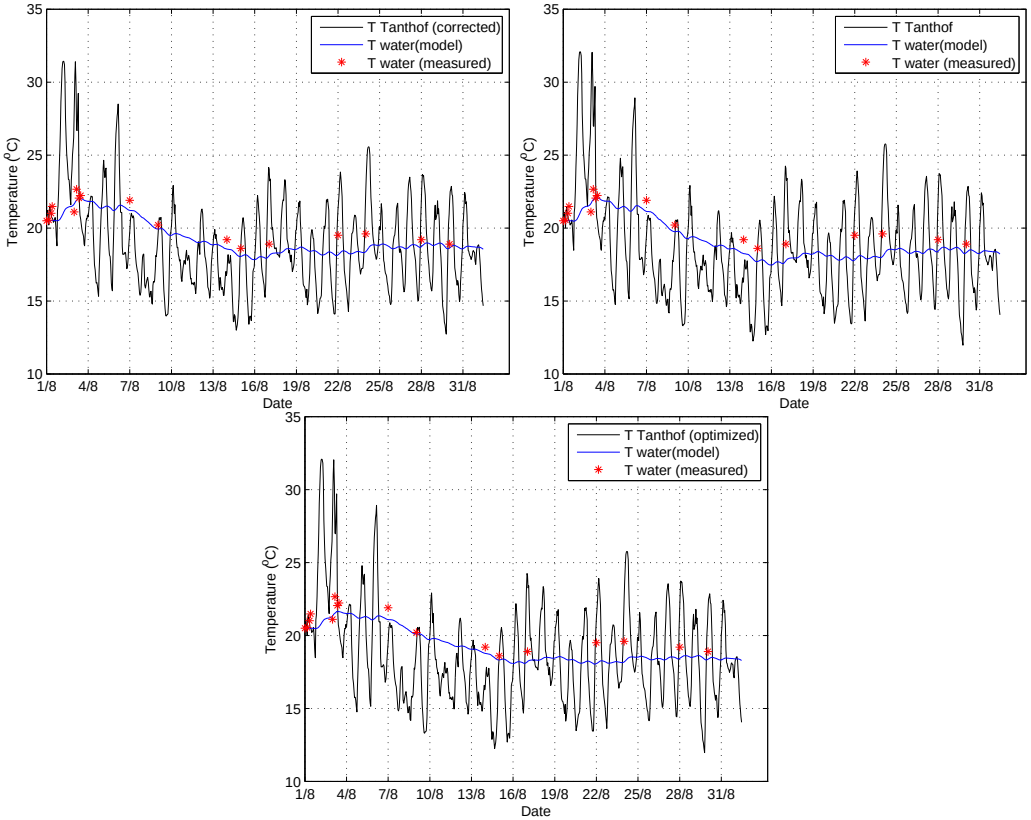

Figure A.3: Modelled and measured water temperature for August for different methodologies.

Appendix B

Statistical error analysis

For the evaluation of the numerical model for the Dissolved Oxygen budget and the conversion of air to water temperature we used the Root Mean Square Error ($RMSE$) and the correlation coefficient (r). The $RMSE$ of a model prediction, X_{model}, with respect to the estimated variable is defined as:

$$RMSE = \sqrt{\frac{\sum_{i=1}^{n} \left(X_{\text{obs},i} - X_{\text{model},i}\right)^2}{n}} \,. \tag{B.1}$$

Where $X_{\text{obs},i}$ and $X_{\text{model},i}$ are respectively the observed and modelled values at time (or position) i. It is straightforward to see that a value of RMSE=0 is ideal.

The Pearson correlation of coefficient (r_{p}) is a qualitative expression of the relationship between the observed and the modelled values. The Pearson correlation coefficient varies from 1 (perfect linear relation) to -1 (perfect negative linear relation), passing by 0 (no relation or vary small). The expression for the Pearson correlation coefficient is given by:

$$r_{\text{p}} = \frac{\sum_{i=1}^{n} \left(X_{\text{obs},i} - \overline{X}_{\text{obs}}\right)\left(X_{\text{model},i} - \overline{X}_{\text{model}}\right)}{\sqrt{\sum_{i=1}^{n} \left(X_{\text{obs},i} - \overline{X}_{\text{obs}}\right)^2 \sum_{i=1}^{n} \left(X_{\text{model},i} - \overline{X}_{\text{model}}\right)^2}} \,. \tag{B.2}$$

Where the same nomenclature of equation (B.1) was used and $\overline{X}_{\text{obs}}$ and $\overline{X}_{\text{model}}$ are the averages of the observed and modelled values, respectively.

The Spearman correlation coefficient is defined as the Pearson correlation coefficient for ranked variables. It assesses how well a monotonic function describes the relation between two variables. A perfect monotonic relation is indicated by a Spearman coefficient of ± 1. Consider the ordered sets of modelled and observed data: $(X_{\text{model},i}, k_{\text{model},i})$ and $(X_{\text{obs},i}, k_{\text{obs},i})$, where $k_{\text{model},i}$ and $k_{\text{obsl},i}$ are the indices that indicate the rank associated with the ordering of the data. Then the Spearman correlation coefficient is given by:

$$r_{\text{s}} = 1 - \frac{6 \sum_{i=1}^{n} \left(k_{\text{model},i} - k_{\text{obs},i}\right)^2}{n\left(n^2 - 1\right)} \,. \tag{B.3}$$

Appendix C

Divers temperature correction

An interesting fact regarding the measured water temperature is that during the period in which water temperature was measured by the divers (4^{th} to 23^{rd} of September), position B showed higher temperatures than position C, see Figure C.1. These temperature differences can be up to 1.5°C, leading to different Dissolved Oxygen saturation levels. These results come into contradiction with the temperature measurements made with the probe (19^{th} of July to 23^{rd} of September), see Table C.1. Here we can see that in most of the cases shown, although the temperatures of the divers have differences up to 0.5°C between positions B and C, the probe has no significant differences in the temperatures. This led us to consider the possibility of a different calibration between the divers. For this reason, we computed the average differences between the probe measurements and the diver measurements see Table C.2. As can be seen, between the divers at positions B and C there is a difference of 0.56°C at the depth of 0.7m and a difference of 0.14°C at the depth of 2.0m. These values were used to correct the temperatures of the divers transforming the temperatures seen in Figure C.1 into the corrected values of Figure C.2.

Table C.1: Temperature comparison between probe and diver measurements.

Date	Temperature Diver (°C)	Temperature Probe (°C)	Temperature Diver (°C)	Temperature Probe (°C)
	Position B, $z = 0.7$m		Position C, $z = 0.7$m	
5^{th} September	18.75	19.62	18.30	19.58
21^{st} September	13.40	14.57	12.95	14.54
23^{rd} September	14.68	15.68	14.55	16.39
	Position B, $z = 2.0$m		Position C, $z = 2.0$m	
5^{th} September	18.17	17.76	17.96	17.76
21^{st} September	-	-	-	-
23^{rd} September	14.47	14.17	14.43	14.19

Table C.2: Average temperature difference between divers and probe.

Depth	Position B	Position C
0.7m	-1.01	-1.57
2.0m	0.36	0.22

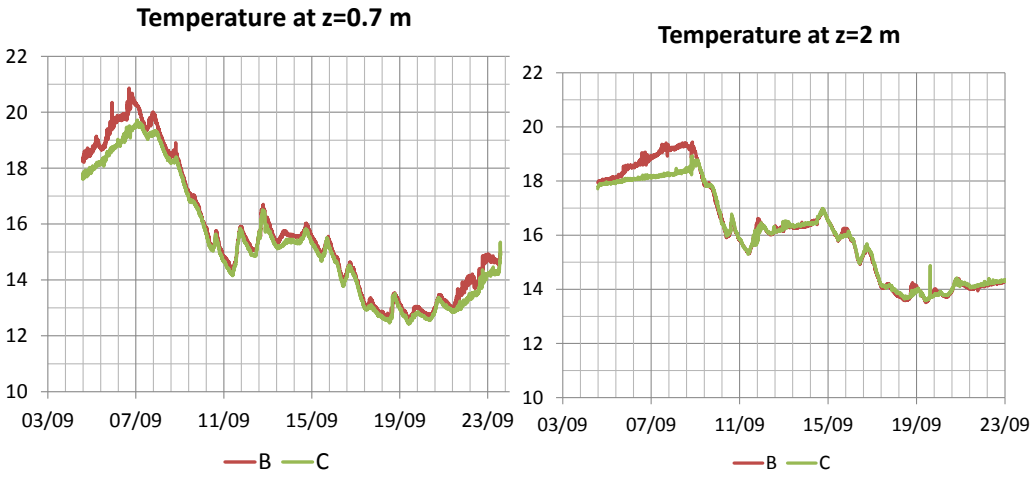

Figure C.1: Temperature measured by divers at positions B and C.

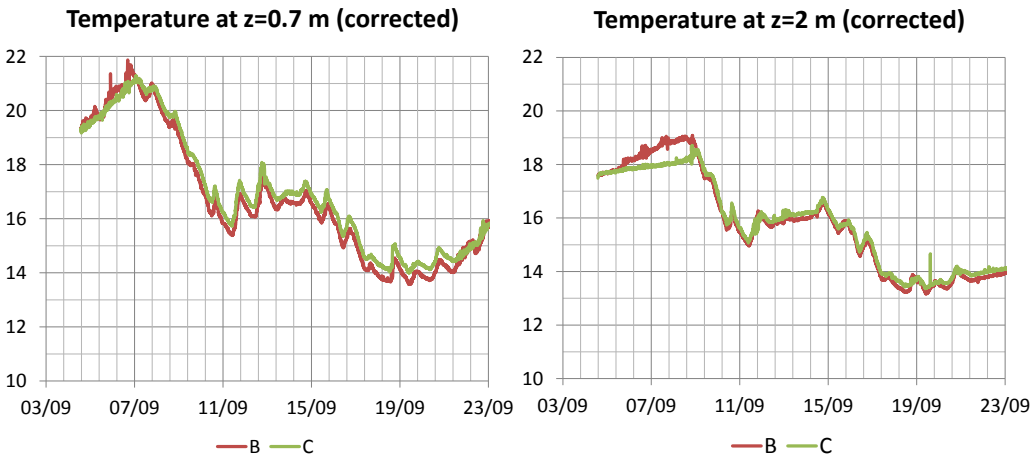

Figure C.2: Temperature measured by divers at positions B and C, corrected.

Appendix D

Field measurement complementary information

Table 5.2 shows the differences in Dissolved Oxygen between the floating houses locations and the open space at each measurement depth. The negative values indicate that the Dissolved Oxygen at the floating houses is lower.

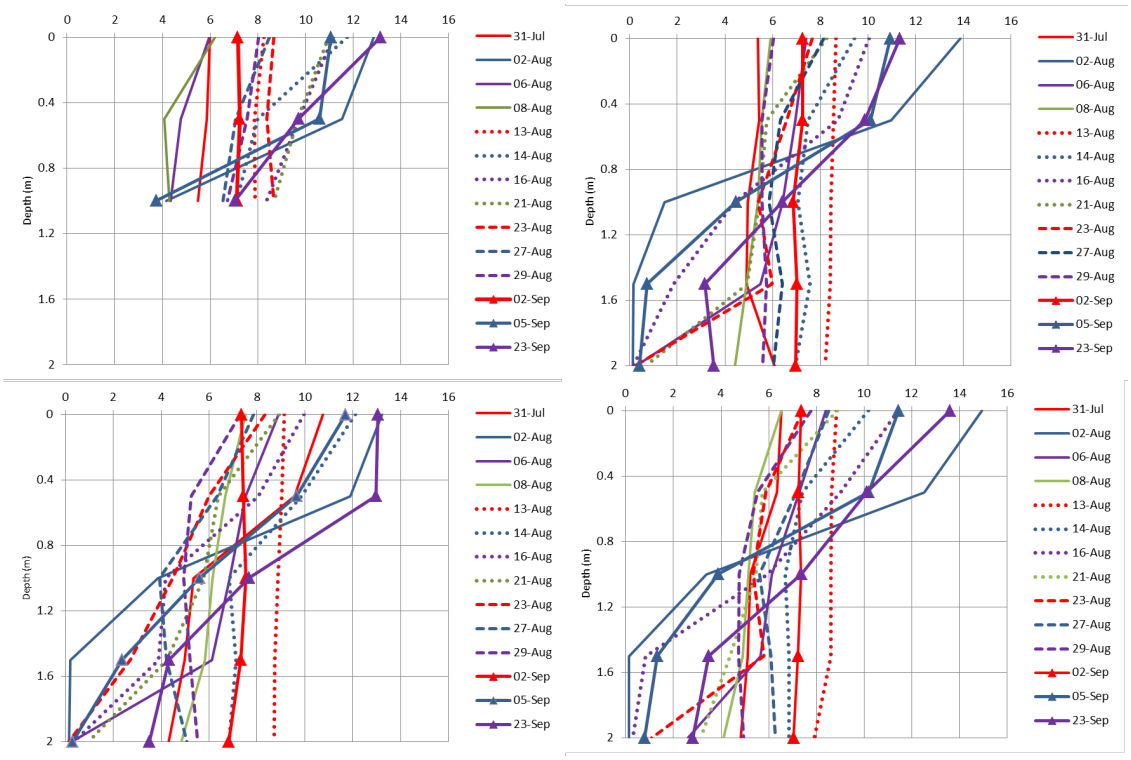

Figure D.1: Vertical Dissolved Oxygen profiles for measurements points A, B, C and D (right to left, top to bottom).

Table D.1: Dissolved Oxygen differences between floating house positions and open space position, $DO_{\mathrm{B}} - DO_{\mathrm{C}}$ (left) and $DO_{\mathrm{D}} - DO_{\mathrm{C}}$ (right).

	$DO_{\mathrm{B}} - DO_{\mathrm{C}}$					$DO_{\mathrm{D}} - DO_{\mathrm{C}}$				
	$z = 0$m	$z = 0.5$m	$z = 1.0$m	$z = 1.5$m	$z = 2.0$m	$z = 0$m	$z = 0.5$m	$z = 1.0$m	$z = 1.5$m	$z = 2.0$m
31-Jul	-5.40	-4.14	-0.40	-0.06	1.75	-4.23	-3.21	-0.14	0.14	0.05
02-Aug	0.66	-0.91	-2.40	-0.03	-0.03	1.71	0.64	-0.47	-0.06	0.03
06-Aug	-1.50	-0.58	-0.42	-0.61	0.04	-0.51	-0.25	-0.73	-0.45	-0.18
08-Aug	-1.60	-1.14	-0.76	-0.92	-0.43	-0.99	-1.27	-1.01	-0.92	-0.07
13-Aug	-0.47	-0.47	-0.42	-0.32	-0.53	-0.29	-0.38	-0.26	-0.14	-0.05
14-Aug	-2.69	-2.37	0.24	0.44	0.13	-1.93	-2.47	-0.14	-0.28	0.00
16-Aug	0.07	0.69	0.21	-2.04	-0.19	1.46	0.95	1.77	-3.06	-0.07
21-Aug	-0.67	-0.63	-0.32	0.70	-0.29	-0.06	-0.65	-0.31	0.14	0.02
23-Aug	-0.65	0.61	0.90	3.25	0.09	-0.90	-0.12	0.86	3.09	0.03
27-Aug	0.29	-0.02	1.92	2.20	0.96	0.67	0.80	1.68	1.86	0.03
29-Aug	-1.26	0.30	0.61	0.52	0.07	0.46	0.27	-0.18	-0.48	0.03
02-Sep	-0.08	-0.19	-0.67	-0.29	0.13	0.00	-0.21	-0.19	-0.09	-0.02
05-Sep	-0.77	0.45	-1.12	-1.64	0.13	-0.25	0.53	-1.72	-1.05	0.11
23-Sep	-1.74	-3.10	-1.25	-1.15	0.03	0.54	-2.86	-0.30	-0.85	-0.03

Appendix E

Vertical profiles of one dimensional model

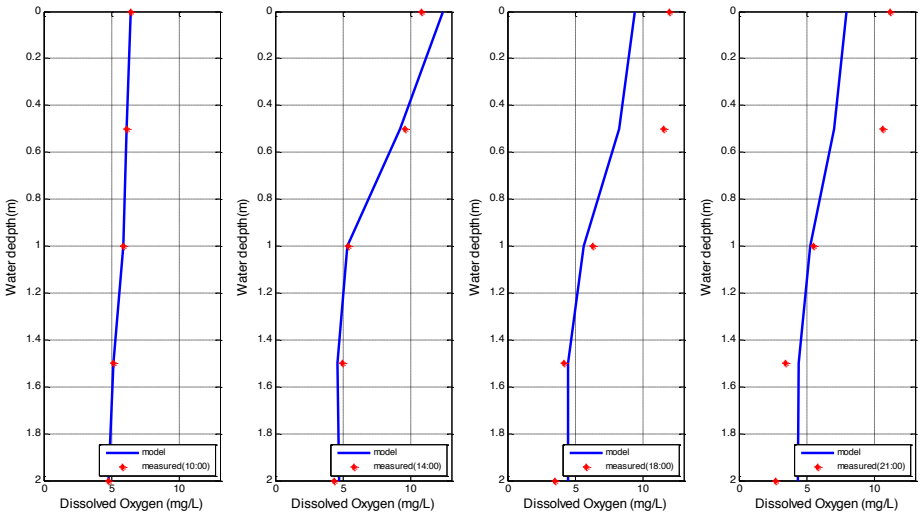

Figure E.1: Vertical Dissolved Oxygen profiles of July 31st.

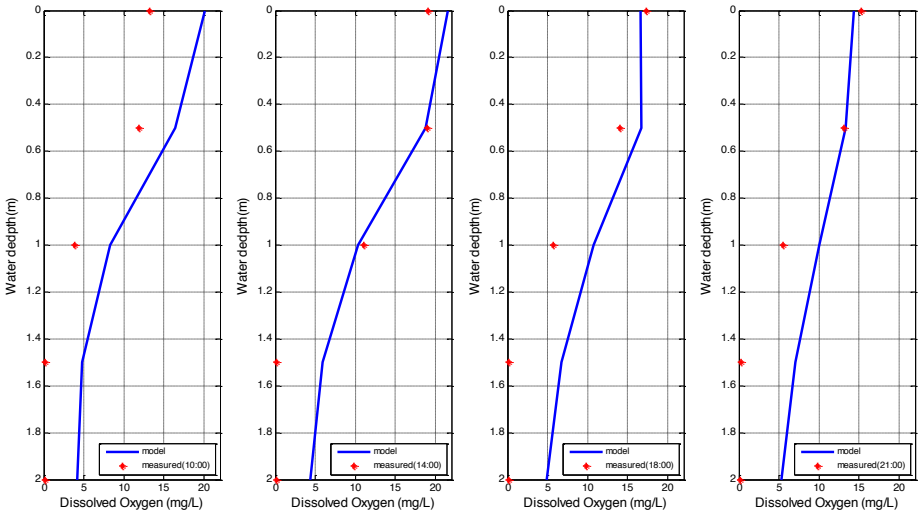

Figure E.2: Vertical Dissolved Oxygen profiles of August 2nd.

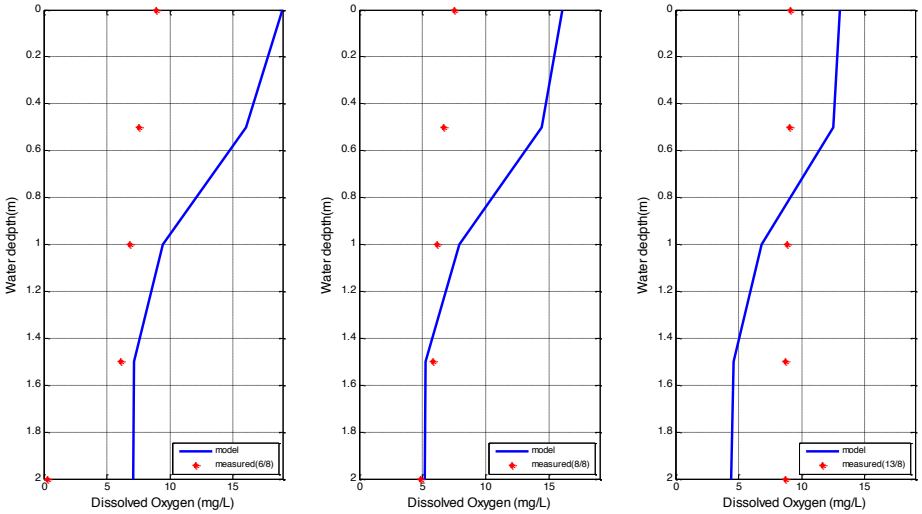

Figure E.3: Vertical Dissolved Oxygen profiles of August 6th, 8th and 13th.

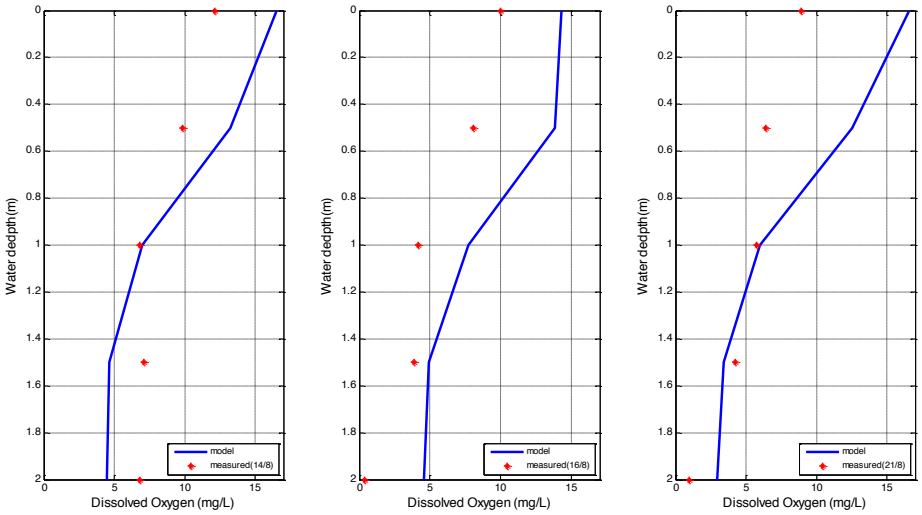

Figure E.4: Vertical Dissolved Oxygen profiles of August 14th, 16th and 21st.

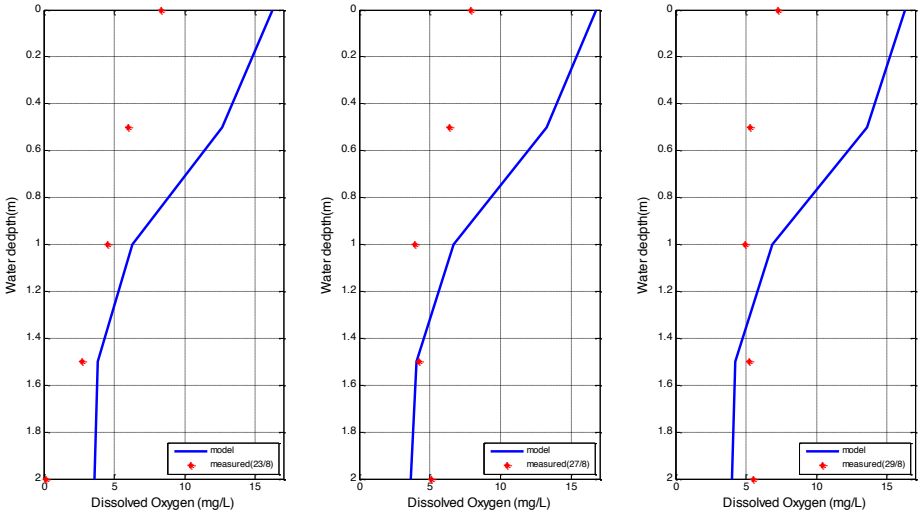

Figure E.5: Vertical Dissolved Oxygen profiles of August 23rd, 27th and 29th.

Appendix F

Zero dimensional code

```
function [O,Pt,Ft,Dt,Rt,St,Osat,t] = OxygenBudgetEvolution_0D(...
                                        O_initial,dt,Chla,alpha,Gmax,...
                                        krs,thetars,YCHO2,kb,BOD,Sb,...
                                        reaeration_model,Secchi,H,...
                                        beta,I0,W,T)
    % OxygenBudgetEvolution computes the Dissolved Oxygen evolution
    % in time given an initial condition and the parameters.
    %
    % INPUTS
    %   O_initial :: initial Dissolved Oxygen concentration (mg/l)
    %   dt :: the time step used in the simulation (h)
    %   Chla:: concetration of the chlorophyll-a (mg/L)
    %   alpha:: mg of oxygen produced per mg of Chloropyll-a (mgO2/mgChla)
    %   Gmax:: Maximum value for algae growth[h-1]
    %   krs:: respiration rate [h-1]
    %   thetars:: temperature adjustment for respiration [h-1]
    %   YCHO2:: ratio of mg Chla to mg oxygen utilised in r
    %           espiration [mgChla/mgO2]
    %   kb:: decomposition rate [h-1]
    %   BOD:: Biological Oxygen demand [mg/L]
    %   Sb:: Sediment Oxygen Demand coefficient[gO2/m^2h]
    %        depending on the trophic state
    %   reaeration_model:: Calculation of the surface oxygen
    %                      transfer velocity [m/h]/ models to choose
    %                      banks wanninkhof
    %   Secchi::Secchi disk depth [m]
    %   H:: Water depth (m)
    %   beta :: effective percentage of solar radiation used
    %   Is :: Solar radiation hourly[W/m^2]
    %   W:: Wind speed (m/s) measured in Tanthof
    %   T:: Water temperature (oC)

    % OUTPUTS
    %   O:: Modeled dissolved oxygen
    %   Pt:: Modeled oxygen production by photosynthesis
    %   Ft:: Modeled oxygen production by reaeration
```

```
37      %   Dt:: Modeled oxygen consumption by decomposition
38      %   Rt:: Modeled oxygen consumption by respiration
39      %   St:: Modeled oxygen consumption by sediment
40      %   Osat:: Estimated Staurated Dissolved Oxygen
41      %   t:: time of the simulation
42
43      % Compute the available solar radiation
44      Is = beta.*I0; %Solar radiation hourly [W/m^2]
45
46      % Determine the number of time steps
47      tSteps = length(I0); % Hours in the month of simulation
48
49      % Compute the extinction coefficient
50      ke=(1.8./Secchi); % Extinction coefficient [m^-1]
51
52      % DECOMPOSITION
53      thetab = (T>20)*1.047 + (T<=20)*1.13; % TEMPERATURE ADJUSTMENT
54                                            % COEFFICIENT [-]
55
56      %% SEDIMENT OXYGEN DEMAND
57      thetas = (T>10)*1.065 + (T<=10)*1.13; % Temperature Adjustment
58                                            % Coefficient [-]
59
60      %% Initialize quantities to compute as zero vectors
61      Pt = zeros(1,tSteps);
62      Ft = zeros(1,tSteps);
63      Dt = zeros(1,tSteps);
64      Rt = zeros(1,tSteps);
65      St = zeros(1,tSteps);
66      Osat = zeros(1,tSteps);
67
68      %% Compute time vector
69      t = dt*(0:tSteps);
70
71      %% Initialize Dissolved Oxygen as a zero vector and assign
72      % the initial value
73      O = zeros(1,tSteps+1);
74      O(1) = O_initial;
75
76      %% Advance in time the oxygen concentration
77
78      for k=1:(tSteps)
79
80          Pt(k) =  Photosynthesis2_0D(H,Is(k),ke,T(k),alpha,Gmax,Chla);
81          Rt(k) = respiration(YCHO2,krs,thetars,T(k),Chla);
82          Dt(k) = Decomposition(kb,thetab(k),T(k),BOD);
83          St(k) = sediment(H,Sb,thetas(k),T(k));
84          Ft(k) = reaeration_flux(W(k),T(k),O(k),H,reaeration_model);
85
86          if O(k)<2 % my sediment oxygen demand is zero when the
87                    % DO levels are less than 2 mg/L [DELWAQ]
88            St(k)=0;
89          end
90
91          O(k+1) = O(k) + dt.* (Pt(k) - Rt(k) -  Dt(k) - St(k)+ Ft(k));
92
93          if O(k+1)<0 % in order to exclude negative values in the
94                      % Dissolved Oxygen  budget
```

```
95              O(k+1)=0;
96          end
97          Osat(k) = Saturated_O2(T(k));
98      end
99
100     Osat(end) = Osat(end-1);
101
102 end
```

Appendix G

One dimensional code

```
1
2  function [O,Pt,Ft,Dt,Rt,St,Osat,t,z_DO] = OxygenBudgetEvolution_1D(...
3                      O_initial,z_initial,dt,NVolumes,nu,Chla,alpha,...
4                      Gmax,krs,thetars,YCHO2,kb,BOD,Sb,reaeration_model,...
5                      Secchi,H,beta,I0,W,T)
6      % OxygenBudgetEvolution_1D computes the Dissolved Oxygen evolution
7      % in 1D in time given an initial condition and the parameters.
8      %
9      % INPUTS
10     %   O_initial :: initial Dissolved Oxygen concentration (in depth,
11     %                from top to bottom) (mg/l)
12     %   z_initial :: depth location of the initial oxygen distribution
13     %   dt :: the time step used in the simulation (h)
14     %   NVolumes :: the number of volumes in which the water column is
15     %               to be divided in.
16     %   nu :: the coefficient of Oxygen diffusion in water
17     %   Chla:: concetration of the chlorophyll-a (mg/L)
18     %   alpha:: mg of oxygen produced per mg of Chloropyll-a (mgO2/mgChla)
19     %   Gmax:: Maximum value for algae growth[h-1]
20     %   krs:: respiration rate [h-1]
21     %   thetars:: temperature adjustment for respiration [h-1]
22     %   YCHO2:: ratio of mg Chla to mg oxygen utilised in respiration
23     %           [mgChla/mgO2]
24     %   kb:: decomposition rate [h-1]
25     %   BOD:: Biological Oxygen demand [mg/L]
26     %   Sb:: Sediment Oxygen Demand coefficient[gO2/m^2h] depending on
27     %        the trophic state
28     %   reaeration_model:: Calculation of the surface oxygen transfer
29     %                      velocity [m/h) / models to choose banks
30     %                      wanninkhof
31     %   Secchi::Secchi disk depth [m]
32     %   H:: Water depth (m)
33     %   beta :: effective percentage of solar radiation used
34     %   Is :: Solar radiation hourly[W/m^2]
35     %   W:: Wind speed (m/s) measured in Tanthof
36     %   T:: Water temperature (oC)
```

```
37
38      % OUTPUTS
39      %   O:: Modeled dissolved oxygen
40      %   Pt:: Modeled oxygen production by photosynthesis
41      %   Ft:: Modeled oxygen production by reaeration
42      %   Dt:: Modeled oxygen consumption by decomposition
43      %   Rt:: Modeled oxygen consumption by respiration
44      %   St:: Modeled oxygen consumption by sediment
45      %   Osat:: Estimated Staurated Dissolved Oxygen
46      %   t:: time of the simulation
47
48      % Compute the available solar radiation
49      Is = beta.*I0; %Solar radiation hourly [W/m^2]
50
51      % Determine the number of time steps
52      tSteps = length(I0); % Hours in the month of simulation
53                           % (August)
54
55      % Compute the extinction coefficient
56      ke=(1.8./Secchi); % Extinction Coefficient [m^-1]
57
58      % Decomposition
59      thetab = (T>20)*1.047 + (T<=20)*1.13; % Temperature Adjustment
60                                            % Coefficient [-]
61
62      % Sediment Oxygen Demand
63      thetas = (T>10)*1.065 + (T<=10)*1.13;     % Temperature Adjustment
64                                                % Coefficient [-]
65
66      % Initialize quantities to compute as zero vectors
67      Pt = zeros(NVolumes,tSteps);
68      Ft = zeros(1,tSteps);          % Reaeration exists only
69                                     % on the surface layer
70      Dt = zeros(NVolumes,tSteps);
71      Rt = zeros(NVolumes,tSteps);
72      St = zeros(1,tSteps);          % Oxygen consumption by
73                                     % sediment exists only on
74                                     % the bottom layer
75      Osat = zeros(1,tSteps);
76
77      % Compute time vector
78      t = dt*(0:tSteps);
79
80      % Compute the spacing vector
81      z_fluxes = linspace(0,H,NVolumes+1)'; % the location of the fluxes
82      z_DO = 0.5*(z_fluxes(2:end)+z_fluxes(1:end-1)); % the location of
83                                                      %the DO densities
84
85      % Compute the spacing
86      dz = z_fluxes(2)-z_fluxes(1);
87
88      % Initialize Dissolved Oxygen as a zero matrix and assign the
89      % initial value
90      O = zeros(NVolumes,tSteps+1);
91
92      % Compute the initial condition at the cell centers/use
93      % interpolation (use pchip to avoid negative values)
94      O_initial_fine = interp1(z_initial,O_initial,z_DO,'pchip');
```

```
95      O(:,1) = O_initial_fine;
96
97      % Initialize the fluxes as zero
98      Q = zeros(NVolumes+1,tSteps+1);
99
100     % Initialize the variation of DO due to diffusion
101     DO_dt_diffusion = zeros(NVolumes,tSteps+1);
102
103     % Advance in time the oxygen concentration
104
105     for k=1:(tSteps)
106         Pt(:,k) =  Photosynthesis2(z_DO,Is(k),ke,T(k),alpha,Gmax,Chla);
107         Rt(:,k) = respiration(YCHO2,krs,thetars,T(k),Chla);
108         Dt(:,k) = Decomposition(kb,thetab(k),T(k),BOD);
109         St(k) = sediment(dz,Sb,thetas(k),T(k));
110         Ft(k) = reaeration_flux(W(k),T(k),O(1,k),dz,reaeration_model);
111
112         if O(end,k)<2 % my sediment oxygen demand is zero when the DO
113                       % levels are less than 2 mg/L [DELWAQ]
114           St(k)=0;
115         end
116
117         % Compute the fluxes between cells due to diffusion
118         Q(2:end-1,k) = (nu/dz)*(O(2:end,k)-O(1:end-1,k));
119
120         % Assign the top and bottom fluxes
121         Q(1,k) = -Ft(k)*dz; % the top flux is the reaeration
122         Q(end,k) = -St(k)*dz; % the bottom flux is the sediment oxygen
123                               % consumption
124
125         % Compute the variation of density of DO due to the diffusion,
126         %reaeration and sediment consumption
127         DO_dt_diffusion(:,k) = (Q(2:end,k)-Q(1:end-1,k))/dz;
128
129         % Compute the DO oxygen evolution
130
131         O(:,k+1) = O(:,k) + dt.* (Pt(:,k) -(z_DO<1.5).* Rt(:,k)...
132                     - Dt(:,k) + DO_dt_diffusion(:,k));
133
134         O((O(:,k+1)<0),k+1) = 0.0; % in order to exclude negative
135                                    % values in the Dissolved Oxygen  budget
136
137         Osat(k) = Saturated_O2(T(k));
138     end
139     Osat(end) = Osat(end-1);
140 end
```

Appendix H

Photosynthesis code

H.1 One dimensional code

```
function P = Photosynthesis2(z,I,eta,T,alpha,Gmax,Chla)
    % INPUTS
    %   z :: depths where to compute photosynthesis production (m)
    %   I :: available solar radiation just below the water surface (w/m^2)
    %   eta :: the light extinction coefficient (m^-1)
    %   T :: the temperature of the water at z
    %   alpha :: the ratio of Chlorophyl to oxygen utilized
    %   Chla :: the concentration of Chlorophyl
    %   Gmax :: the algae growth factor
    %
    % OUTPUTS
    %   P :: oxygen production by photosynthesis at depth k [gO2/L]

    if I < 10
        P = zeros(size(z));
    else
        Pm = alpha*Gmax*((1.066).^(T-20))*Chla;
        % compute the optical depth
        tau = eta.*z./log(2);

        Ik = 1.5625.*T;
        sigma = ((log(I)-log(0.5*Ik))/log(2))*sqrt(2/pi);

        P = Pm.*exp(-(tau.*tau)./(2*sigma.*sigma));
    end
end
```

H.2 Zero dimensional code

```
function P  = Photosynthesis2_0D(depth,I,eta,T,alpha, Gmax,Chla)
    % INPUTS
    %   depth : depth
    %   I : available solar radiation just bellow the water surface
    %   eta : the light extinction coefficient
    %   T : the temperature of the water at z
    %   alpha : the ratio of Clorophyl to oxygen utilized
    %   Chla : the concentration of Chlorophyl
    %   Gmax : the algae growth factor
    %
    % OUTPUTS
    %   P :: depth averaged oxygen production by photosynthesis [gO2/L]

    z = linspace(0,depth,100)';
    P = mean(Photosynthesis2(z,I,eta,T,alpha,Gmax,Chla));
  end
```

Appendix I

Reaeration code

I.1 Reaeration flux

```
function F=reaeration_flux(W,T,O,D,model)
    % W is the wind speed
    % T is the water temperature

    if strcmp(model,'banks')
        % use Riley model for the rearation coefficient
        ka = rearation_k_Banks(W)./24;% convert to hours

    elseif strcmp(model,'wanninkhof')
        % use Stefan model for the rearation coefficient
        ka = rearation_k_Wanninkhof(W)./24;% convert to hours
    else
       disp('This model does not exist!')
    end

    Os = Saturated_O2(T);
    F=(ka./D).*(Os-O);
end
```

I.2 Saturated Dissolved Oxygen

```
function Cs = Saturated_O2(T)
    % Calculate the saturated oxygen concentration based on water
    % Temperature

    Cs=14.652-0.4102*T+7.99*(10^-3)*(T.^2)-7.7774*(10^-5)*(T.^3);

end
```

I.3 Banks reaeration coefficient

```
function k = rearation_k_Banks(W)
    k = ((0.728.*W^0.5)-(0.317.*W)+(0.0372.*W^2));  %
end
```

I.4 Wanninkof reaeration coefficient

```
function ka = rearation_k_Wanninkhof(W)
    %Sct=13750*(0.010656*exp(-0.0627*T)+0.00495); % Calculation of Schmidt
                                                  % number
    Sct=500; %for lakes Sct is taken 500
    ka=((0.108.*W.^(1.64)).*((600./Sct).^(0.5)));
end
```

Appendix J

Respiration code

```
function R=respiration(YCHO2,krs,thetars,T,Chla)
    % YCHO2 is the ratio of mg of chlorophyll-a to mg of oxygen used in
    % respiration [-]
    % k respiration rate [d-1]
    % theta temperature adjustment coefficient [-]
    % Chla specified chlorophyll a concetration [ug/L]

    R=(1./YCHO2).*(krs).*thetars.^(T-20).*Chla;
end
```

Appendix K

Decomposition code

```
function D=Decomposition(kb,thetab,T,BOD)
    % kb BOD demand rate [d-1]
    % theta temperature adjustment coefficient [-]
    % BOD biological oxygen demand [mg/L]

    D=(kb).*thetab.^(T-20).*BOD;
end
```

Appendix L

Sediment oxygen demand code

```
function S=sediment(H,Sb,thetas,T)
    % Sb Sediment Oxygen Demand rate [g/m^2d]
    % thetas temperature adjustment coefficient [-]
    % H depth of water body [m]

    S=(1./H).*(Sb).*thetas.^(T-20);
end
```

Appendix M

Conversion of air to water temperature code

```
function Tw = AirTemperatureConverter(Tw0,Ta,k,dt)
% Physical converter for the air temperature.
%
% Given an air temperature (Ta) in time and the heat transfer
% coefficient k, the AirTemperatureConverter function computes the
% corresponding surface water temperature in time.
%
% INPUTS
%
%   Tw0 : The initial water temperature. The water temperature at
%         the time step 0. (oC)
%   Ta  : The air temperature in time. It is an array with number of
%         elements corresponding to the number of time steps. (oC)
%   k   : The heat transfer coefficient. It is a number. (1/s)
%   dt  : The time step at which the air temperature is given and at
%         which the water temperature will be computed. (s)
%
% OUTPUTS
%
%   Tw : The water temperature in time. (oC)

    % allocate memory space for water temperature Tw
    Tw = zeros(size(Ta));

    % initialize the water temperature
    Tw(1) = Tw0;

    % convert the air temperature in time according
    for tStep=2:length(Ta)
        Tw(tStep) = (1-exp(-k*dt))*Ta(tStep) + exp(-k*dt)*Tw(tStep-1);
    end
end
```

Appendix N

Discretization of the diffusion term

The diffusion term in (4.15), page 33, is given by:

$$D = \frac{\partial}{\partial z}\left(k_z \frac{\partial C}{\partial z}\right) . \tag{N.1}$$

First we convert this equation into a system of two equations:

$$\begin{cases} q = k_z \dfrac{\partial C}{\partial z} \\ D = \dfrac{\partial q}{\partial z} \end{cases} . \tag{N.2}$$

Then we just discretize each of them. The first equation is discretized using finite differences as:

$$q_i = k_z \frac{C_i - C_{i-1}}{\Delta z} . \tag{N.3}$$

Where q_i and C_i are located in between two cells and at the center of the cells, respectively, see Figure N.1. The second equation is discretized using finite differences as:

$$D_i = \frac{q_{i+1} - q_i}{\Delta z} . \tag{N.4}$$

Where D_i is located in the center of the cells, see Figure N.1.

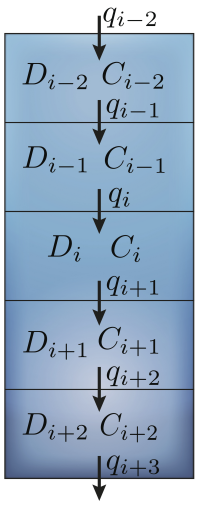

Figure N.1: Location of the discretized quantities in the diffusion term.

Appendix O

Weather conditions of simulation period

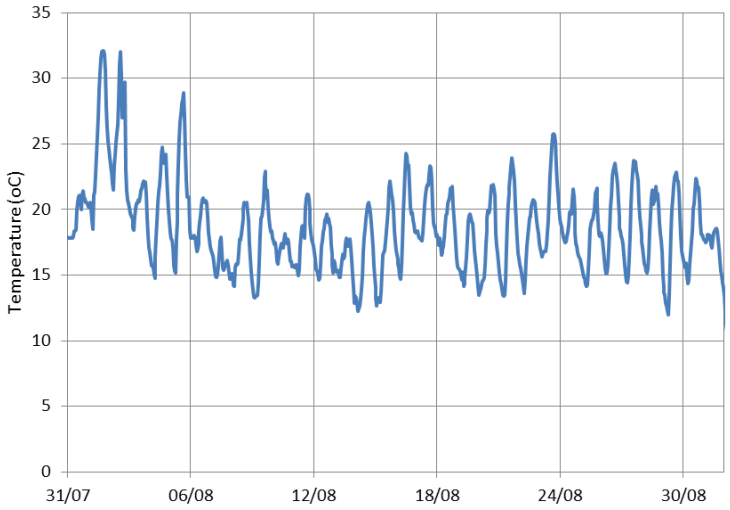

Figure O.1: Temperature during 31st of July and 31st of August.

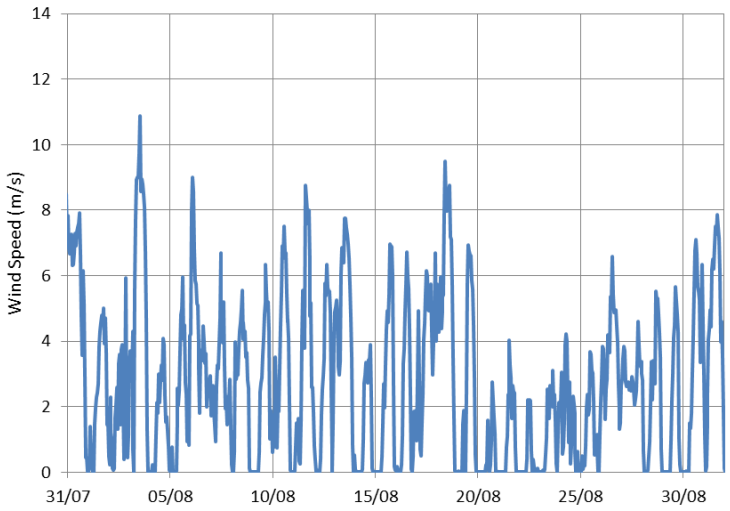

Figure O.2: Wind speed during 31st of July and 31st of August.

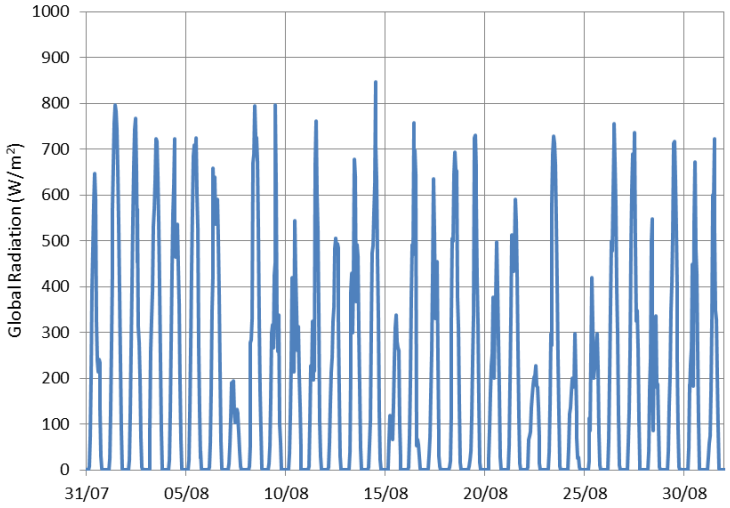

Figure O.3: Global radiation during 31st of July and 31st of August.

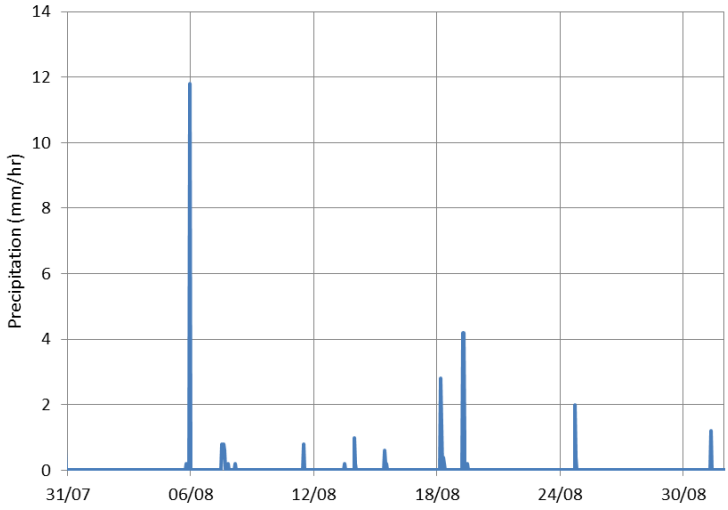

Figure O.4: Precipitation during 31st of July and 31st of August.